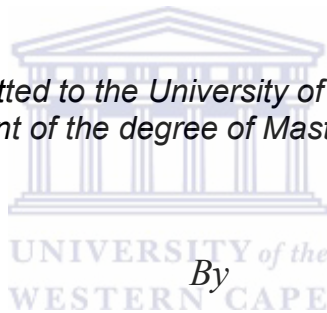




UNIVERSITY *of the*
WESTERN CAPE

**A spatial-temporal conceptualization of groundwater flow
distribution in a granite fractured rock aquifer within the
southern supersite research catchment of the Kruger National
Park**

*Dissertation submitted to the University of the Western Cape in the
fulfilment of the degree of Master of Science*



Ashton Van Niekerk

Department of Earth Sciences
Faculty of Natural Sciences, University of the Western Cape

Supervisor

Dr.Jacobus.M Nel

Co-supervisors

Dr.Edward.S Riddell and Mr.Abraham.C.T Scheepers

September 2014

Cape Town, South Africa

Abstract

A spatial-temporal conceptualization of groundwater flow distribution in a granite fractured rock aquifer within the southern supersite research catchment of the Kruger National Park

Ashton Van Niekerk

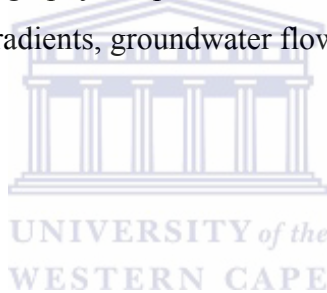
MSc Thesis

Department of Earth Science

University of the Western Cape, South Africa

Keywords:

Electrical resistivity tomography, air percussion drilling, borehole lithology logs, aquifer tests, hydraulic gradients, groundwater flow processes, fluid logging, Kruger National Park.



Abstract:

Understanding the hydrogeology of fractured or crystalline rocks is complicated because of complex structure and a porosity that is almost exclusively secondary. These types of geologies exhibit strong heterogeneities and irregularities contrasted in hydraulic properties, spacing and flow direction within fractured rock aquifers. Therefore it is important to develop a conceptual model based on site specific data such as the hydraulic roles between groundwater and nearby hillslope/surface water bodies in order to understand its movement within the environment. Therefore this study intends to develop a hydrogeological conceptual model associated with the dominant groundwater flow processes at a 3rd order scale within the Kruger National Park (KNP).

Electrical resistivity Tomography (ERT) surveys were conducted in the KNP in the 3rd order supersite catchments namely the southern granite (Stevenson Hamilton). This supersite is representative of the granite geology and land systems in the Southern region of KNP

These ERT surveys were used to characterize the hydrogeological components of weathering and depth to water level using the subsurface resistivity distribution. The initial ERT surveys conducted along the 1st order hillslope suggested that the weathering depths were deeper at the riparian zone and shallower at the crest. The weathering depth at the 2nd order hillslope was expected to be deeper at the riparian zone than at the crest. The weathering depth for the 3rd order hillslope interpretation was expected to be shallower at the riparian than at the crest. The surveys illustrated low resistivity values ranging from 3-75 Ωm at a depth of 8-12m suggesting possible depth to groundwater across the 3 hillslopes. It was interpreted that two zones of saturation could be explored for groundwater along each hillslope, namely the low resistivity (3-75 Ωm) weathered aquifer and high resistivity (1875-5484 Ωm) hard rock aquifer. The close banding of resistivity values ranging between 219-641 Ωm suggest possible depth of weathering /hard rock interface.

Based on the initial ERT survey interpretations, boreholes were drilled providing actual subsurface results in the form of borehole drilling logs, water levels, hydraulic data and in-situ groundwater quality parameters. Integrating the ERT survey data with the results from the intrusive measurements enabled an updated conceptualization of groundwater flow characteristics and distribution across the southern granite supersite.

The concluding findings suggest that two aquifer types exist on the southern granite supersite namely, a weathered (average depth ranging 383-328 mamsl) and hard rock (average depth ranging 364-299 mamsl) granite/gneiss aquifer. The blow out yields obtained from the air percussion drilling ranged from 0.01-1.25 L/s. Hydrogeological processes and characterization show that the general groundwater flow direction in the weathered and hard rock aquifer extends from the 1st order hillslope towards the 3rd order hillslope mimicking the topography. The weathered aquifer flow system responds to localized processes such as piston recharge, indirect surface water recharge and groundwater water discharge via interflow. This was due to the relatively rapid response time of 2-3 weeks in

groundwater levels to the major sequence of rainfall events over the hydrological year and the freshening out or decrease in specific conductance (SC) values during the fluid logging. The hard rock aquifer is part of a regional groundwater flow system. This is owed to the lengthy response time lags of 2-3 months in groundwater levels to the major sequences of rainfall events over the hydrological year. The SC fluids logs conducted over the wet and dry seasons did not vary significantly for the boreholes drilled into the hard rock aquifer, suggesting no active influx of localized fresh (low SC) groundwater or rainfall. This also supports a regional groundwater flow system. Due to the generally low transmissivity (ranging 9.50E-08 -11.2 m²/day) values obtained during the borehole pump and slug tests and inclining trend of groundwater levels after the wet season, suggest these ephemeral hillslope landscapes is likely to act as hydraulic boundary areas. In that they contribute during the dry season to the regional hydraulic head generating baseflow to perennial streams.



Declaration

I declare that **A spatial-temporal conceptualization of groundwater flow distribution in a granite fractured rock aquifer within the southern supersite research catchment of the Kruger National Park** is my own work, that it has not been submitted for any degree or examination in any other university, and that all the sources I have used or quoted have been indicated and acknowledge by complete references.

Full name: Ashton Van Niekerk

Date: 04 September 2014

Signed.....



Acknowledgements

This thesis would not have been possible without the assistance of many individuals and institutions. I would like to express my sincerest appreciation to the following:

- My supervisor, Dr. Jacobus. M Nel from Groundwater Consulting Services (GCS) for his assistance and mentorship.
- My co-supervisors, Dr. Edward. S Riddell from SANParks scientific services for his assistance and mentorship and Mr. Abraham. C.T Scheepers from Earth Science Department, University of the Western Cape for his assistance.
- Prof. Simon Lorentz for the opportunity of working on the supersite project.
- The Water Research Commission for funding this project
- The Department of Water affairs for partial funding of this MSc, Hans Wolmerans for his assistance during the supersite drilling campaign and the drilling team of Rangers Shisana for drilling the supersite boreholes.
- My colleagues Mr. Daniel Fundisi and Ms. Faith Jumbi for their assistance in fieldwork.
- Mr. Matthys Dippenaar from the University of Pretoria, Geology department for analysing the borehole lithology log samples and the characterisation of the southern granite supersite geology.
- Prof. Piet Le roux and Dr. George van Zijl for the hydrogeology studies and soil surveys of the southern granite supersite.
- SANParks staff for their continued support, in particular Mr Robin Petersen from Scientific Services for his mentorship and friendship, the game guards, in particular Mr. Annoit Machele for his vigilance and assistance in the field.
- The University of the KwaZulu-Natal, for the Abem resistivity instrumentation.
- Mr. Thomas Rowe from the University of KwaZulu-Natal, Water Resources Department for assistance in field work.

- Mr. Martin de Klerk, from Cape Geophysics for assistance with the ERT survey interpretations.
- Mr. Shamiel Davids, for his assistance with field work equipment.
- My family and friends for their continued support and encouragement throughout this thesis.



Abbreviations and acronyms

2D	Two dimensions
3D	Three dimensions
%	Percentage
API	Antecedent Precipitation Index
°C	Degrees Celsius
CRD	Cumulative Rainfall Departure
DWA	Department of Water Affairs
dH	Change in hydraulic head
dH/dT	Change in hydraulic head with change in time
EC	Electrical conductivity
ERT	Electrical Resistivity Tomography
FL	Fluid logging
GPS	Global positioning system
h	Hydraulic head
K	Hydraulic conductivity
Km	Kilometres
KNP	Kruger National Park
KNPRRP	Kruger National Park Rivers Research Programme
L/s	Litres per second
mS/cm	Millisiemens per centimetre
m ² /d	Metres squared per day
m	Meters
mamsl	Metres above mean sea level
mm	Millimetres
MS	Microsoft

Ωm	Ohm metre
RMS	Root mean square
SANParks	South African National Parks
SASW	Spectral analysis of surface waves
SC	Specific conductance
T	Transmissivity
YSI	Yellow Springs Incorporated
W/m ²	Watt per square meter
WRC	Water Research Commission



Glossary

Catenal elements

Areas that have distinct hydrological regimes which are both cause and consequence of a particular combination of plant cover, soil, slope characteristics (e.g. gradient, curvature and aspect) and slope position (Cullum and Rogers, 2011).

Groundwater Recharge

The entry into the saturated zone of the water made available at the water table surface, together with the associated flow away from the water table within the saturated zone (Freeze and Cherry, 1979).

Groundwater Discharge

The removal of water from the saturated zone across the water table surface, together with the associated flow toward the water table within the saturated zone (Freeze and Cherry, 1979).

Hard rock zone

This includes the variably fractured fresh bedrock and the saprock or weathered bedrock (Wright, 1992).

Hydraulic conductivity

It is the ease with which a fluid can move through an aquifer medium depending on the physical properties of the medium (grain size, grain shape, pore size, fracture arrangement and density) and the fluid (density, viscosity, gravitational force) (Kresic, 2007).

Interflow (soils)

Interflow (A/B horizon): Duplex soils where the textural discontinuity facilitates build-up of water in the topsoil. Duration of drainable water depends on rate of ET, position in the hillslope (lateral addition/release), and slope (discharge in a predominantly lateral direction) (Van Tol et al., 2013).

Interflow (soil / bedrock): Soils overlying relatively impermeable bedrock. Hydromorphic properties signify temporal build of water on the soil/bedrock interface and slow discharge in a predominantly lateral direction (Van Tol et al., 2013).

Interflow (groundwater)

The rapid flow of water along essentially unsaturated flow paths, water that infiltrates the subsurface and moves both vertically and laterally before discharging into other water bodies i.e. becoming part of the regional groundwater flow system (DWA, n.d.).

Perched water table

The existence of a low permeability medium or layer in a high permeable formation can lead to the formation of a discontinuous saturated lens, with unsaturated conditions existing both above and below the low permeable layer (Freeze and Cherry, 1979).

Recharge (soils)

Soils without any morphological indication of saturation. Vertical flow through and out of the profile into the underlying bedrock is the dominant flow direction. These soils can either be shallow on fractured rock with limited contribution to evapotranspiration or deep freely drained soils with significant contribution to evapotranspiration (Van Tol et al., 2013).

Supersite

Areas within KNP that are selected as examples of catchments characteristic of a certain physiographic zone. Research projects will be focused on these areas, aiming to construct a holistic, transdisciplinary description and understanding of the ecological processes and interactions that operate within each physiographic zone (Cullum and Rogers, 2011).

Sodic site

According to Cullum and Rodgers (2011) in areas where the A horizon is either very thin or totally absent are inhospitable to most plants. These are 'sodic sites', which are very open, containing only sparse cover of salt resistant shrubs such as

Euclea divinorum. The accumulated salts in these areas and the high nutrient content of the soil produce highly palatable grasses that are preferred grazing sites for many herbivores early in the season. By the end of the wet season, these sites are often almost devoid of cover, appearing as bare patches.

Static water level

The groundwater level in a borehole not influenced by abstraction or artificial recharge (DWA, n.d.).

Transmissivity

It is the product of hydraulic conductivity of the aquifer material and the saturated thickness of the aquifer (Kresic, 2007).

Vadose/unsaturated zone

That part of the geological stratum above the water table where interstices and voids contain a combination of air and water (DWA, n.d.).

Water table

The surface on which the fluid pressure in the pores of a porous medium is exactly atmospheric (Freeze and Cherry, 1979).

Water level

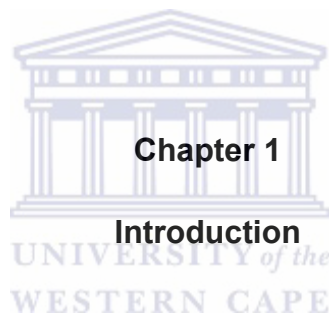
Whereby the water table is revealed by the level at which water stands in a borehole open along its length and penetrating the surficial deposits just deeply enough to encounter standing water in the bottom (Freeze and Cherry, 1979).

Weathered zone

According to Wright (1992) the regolith or weathered zone consists of the collapsed zone and the saprolite. Since weathering is most effective in the vadose zone and the zone of water table fluctuations, there is a tendency to develop subdivisions into an upper and lower saprolite relative to current (or previous) water levels.

TABLE OF CONTENTS

Abstract	I
Declaration	IV
Acknowledgements	V
Abbreviations and acronyms	VII
Glossary	IX
Table of contents	XII
List of figures	XIX
List of tables	XXVII



1.1	Background	1
1.2	Main aim	2
1.3	Objectives	2
1.4	Key questions	2
1.5	Scope and outline of the thesis	3

Chapter 2

Literature review

2.1	Introduction	4
2.2	Groundwater in the environment	4
2.2.1	Groundwater flow systems	6
2.2.2	Groundwater fluctuations	8
2.3	Hydrogeological regimes within Kruger National Park savanna landscape	10
2.4	Groundwater in Kruger National park	12
2.5	The approach for developing a hydro geological conceptual model, application to the southern granite supersite	12
2.6	Literature addressing site specific scale hydrogeological investigations adopted for the southern granite supersite	13
2.6.1	Introduction to geophysical surveys: Electrical resistivity method	13
2.6.2	General Electrical Resistivity Tomography (ERT) theory	15
2.6.3	ERT electrode configuration	18
2.6.4	2D electrical resistivity profiling	19
2.7	Borehole drilling	19
2.7.1	Introduction	19

2.7.2	Drilling methods applicable for hard rock environments	21
2.8	Aquifer tests	22
2.8.1	Introduction	22
2.8.2	Single borehole pump out test	24
2.8.3	Slug borehole test	24
2.9	Analysis of aquifer test solutions	25
2.9.1	Theis equation	26
2.9.2	Cooper-Jacob equation	27
2.9.3	Pump test drawdown correction factor	27
2.9.4	Hantush equation	28
2.9.5	Bouwer and Rice equation	28
2.10	Fluid logging	30
2.10.1	Fluid Logging application techniques	30

Chapter 3

Study description

3.1	Introduction	32
3.2	Location	32
3.3	Hillslope soil and vegetation	34
3.4	Topography	35
3.5	Climate and rainfall	36

3.6	Geology	37
-----	---------	----

Chapter 4

Materials and Methods

4.1	Introduction	39
4.2	Site or transect selection for ERT surveys	39
4.3	ERT surveys method	40
4.4	Air percussion drilling	42
4.4.1	Air percussion drilling method	43
4.4.2	Borehole lithology logs	44
4.5	Monitoring	45
4.5.1	Groundwater level trends	45
4.5.2	Fluid logging	48
4.5.3	Meteorologic data	50
4.6	Aquifer properties and characterisation	52
4.6.1	Pump test	52
4.6.2	Slug test	53
4.7	Data analysis	54
4.7.1	Pump test	54
4.7.2	Slug test	55

Chapter 5

Results and Discussion: Spatial characterisation

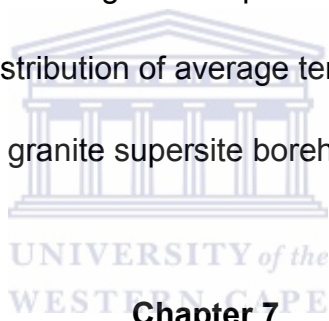
5.1	Introduction	56
5.2	Geophysical and borehole lithology log characterisation	56
5.2.1	Southern granite First order transect	57
5.2.2	Southern granite First/second order triangulation transect	61
5.2.3	Southern granite Second order transect	64
5.2.4	Southern granite Third order transect	67
5.2.5	Southern granite Third order triangulation transect	71
5.3	Hydraulic characterisation for the southern granite supersite boreholes	73
5.3.1	Transmissivity	75
5.4	Groundwater flow direction and gradients	77

Chapter 6

Results and discussion: Spatial – Temporal characterisation

6.1	Introduction	81
6.2	Time series rainfall	81
6.3	Time series groundwater levels and rainfall	83
6.3.1	First order boreholes	83
6.3.2	First/second order triangulation boreholes	86
6.3.3	Second order boreholes	87

6.3.4	Third order boreholes	90
6.4	General discussion	96
6.5	In-situ parameters/fluid logging	96
6.5.1	First order boreholes	97
6.5.2	First/second boreholes triangulation boreholes	99
6.5.3	Second order boreholes	101
6.5.4	Third order boreholes	104
6.5.5	Spatial distribution of average specific conductance for the southern granite supersite boreholes	110
6.5.6	Spatial distribution of average temperatures for the Southern granite supersite boreholes	112



Chapter 7

Synthesis: Hydro-geological conceptual site model

7.1	Introduction	114
7.2	Discussion	114
7.2.1	First order hillslope	114
7.2.2	Second order hillslope	115
7.2.3	Third order hillslope	116
7.2.4	General conclusion	116

Chapter 8

Conclusions and Recommendations

8.1	Conclusion	118
8.2	Recommendations for future research	120
8.3	Recommendations for management	121
	References	122
	Appendix CD	136



List of figures

- Figure 2.1 A demonstration of a concept that groundwater can interact with all types of surface water at many different terrains at many different places throughout the landscape (Winter et al., 1998). (M=mountains, G=glacial, K=karst, R=riverine (small), V=riverine (large) and C=coastal). 6
- Figure 2.2 Schematic illustrating the distribution of downward, lateral and upward components of groundwater flow from nested boreholes or piezometers (Winter et al., 1998). 7
- Figure 2.3 Three dominant flow systems within a groundwater flow system (Toth, 1963). 8
- Figure 2.4 Schematic of groundwater level response or rise in relation to the distance of area contributing to the response or rise in water level (Kirchner, 2003). 10
- Figure 2.5 A conventional Wenner and Schlumberger electrode array, C1 and C2 – current electrodes, P1 and P2 – potential electrodes (Loke, 2004). 17
- Figure 2.6 Typical resistivity values for geological materials (Abem, 2010). 18
- Figure 2.7 Diagram illustrating factors influencing the design of boreholes (Kresic, 2007). 21
- Figure 2.8 Trends in water level obtained during a pump test (Heath, 1983). 24
- Figure 2.9 Schematic cross section of a pumped aquifer (Kruseman and De Ridder, 1994). D: Aquifer saturated thickness, S: Drawdown, Q: Discharge. 25

Figure 2.10	A graph devised by Bouwer and Rice (1976) to estimate a value for the R_e / r_w relationship.	30
Figure 3.1	Location of the southern granite supersite with respect to the N'waswitshaka basin, Kruger National Park and north eastern South Africa.	33
Figure 3.2	Soil hydrological map with groups of soils discussed above based on their expected hydrological responses for the southern granite supersite (Van Zijl, 2013).	35
Figure 3.3	Topography across the southern granite supersite catchment.	36
Figure 3.4	Daily rainfall over the hydrological season September 2012 to September 2013.	37
Figure 3.5	The locations of survey samples taken for the geological characterisation of the southern granite supersite (Dippenaar, 2013).	38
Figure 4.1	An Abem Signal Averaging System (SAS) 1000/4000 Terrameter and switching unit powered by a 12 volt battery with 64 steel probes and clips to connect to four 100m cables with 21 take outs on each to form electrodes.	41
Figure 4.2	Supper rock 5000 air percussion rig on a 10 ton 6x6 truck with 24 bar 900CFM compressor used for drilling the southern granite supersite boreholes.	42
Figure 4.3	Schematic diagram of the piezometric or shallow and deep borehole construction.	44
Figure 4.4	Borehole lithology log of weathered material (green highlighted section) and hard rock material (yellow highlighted section). The	

	black highlighted section indicates the depth at which a water strike was encountered.	45
Figure 4.5	Schematic representation of groundwater hydraulic heads (H1 and H2) and gradient (Kresic, 2007).	46
Figure 4.6	Use of a Solinst™ water level (Dip) meter to measure groundwater level.	47
Figure 4.7	A Solinst™ level loggers used to measure water levels in the streams.	47
Figure 4.8	Yellow Spring Incorporated (YSI) 600XLMD sonde multi-parameter in-situ monitoring device.	49
Figure 4.9	Southern granite supersite weather station.	51
Figure 4.10	Location of site instrumentation (and black lines represent ERT traverses).	51
Figure 4.11	Equipment used during a pump test.	53
Figure 4.12	Equipment required to perform a slug test.	54
Figure 5.1	Initial and final interpretation of 2D ERT traverses coupled with topography data, satellite imagery and estimated and actual positions of groundwater level and weathering.	59
Figure 5.2	Borehole lithology log of the southern granite 1st order riparian 61m and crest 103m boreholes, the green highlighted section indicates weathered material, the yellow highlighted section indicates hard rock material and the black blocks indicate water strike positions.	60
Figure 5.3	2D ERT traverse coupled with actual groundwater level and weathering positions (Topographic detail excluded) of the 1st / 2nd order triangulation borehole position.	62

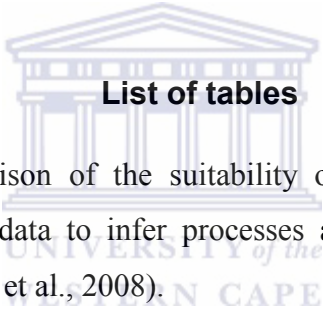
- Figure 5.4 Borehole lithology log of the southern granite 1st/2nd order triangulation 61m borehole, the green highlighted section indicates weathered material and the yellow highlighted section indicates hard rock material. 63
- Figure 5.5 Initial and final interpretation of 2D ERT traverses coupled with topography data, satellite imagery and estimated and actual positions of groundwater level and weathering. 65
- Figure 5.6 Borehole lithology logs of the southern granite 2nd order riparian 49m and crest 55m borehole, the green highlighted section indicates weathered material and the yellow highlighted section indicates hard rock material. 66
- Figure 5.7 Initial and final interpretation of 2D ERT traverses coupled with topography data, satellite imagery and estimated and actual positions of groundwater level and weathering. 68
- Figure 5.8 Borehole lithology log of the southern granite 3rd order riparian 43m and mid-slope 49m boreholes, the green highlighted section indicates weathered material, the yellow highlighted section indicates hard rock material and the black block indicates the water strike position. 69
- Figure 5.9 Borehole lithology log of the southern granite 3rd order crest 55m borehole, the green highlighted section indicates weathered material, the yellow highlighted section indicates hard rock material and the black block indicates the water strike position. 70
- Figure 5.10 2D ERT traverse coupled with actual groundwater level and weathering positions (Topographic detail excluded) of the 3rd order triangulation borehole position. 71
- Figure 5.11 Borehole lithology log of the southern granite 3rd order triangulation 61m borehole, the green highlighted section indicates

	weathered material, the yellow highlighted section indicates hard rock material.	72
Figure 5.12	Data acquired during a pump test for the southern granite 1st order riparian position 61m borehole, a=drawdown, b=recovery and c=pump test Cooper - Jacob macro (Van Tonder et al., 2001).	74
Figure 5.13	Data acquired during a slug test for the southern granite 3rd order crest position 34m borehole, a=recovery and b=slug test excel macro (Halford and Kuniansky, 2005).	75
Figure 5.14	Transmissivity values for the southern granite supersite boreholes calculated using the Cooper-Jacob and Huntush (wedge shaped) solutions.	76
Figure 5.15	Transmissivity values for the southern granite supersite boreholes calculated using the Bouwer and Rice solution.	77
Figure 5.16	General groundwater flow direction of the boreholes drilled into the hard rock aquifer during the dry season (date of water level taken: 27-Sep-13).	78
Figure 5.17	General groundwater flow direction of the boreholes drilled into the weathered aquifer during the dry season (date of water level taken: 27-Sep-13).	79
Figure 5.18	General groundwater flow direction of the boreholes drilled into the hard rock aquifer during the wet season (date of water level taken: 28-Jan-13).	79
Figure 5.19	General groundwater flow direction of the boreholes drilled into the weathered aquifer during the wet season (date of water level taken: 28-Jan-13).	80
Figure 6.1	Daily rainfall intensities for the southern granite supersite from September 2012 to September 2013.	82

Figure 6.2	Cumulative rainfall for the southern granite supersite from September 2012 to September 2013.	82
Figure 6.3	API for the southern granite supersite illustrating the 3 major rainfall sequences during September 2012 to September 2013.	83
Figure 6.4	1st order crest position 103m borehole water level response to rainfall over the hydrological season September 2012 to September 2013.	85
Figure 6.5	1st order crest position 17m borehole water level response to rainfall over the hydrological season September 2012 to September 2013.	85
Figure 6.6	1st order riparian position 61m borehole water level response to rainfall over the hydrological season September 2012 to September 2013.	86
Figure 6.7	1st /2nd order triangulation position 36m and 61m borehole water level response to rainfall over the hydrological season September 2012 to September 2013.	87
Figure 6.8	2nd order crest position 40m and 55m borehole water level response to rainfall over the hydrological season September 2012 to September 2013.	89
Figure 6.9	2nd order riparian position 28m and 49m borehole water level response to rainfall over the hydrological season September 2012 to September 2013.	90
Figure 6.10	3rd order crest position 34m and 55m borehole water level response to rainfall over the hydrological season September 2012 to September 2013.	94

Figure 6.11	3rd order mid-slope position 23m, 26m and 49m borehole water level response to rainfall over the hydrological season September 2012 to September 2013.	95
Figure 6.12	3rd order riparian position 20m and 43m borehole water level response to rainfall over the hydrological season September 2012 to September 2013.	95
Figure 6.13	3rd order triangulation position 34m and 61m borehole water level response to rainfall over the hydrological season September 2012 to September 2013.	96
Figure 6.14	Specific conductance quarterly fluid log for the 1st order crest position 103m borehole.	98
Figure 6.15	Specific conductance quarterly fluid log for the 1st order crest position 17m borehole.	98
Figure 6.16	Specific conductance quarterly fluid log for the 1st order riparian position 61m borehole.	99
Figure 6.17	Specific conductance quarterly fluid log for the 1st /2nd order triangulation position 61m borehole.	100
Figure 6.18	Specific conductance quarterly fluid log for the 1st /2nd order triangulation position 36m borehole.	101
Figure 6.19	Specific conductance quarterly fluid log for the 2nd order crest position 55m borehole.	102
Figure 6.20	Specific conductance quarterly fluid log for the 2nd order crest position 40m borehole.	103
Figure 6.21	Specific conductance quarterly fluid log for the 2nd order riparian position 49 m boreholes.	103
Figure 6.22	Specific conductance quarterly fluid log for the 2nd order riparian position 28 m boreholes.	104

Figure 6.23	Specific conductance quarterly fluid log for the 3rd order crest position 55m borehole.	106
Figure 6.24	Specific conductance quarterly fluid log for the 3rd order crest position 34m borehole.	107
Figure 6.25	Specific conductance quarterly fluid log for the 3rd order mid-slope position 49m borehole.	107
Figure 6.26	Specific conductance quarterly fluid log for the 3rd order mid-slope position 26m borehole.	108
Figure 6.27	Specific conductance quarterly fluid log for the 3rd order riparian position 43m borehole.	108
Figure 6.28	Specific conductance quarterly fluid log for the 3rd order riparian position 20m borehole.	109
Figure 6.29	Specific conductance quarterly fluid log for the 3rd order triangulation position 61 m borehole.	109
Figure 6.30	Specific conductance quarterly fluid log for the 3rd order triangulation position 34m borehole.	110
Figure 6.31	Spatial distribution of specific conductance for the southern granite supersite deep boreholes during the dry season combined averaged value fluid logs of May 2013 and August 2013.	111
Figure 6.32	Spatial distribution of specific conductance for the southern granite supersite deep boreholes during the wet season combined averaged value fluid logs of November 2012 and February 2013.	111
Figure 6.33	Spatial distribution of specific conductance for the southern granite supersite shallow boreholes during the dry season combined averaged value fluid logs of May 2013 and August 2013.	112

Figure 6.34	Spatial distribution of specific conductance for the southern granite supersite shallow boreholes during the wet season combined averaged value fluid logs of November 2012 and February 2013.	112
Figure 6.35	Spatial temperature distribution for the southern granite supersite deep boreholes during the hydrological season fluid logs of November 2012 and August 2013.	113
Figure 6.36	Spatial temperature distribution for the southern granite supersite shallow boreholes during the hydrological season fluid logs of November 2012 and August 2013.	113
Figure 7.1	A hydrogeological conceptual site model of the southern granite supersite.	117
 <p>List of tables</p>		
Table 2.1	A comparison of the suitability of a measurement method for obtaining data to infer processes at the desired watershed scale (Robinson et al., 2008).	15
Table 2.2	A summary of various borehole drilling methods (Kresic, 2007).	22
Table 4.1	Site names and their respective hillslope/stream order positions within the southern granite supersite.	52

Chapter 1

Introduction

1.1. Background

Predicting the natural groundwater flow direction in crystalline rock aquifers can be related to the topography as, groundwater moves from high piezometric levels (often high lying areas) towards lower piezometric levels (often low lying areas associated with streams) where it discharges as springs or bank channel seepage into streams (Kresic and Mikszewski, 2013). However, understanding the hydrogeology of fractured or crystalline rocks is complicated because of complex structure, porosity that is almost exclusively secondary and the relationship with weathering processes. These can exhibit strong heterogeneities and irregularities in the contrast in hydraulic properties, spacing, flow direction and clogging by secondary clays within fractured rock aquifers (Kresic and Mikszewski, 2013; Lemieux et al., 2006; Freeze and Cherry, 1979; Wright, 1992). Therefore, it is important to develop a conceptual model based on site specific data such as hydraulic roles between groundwater and nearby hillslope/surface water bodies in order to understand its movement within the environment. In addition, a conceptual model would provide useful information or identify gaps in data sets that need to be addressed before a quantitative or numerical model can be constructed.

A current Water Research Commission (WRC) project was initiated to establish a multi-disciplinary research project which compares ephemeral landscape interactions between surface water, groundwater and vadose zone for two dominant geologies (granite and basalt) in Kruger National Park (KNP). These particular ephemeral landscapes were confined to the first, second and third order stream catchments according to the methods of Strahler (1957). The WRC research project focused on two ‘supersite research catchments’, namely southern granite (Stevenson Hamilton) and southern basalt (Nhlowa) supersites.

The basis for developing these supersite catchments were rooted from the fact that the scale at which many hydrological studies were carried out in the KNP

favoured a regional scale and not much has focused on the localized hillslope scale towards the larger perennial watersheds. Furthermore, hydrological research had the tendency of focusing on perennial streams. These perennial streams cover 600 km of KNP as opposed to the ephemeral streams that make up 30 000 km (Rogers and O’Keeffe, 2003). This information was suggestive of a hydrological knowledge gap within these particular landscapes.

This thesis forms part of the WRC research providing the groundwater component of the southern granite supersite (Stevenson Hamilton). The thesis attempts to conceptualize the spatial temporal distribution of groundwater flow processes down to the 3rd order hillslope scale to inform the greater WRC project of its potential role in interacting with the vadose zone and surface water streams.

1.2. Main aim

The main aim is to determine dominant groundwater flow processes within the southern granite supersite

1.3. Objectives

The following objectives were set for this thesis

- To identify potential groundwater flow paths in the southern granite supersite; and
- To develop a conceptual model describing the role of groundwater in groundwater/surface water/vadose zone interaction of the southern granite supersite

1.4. Key questions

The following key questions were used to achieve the above objectives:

- What are the subsurface lithological characteristics of the southern granite supersite?
- What is the groundwater flow paths associated within the southern granite supersite?

- What is the link with groundwater in relation to rainfall, vadose zone and surface water processes?

1.5. Scope and outline of the thesis

Chapter 1 provides the general background, problem statement, main aim, objectives and key questions of the thesis.

Chapter 2 outlines a theoretical basis for the state of knowledge of hydrogeological regimes within the surface water/vadose zone/groundwater interaction environment as well as the state of knowledge for Kruger National Park savanna landscapes. Furthermore a description of qualitative methodologies will be discussed in order to conceptualize the distribution of groundwater.

Chapter 3 provides an overview of the location, hillslope soil, vegetation, topography, climate, rainfall and geology of the southern granite supersite.

Chapter 4 outlines the site specific materials and methods used to achieve the study objectives.

Chapter 5 provided a spatial characterisation of the southern granite supersite groundwater distribution.

Chapter 6 provides a spatial-temporal characterisation of the southern granite supersite groundwater distribution.

Chapter 7 consolidates chapter 5 and 6 to achieve a site specific conceptualization of the spatial – temporal groundwater water distribution of the southern granite supersite.

Chapter 8 provides a conclusion and recommendation to the study

Chapter 2

Literature review

2.1 Introduction

The scope of this chapter is to outline a theoretical basis for the state of knowledge of hydrogeological regimes within the general environment and Kruger National Park savanna landscapes. Furthermore a description of qualitative methodologies will be discussed in order to characterize the distribution of groundwater. This would provide insight for the investigation of potential groundwater flow processes associated with the localized 3rd order hillslope scale of the southern granite supersite.

2.2 Groundwater in the environment

The hydrological cycle is commonly portrayed in a simplified diagram that shows only the major transfers of water between the ocean and continents. In order to understand hydrological processes and the managing of water resources, the water cycle has to be viewed at a broader range of scales and having an extensive variability in space and time (Winter et al., 1998).

The movement of water in the atmosphere and on the ground surface is relatively easy to visualize, but the movement of groundwater is not. Groundwater moves from flow paths of varying lengths from areas of recharge to areas of discharge (Winter et al., 1998). The generalized flow path of groundwater starts at the water table and migrates through the groundwater flow system and exists at the stream or at a pumped well (Winter et al., 1998). The source of water to the water table or groundwater recharge is precipitation through the unsaturated or vadose zone (Winter et al., 1998). The precipitation such as rainfall which contributes to groundwater recharge can be manipulated in various ways. A study was done by Wenniger et al. (2008) in order to develop a general understanding of the rainfall-runoff dynamics, a simple time series analysis was performed by dividing the precipitation into separate events for a specific hydrological year. In addition a study conducted in eight drainage basins in Greece estimated the time lag of

rainfall events which contributed to runoff using the API (Nikas et al., 2007). Gabrielli et al. (2012) also discovered that particular thresholds exist in the amount of rainfall that contributes to a rise in water levels.

According to Wenninger et al. (2008) a method has been devised in order to develop a simple time series analysis by grouping precipitation into particular rainfall events for a given hydrological year. This analysis is known as an Antecedent Precipitation Index (API). The API equation is as follows (Kohler and Linsley, 1949):

$$I = b_1P_1 + b_2P_2 + b_3P_3 + \dots + b_iP_i \quad \text{Equation 2.1}$$

- Where P_i is the amount of precipitation which occurred i days prior to the storm under consideration,
- b_i is a constant which is assumed to be some function of time such as $b_i = 1/i$

If a day-day value index (I) is required, there is a considerable advantage in assuming that b_i decreases with time according to a logarithmic recession rather than as a reciprocal. Therefore the following equation would be used:

$$I_t = I_0 k^t \quad \text{Equation 2.2}$$

Where:

t is the number of days between I_t and the initial index I_0 , thus the index for any day is equal to that of the previous day multiplied by the factor k with values that range from 0.85 to 0.90.

In unconfined aquifers flow paths (local and intermediate flow systems) near the stream can have extensive lengths and corresponding travel times of days to a few years while the longest flow paths (regional flow systems) near the stream can have travel times that may range from decades to millennia (Winter et al., 1998).

Therefore a host of hydrological process studies at multiple scales have been investigated in order to determine key factors such as dominant flow processes

which could be upscaled to landscape or regional scale to provide catchment conceptualization and hydrological prediction (Tetzlaff et al., 2010)

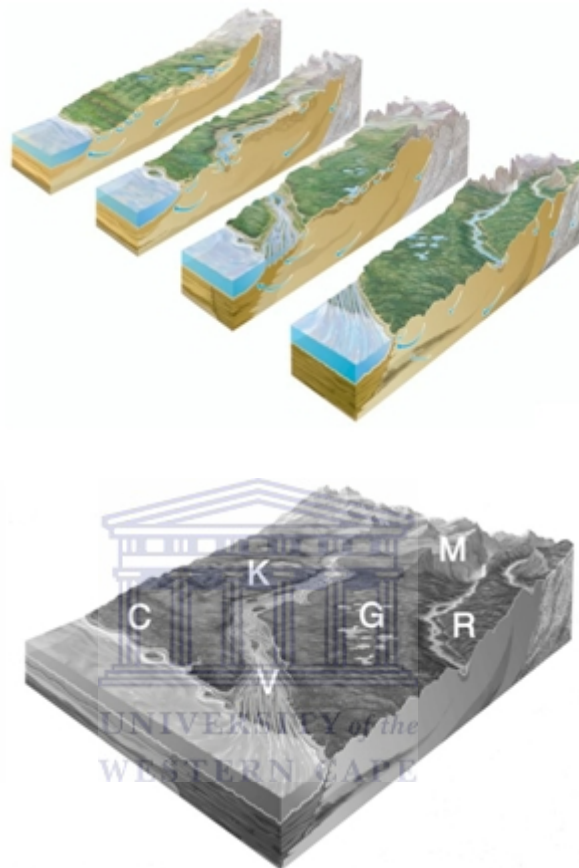


Figure 2.1 A demonstration of a concept that groundwater can interact with all types of surface water at many different terrains at many different places throughout the landscape (Winter et al., 1998). (M=mountains, G=glacial, K=karst, R=riverine (small), V=riverine (large) and C=coastal).

2.2.1 Groundwater flow systems

The groundwater flow system as a hole in reality is a three dimensional flow field (see Figure 2.3). A vertical section of a flow field indicates how potential energy or hydraulic head (h) is distributed beneath the water table in the groundwater system and how energy distribution can be used to determine vertical components of flow near a surface water body (Winter et al., 1998). Flow fields can be mapped in a process similar to water table contour maps i.e. geo-statistical

methods such as kriging, instead vertically distributed boreholes need to be used instead of water table boreholes, i.e. borehole nests whereby boreholes are drilled to different depths in the same location and screened only in a particular section of the groundwater system providing hydraulic heads representative of that section (see Figure 2.2).

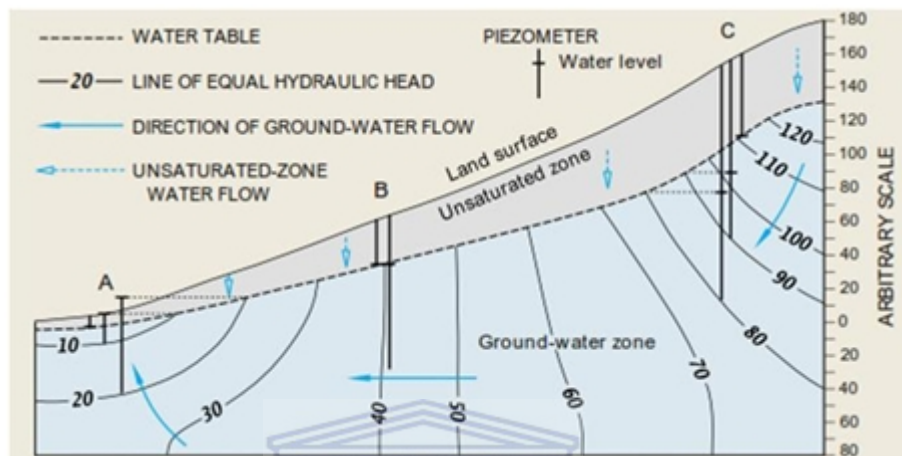


Figure 2.2 Schematic illustrating the distribution of downward, lateral and upward components of groundwater flow from nested or piezometric boreholes (Winter et al., 1998).

Local flow systems are the most dynamic and the shallowest flow systems, therefore they have the greatest interchange with surface water bodies (Winter et al., 1998). Given the low rainfall in semi-arid environments the understanding of localized hydrological flow processes within a catchment would provide insight as to how precipitation is distributed, storage of water in surface water, vadose zone and groundwater systems (Wenninger et al., 2008 and Tetzlaff et al., 2010). In literature there exists a knowledge gap within the understanding of these semi-arid localized scaling of integrated hydrological processes. Therefore this incongruity calls for new approaches to integrate different fields within the hydrological process realm (Tetzlaff et al., 2010). Studies have been carried out in order to improve the understanding of these systems such as the use of a regional calibrated flow model to calculate flow fluxes of boundary cells for a local scaled model (Ebraheem et al., 2003). Ochoa et al. (2013) showed that shallow groundwater systems can be an important determinant of hydrologic resilience in

the face of climate variability. Furthermore Ochoa et al. (2013) carried out an investigation to gain knowledge of the interconnectedness of different hydrologic processes of water distribution within the catchment. Through this study it was found that the localized groundwater system played an important role in terrestrial and aquatic habitat functionality and vice versa by means of groundwater recharge.

Local flow systems can be underlain by intermediate and regional flow systems. Water in the deeper flow systems have longer flow paths and longer contact time with subsurface material, therefore the water generally contains more dissolved chemicals i.e. higher specific conductance. The deeper flow paths also eventually discharge into surface water bodies where they can have an effect on surface water chemical composition (Winter et al., 1998).

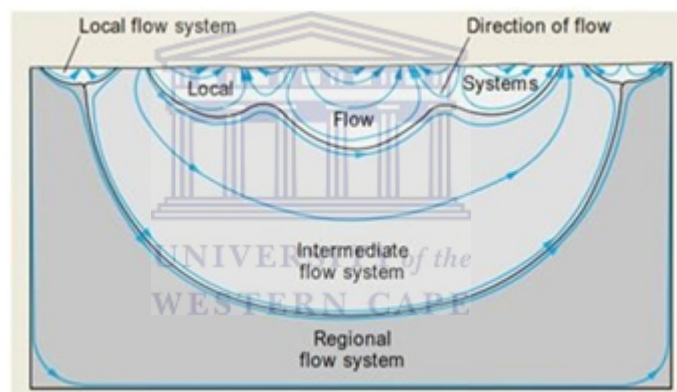


Figure 2.3 Three dominant flow systems within a groundwater flow system (Toth, 1963).

2.2.2 Groundwater fluctuation

The measurement of groundwater level fluctuation in boreholes or piezometers are important for groundwater studies because one can gather a good conceptual understanding of a particular study site, i.e. within a catchment deeper water levels typically indicate recharge zones and shallower water levels indicate discharge zones (Freeze and Cherry, 1979). These recharge and discharge areas can be mapped using indicators such as piezometric nest (different depths) boreholes and hydrochemical trends (Freeze and Cherry, 1979). The piezometric nests would show upward flow component in discharge areas and downward flow

component in recharge areas (see Figure 2.2). In addition temperature profiles of boreholes can be used as a surrogate to piezometric head measures whereby cooler temperatures are suggestive of recharge areas and warmer temperatures indicate discharge areas (Anderson, 2005). The hydrochemical trends infer that the general specific conductance (SC) increases along flow paths (Freeze and Cherry, 1979). Therefore water from recharge areas is usually fresh (low SC content) and discharge areas often have high SC content (Freeze and Cherry, 1979).

The fluctuations in groundwater levels could result from various hydrodynamic phenomena which could be natural such as distance from recharge areas (see Figure 2.4), recharge/discharge processes, evaporation, transmissivity, hydraulic conductivity and storativity or man induced such as groundwater abstraction for water supply or a combination of the phenomena (Freeze and Cherry, 1979; Kirchner, 2003). Therefore in order to correctly interpret the change in groundwater levels it is important to understand these phenomena (Freeze and Cherry, 1979).

The following example of groundwater level fluctuations will be discussed:

- groundwater recharge processes

Recharge processes:

Direct recharge is water added to the groundwater reservoir in excess of soil moisture deficits and evapotranspiration by direct vertical percolation through the unsaturated zone (Lerner et al., 1990). This could occur as a piston-type flow or translatory flow, a process whereby precipitation moves past the root zone and remain in storage in the unsaturated zone until it is displaced downwards by the subsequent infiltration or percolation event (Kresic, 2007). A study conducted by Gomo et al. (2012) suggested in an investigation of groundwater recharge in an alluvial environmental setting that the steady rise in water levels in response to rainfall events would likely be associated with piston recharge process. Indirect recharge is the movement of water from surface-water bodies, such as streams and rivers, to an underlying aquifer (Lerner et al., 1990).

Furthermore, a concept in which the area of recharge is related to the response in a recharge event could provide additional insight with regards to recharge processes (see Figure 2.4). A rapid response would indicate a more localized recharge process and a more gradual response would indicate a possible regional recharge process.

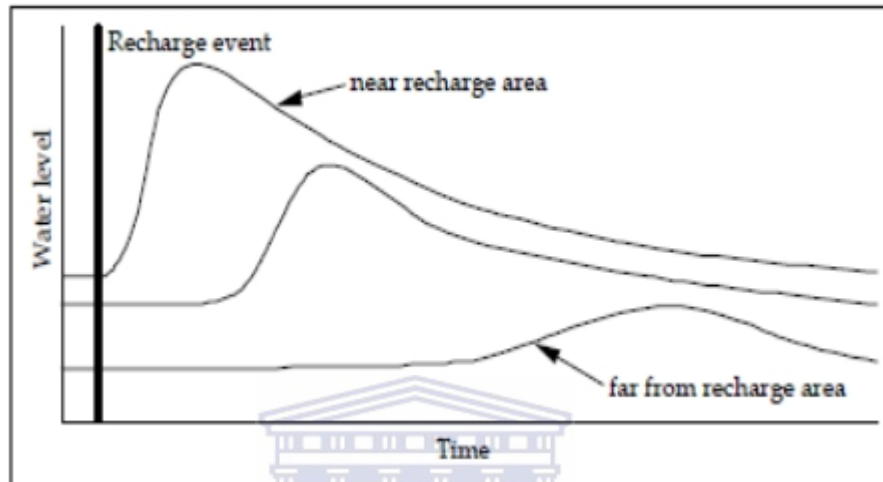


Figure 2.4 Schematic of groundwater level response or rise in relation to the distance of area contributing to the response or rise in water level (Kirchner, 2003).

2.3 Hydrogeological regimes within the Kruger National Park savanna landscape

The KNP has an extensive history of research done on its rivers and water resources such as the Kruger National Park Rivers Research Programme (KNPRRP) which devised a multi-disciplinary approach to determine the hydrological and geomorphological drivers for river system heterogeneity, through the monitoring of biotic responses (Rogers and O’Keeffe, 2003). This was done in effort to better understand ecosystem dynamics for the larger perennial rivers of KNP and ultimately be incorporated into policy and decision-making for ecosystems and water resource management. Furthermore, large scale perennial river research included a modelling approach to investigate the spatial

variability, magnitudes and probabilities of the floods which occurred during February 2000 in the Sabie catchment (Smithers et al., 2001).

Additional research was done on the Sabie River by Birkhead et al. (1995) which provided significant insight to the longitudinal flow of groundwater gradients in relation to the river stage fluctuations which resulted in temporal alternation of recharge and discharge between the river and groundwater throughout the year. The Department of Water Affairs in collaboration with South African National Parks (SANParks) have established a groundwater monitoring network in KNP whereby it was discovered that on a park wide scale the groundwater water levels have a tendency of decreasing based on data from the year 2007 to date (Du Toit et al., 2009). However in some cases certain boreholes such as the Matlari borehole located in the Skukuza section in the riparian zone of a 5th order ephemeral stream tributary to the Sabie River tends to have an increasing trend in water levels (Du Toit et al., 2009). A study undertaken by Petersen (2011) made use of a combination of the Cumulative Rainfall Departure (CRD) method and stable isotopes to infer dominant recharge processes and surface water groundwater interactions that occur in granitic and basaltic geologic types within the southern KNP region. It was concluded with the combination of the CRD method and stable isotopic compositions that the dominant recharge flow processes occurring in the southern region of KNP are a combination of direct recharge piston flow and indirect recharge via preferred pathways particularly streams and rivers. It was also found that at 6th and 7th order ephemeral/seasonal groundwater was contributing to these streams.

A host of vadose zone hydrological process studies have also been completed such as the attempt to describe the distribution of soil nutrients along the catena or hillslope and linking it to the dynamics of soil moisture levels on the upper parts of the catena in the Sabi-Sand game reserve by Ben-Shahar (1990). Furthermore, at two long term monitoring sites, the Sabie-Nkhulhu experimental exclosures (on granite) and the dryer Letaba experimental exclosure (on granite) Lorentz et al. (2006) examined soil moisture behaviours within the sections of the large granitic hillslope catena along the Sabie & Letaba Rivers respectively. Catena can be

defined as a series of soils and associated vegetation linked by their topographic relationship (Cullum and Rogers, 2011). These catenas consist of catenal elements which are areas that have distinct hydrological regimes which are both cause and consequence of a particular combination of plant cover, soil, slope characteristics (e.g. gradient, curvature and aspect) and slope position (Cullum and Rogers, 2011). In summary the crest soils were dominated by rapid vertical movement of water toward the weathered saprolitic zone where minimal lateral flows were expected following large rainfall events. The midslope soils only responded to high rainfall events in the wet season. The riparian zone soils responded to both rainfall inputs and lateral seepage from the rivers

2.4 Groundwater in Kruger National Park

Based on a study by Fischer et al. (2009) the aquifers of the KNP mainly occur in crystalline hard rock lithologies. These crystalline rocks are usually fractured to various degrees and have relatively low hydraulic conductivities. Groundwater occurrence is mainly in water filled joints, fractures, faults, zones of weathering and structures such as dyke intrusions. The fractured aquifer systems of KNP mostly form anisotropic and heterogeneous groundwater bodies as the geometry and arrangement of fractures, joints and faults are influenced by various tectonic features. According to Wright (1992) as cited by Fischer et al. (2009) basement aquifers generally develop within the weathered residual overburden i.e. the regolith as well as in the fractured bedrock. Examples of groundwater exchanges commonly occur between saturated regolith and alluvium with adjacent underlying bedrock. As a result of this weathering profile and the relatively shallow depths to groundwater ranging mainly from 3m to 11m below the ground surface it is reasonably safe to expect mainly unconfined aquifers within KNP.

2.5 The approach for developing a hydrogeological conceptual model, application to the southern granite supersite

Robust groundwater model conceptualization includes the selection of the correct spatial and temporal scales at which data would be collected (Kresic and Mikszewski, 2013). A hydrogeological model describes various natural and

anthropogenic factors that govern and contribute to the movement of groundwater in the subsurface (Kresic and Mikszewski, 2013). The main objective would be to provide a visualisation concept of necessary text, pictures and animation where all the information about the site is logical and could be implemented at any point during project for decision making (Kresic and Mikszewski, 2013).

Depending on the groundwater system of interest the basic components included in the build up of a conceptual model would include in some instances mandatory aspects such as i.e. within unconfined aquifers the comparison of hydraulic gradients of nearby surface water bodies (stream, lakes, drainage ditches) with respect to groundwater movement (Kresic and Mikszewski, 2013). Other components would include geological descriptions, sources of water into the system, sinks within the system, physical boundaries, interpretation of geophysics data, geochemical information and previous findings or other data that are of relevance (Leon, 2003).

Special attention should be given to the distribution of heterogeneity in the subsystem. The heterogeneity can be a result of physical and/or chemical weathering. The heterogeneity of fractured rock aquifers can have important implications on how groundwater processes are measured. The fundamental characteristic of fractured rock aquifers has extreme spatial and temporal variability in hydraulic conductivity, and hence groundwater flow rate (Cook, 2003). Identification of the vertical flow distribution in aquifers is an important component of the conceptual model and understanding the spatial distribution of flow (Maurice et al., 2011).

2.6 Literature addressing site specific scale hydrogeological investigations adopted for the southern granite supersite:

2.6.1 Introduction to geophysical surveys: Electrical resistivity method

Various geophysical methods have been used widely to characterize and conceptualize hydrogeological studies (see Table 2.1). The electrical methods which are often used and consist of many methods, whereby some make use of

naturally occurring fields within the earth and other require an induction of currents penetrating the ground surface (Kearey and Brooks, 1984). The electrical resistivity method infers horizontal and vertical discontinuities in the electrical properties of the ground and commonly used in hydro-geological investigations (Kearey and Brooks, 1984). For instance, the provision of imagery depicting subsurface resistivity distribution proved to be vital in the characterization of regolith structures which was influential in weathering patterns at the edges of a lateritic plateau overlying ultramafic rocks in the north western region of New Caledonia (Southwest Pacific) (Beauvais et al., 2006). This technique also proved to be very useful to explore thick lateritic weathering mantles bearing stepped land surfaces capped with ferricrete over granitic bedrock in West Africa as it is able to instantaneously document the vertical and lateral variations of resistivity (Beauvais et al., 1999). In terms of obtaining a 2-D integrated image which targets the shallow (vadose zone) and deep (fractured rock), this method proved to be adequate (Loke, 1999). The 2D resistivity images produce an approximate picture of the true subsurface resistivity distribution and depend on the type of array used i.e. pole –pole array gives an extensive horizontal coverage, while the Wenner array decreases much more rapidly with an increase in electrode spacing. A study done by (Singh, 2005) added that the Schlumberger array used in the resistivity methods have been assessed for a correlation relationship for hydraulic permeability and transmissivity with electrical resistivity in a range with both alluvial (porous medium) and fractured hard rock aquifers.

Other applications of electrical resistivity surveys have hinted to provide a method that offers quick and relatively inexpensive imaging of subsurface resistivity patterns to a depth of several tens to hundreds of meters (Panek et al., 2010). Electrical resistivity surveys were used in combination with Spectral Analysis of Surface Waves (SASW) method to determine soil depths in a 500 m ranged Mediterranean hillslopes (Southern France) with increasing soil depths along the slope (Coulouma et al., 2011). Therefore ERT has multiple applications to investigate and gain insight into the subsurface information on fluid flow behaviour (both present and predicted) needed to assess the contamination impact of spills and plumes and the planning and assessment of remediation efforts

(Sandberg et al., 2002). In essence electrical resistivity surveys prove to be useful for geo-hydrological studies as many geological and hydrological features such as clay layers, variable moisture content, high salinity are fairly simple targets for electrical resistivity methods (Robinson et al., 2008) Furthermore, the instrumentation is relatively cost effective, robust and easy to operate.

Table 2.1 A comparison of the suitability of a measurement method for obtaining data to infer processes at the desired watershed scale (Robinson et al., 2008).

Type of geophysics techniques	Various watershed scales				
	Point /Profile/Transect	Catchment	Sub-watershed	Watershed	Sub-basin Basin
Airborne					
Microwave remote sensing	*	*	*	*	*
Airborne electromagnetic	*	*	*	*	*
Airborne time domain electromagnetic	*	*	*	*	*
Aeromagnetic	*	*	*	*	*
Ground based					
Time domain electromagnetic	*	*	*	*	*
Magnetotelluric	*	*	*	*	*
Audio magnetotelluric	*	*	*	*	*
Electromagnetic induction	*	*	*	*	*
Ground penetrating radar	*	*	*	*	*
Electrical resistivity imaging	*	*	*	*	*
Induced polarization	*	*	*	*	*
Electromagnetic water content sensors	*	*	*	*	*
Seismic	*	*	*	*	*
Gravity	*	*	*	*	*
Microgravity	*	*	*	*	*
Magnetic	*	*	*	*	*
Magnetic resonance sounding	*	*	*	*	*



2.6.2 General Electrical Resistivity Tomography (ERT) theory

Spatial identification of subsurface lithological characteristics can be characterized using electrical resistivity tomography geophysics technique. Electrical resistivity profiling provides valuable data of the subsurface geological material distribution and results depend on soil/rock properties, water content and salinity (Loke, 2004). According to Kearey and Brooks, (1984) electrical resistivity data is collected when an electrical current passes into the ground through a pair of current electrodes and the potential drop is measured across a pair of potential electrodes (see figure 2.5). The spacing of the electrodes controls the depth of penetration. At each setup an apparent resistivity is calculated on the basis of the measured potential drop, the applied current and the electrode spacing.

The resistivity of various materials and minerals is defined as the resistance in ohms between the opposite faces of a unit cube of the material or mineral, hence the SI unit of resistivity is the ohm metre (Ωm) (Kearey et al., 2002). Most rock-forming minerals can serve as insulators in that an electrical current can be transferred via the passage of ions in primary/secondary pores or cracks containing water (Kearey et al., 2002). Therefore secondary porosity such as fractures and weathering is a major control of the resistivity of granite/gneiss rocks, and that resistivity generally increases as porosity decreases (Kearey et al., 2002; Abem, 2010).

According to Kearey et al. (2002) the interpretation of ERT involves making the assumption that subsurface layers are horizontal and isotropic. However the assumption of isotropy can be incorrect for various subsurface layers, whereby geological features such as clay or shale would produce greater resistivity in a perpendicular direction than parallel to the direction of the feature. The effects of anisotropy are depth-dependent such as the reduction with depth of the degree of weathering, and the increase with depth of both compaction of sediments and salinity of pore fluids. Other geological features such as faults give rise to lateral inhomogeneities which can affect ERT interpretations.

However the resistivity of different type of soil and rock may vary seen in Figure 2.6. These variations in soil and rock types will reflect changes in physical properties (Abem, 2010). Whereby crystalline rock is highly resistive, apart from certain ore minerals, but weathering commonly produces less resistive clay-rich saprolite.

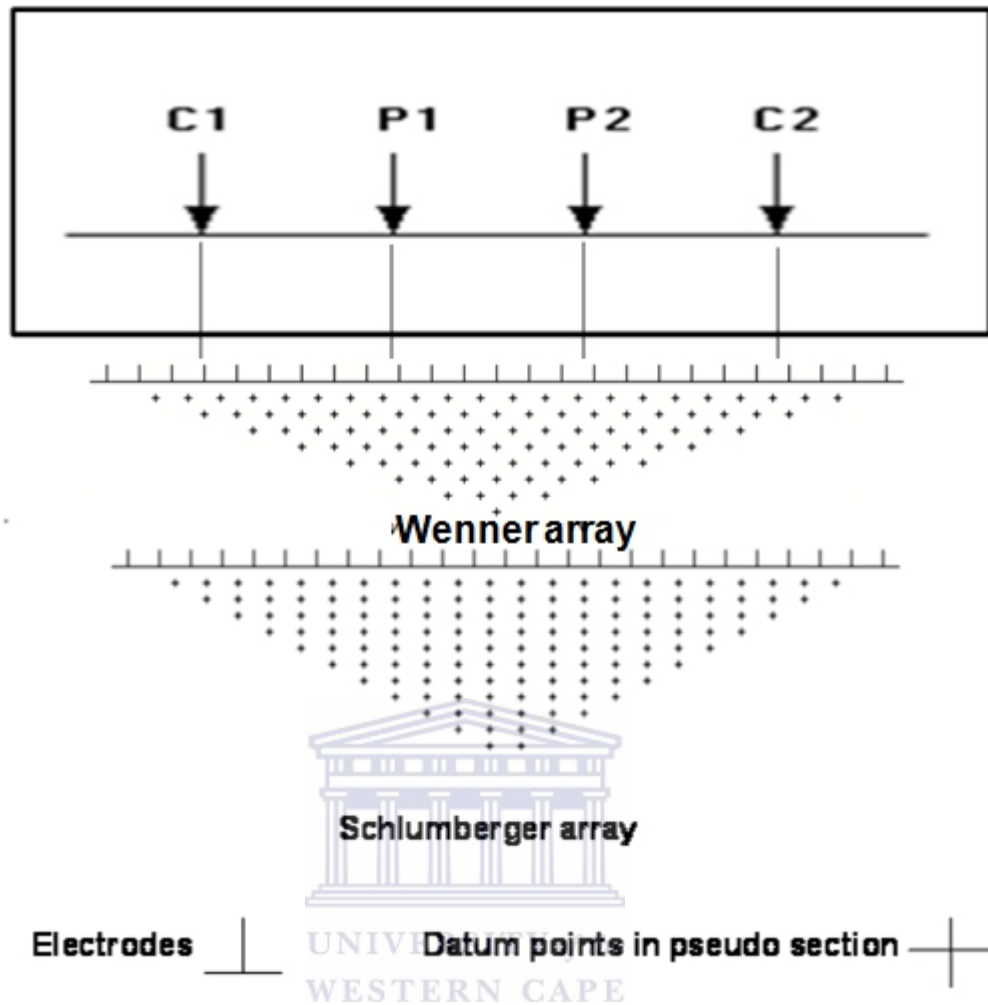


Figure 2.5 A conventional Wenner and Schlumberger electrode array, C1 and C2 – current electrodes, P1 and P2 – potential electrodes (Loke, 2004).

Furthermore, Loke, (1999) specifies the resistivity measurements calculated from an apparent resistivity (ρ_a) value:

$$\rho_a = kV/I \quad \text{Equation 2.3}$$

Where:

- $V=$ is the voltage
- $I=$ is the current; and
- $k=$ is the geometric factor which depends on the arrangement of the four electrodes.

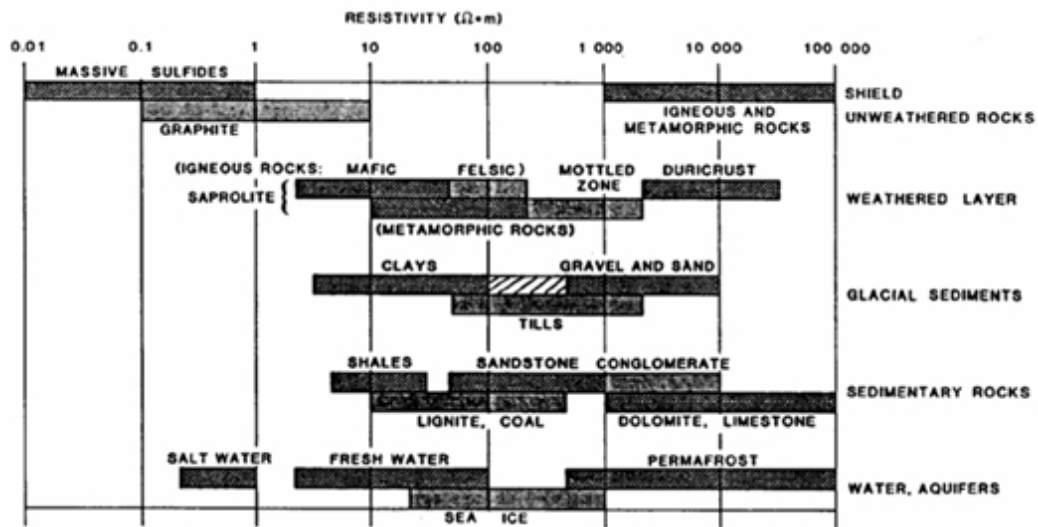


Figure 2.6 Typical resistivity values for geological materials (Abem, 2010).

2.6.3 ERT Electrode configurations

Many configurations exist and are used occasionally in specialized surveys but only two are commonly used, namely the Wenner and Schlumberger arrays (Kearey et al., 2002):

- The Wenner array is a simple setup with the current and potential electrodes being maintained at an equal spacing. The efficiency of using the Wenner array can be increased by using a multicore cable to which a number of electrodes are permanently attached at standard separations. However surveying with the Wenner array all four electrodes need to be moved between successive readings. This labour is reduced when using the Schlumberger array in which the inner potential electrodes have a smaller spacing in proportion to the outer current electrodes.
- The Schlumberger array is moderately sensitive to both horizontal and vertical structures, in areas where complex type of geological structures are expected. This array best suits an integrative study in that it provides adequate shallow resolution during wider spaced electrodes. The further spaced electrodes would accommodate resolution of the deeper subsurface.

2.6.4 2D Electrical resistivity profiling

2D electrical resistivity models can be formulated whereby horizontal and vertical changes in resistivity are taken into account. This is beneficial in the identification of property changes between the shallow and deep subsurface. According to Loke, (2004) generally the 3D model would provide the best results but the 2D produces accurate results and is more cost effective in comparison to the 3D model. These models are also known as pseudosections.

The pseudosection displays an approximate picture of the true subsurface resistivity distribution. However the pseudosections illustrate a distorted picture of the subsurface because the shapes of the contours depend on the type of array used as well as the true subsurface resistivity. Among the characteristics of an array that should be considered are:

- The depth of investigation,
- The sensitivity of the array to vertical and horizontal changes in the subsurface resistivity,
- The horizontal data coverage and
- The signal strength.

2.7 Borehole drilling

2.7.1 Introduction

Boreholes have been drilled for domestic and public supply, as well as for monitoring purposes throughout the world. The monitoring of boreholes can be split into 4 types namely, ambient, source, case preparation and research monitoring. Research monitoring involves the collection of data far beyond other monitoring types (Barcelona et al., 1983). The collection of this type of data is rigorous and demanding although constructed to obtain site specific research objectives (Barcelona et al., 1983). Therefore careful thought has to be given to the design of monitoring boreholes.

The basis for borehole design depends on factors such as expected yield, depth to aquifer productive zone and physical and chemical characteristics of the porous

medium and groundwater (see Figure 2.7). Pilot drilling and geophysical surveys are often used to drill the “ideal” borehole construction. These types of studies provide key information such as depth to and thickness of water bearing intervals in the aquifer, grain size, and permeability of the targeted intervals, physical and chemical characteristics of the porous media and groundwater (Kresic, 2007). The water bearing zone in which the borehole screen lined with gravel pack would be placed is an important factor since this is where groundwater enters the borehole (Kresic, 2007). The gravel serves as a filter and allows for the removal of formation material during borehole development. However certain boreholes drilled in stable rock are in most cases completed as an open borehole intersecting possible fractures to maximize borehole yield (Kresic, 2007). This type of borehole would be cased off in the upper unconsolidated section of the well and grouted to prevent possible contamination from the land surface or short-circuiting of groundwater along the boring walls (Kresic, 2007).

Subsurface material characterisation can be done using the South African National Standard (SANS) 633, reference 7114/633/DL, profiling and percussion and core borehole logging in South Africa for engineering purposes, Section 4.3.3.

According to Driscoll, (1986) there are four to five components that usually make up a drilling method namely, physical drilling, installation of casing, placing a well screen and filter pack, if required, grouting to provide sanitary protection and development of the well to ensure sediment free and maximum yield wells. Furthermore, these components may occur simultaneously depending on the method of drilling. Usually the drilling designs employed are based on geological setting and borehole depth. The diagram below illustrates factors influencing borehole design and construction.

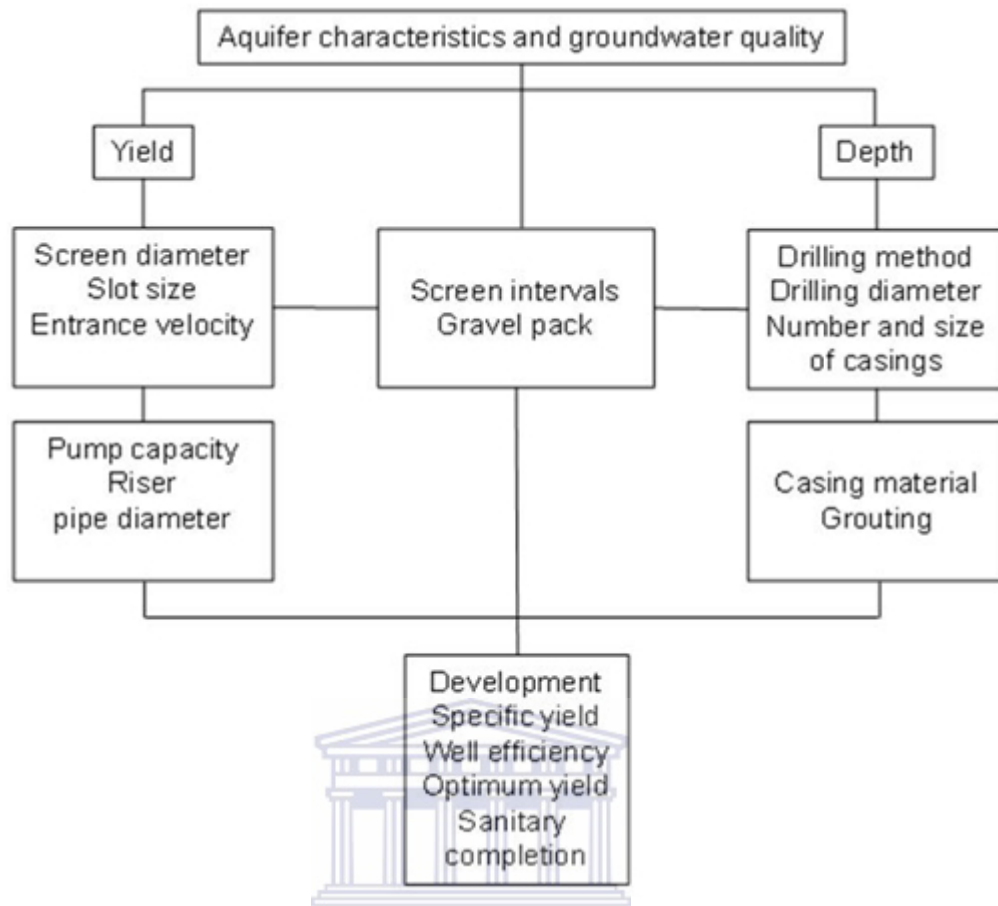


Figure 2.7 Diagram illustrating factors influencing the design of boreholes (Kresic, 2007).

2.7.2 Drilling methods applicable for hard rock environments

Various drilling methods could be suitable but it is important to understand the geological environment that is to be investigated and adjust the relevant drilling technique bearing in mind its physical limitations to the specific application (Australian Drilling Industry Training Committee Limited, 1997; see Table 2.2).

The air rotary method is most often used in hard rock environments. In this method a powerful air compressor provides the drilling rod and bit with a cutting force to penetrate unconsolidated and consolidated material. The cuttings are brought to the surface by compressed air and deposited on the ground surface for sampling. For remote environmental settings the air percussion drilling method is favourable due to the following advantages (Australian Drilling Industry Training Committee Limited, 1997):

- It is particularly suited to water well work as it permits collection of detailed information on each water horizon as it is penetrated, this provides characterization of boreholes.
- In general it can drill in a greater variety of lithologies than other drill types.
- It produces high quality samples in unconsolidated formations which is ideal for borehole logs and characterization of boreholes.

Table 2.2 A summary of various borehole drilling methods (Kresic, 2007).

Characteristics:	Drilled							
	Dug	Bored	Driven	Jetted	Percussion	Rotary		
Maximum practical depth in (m)	15	30	15	30	300	300	250	
Range in diameter in (cm)	1-6m	5-75	3-6	5-30	10-46	10-61	10-25	
Unconsolidated material:								
Silt	*	*	*	*	*	*	*	
Sand	*	*	*	*	*	*	*	
Gravel	*	*			*	*		
Glacial till	*	*			*	*		
Shell and limestone	*	*		*	*	*		
Consolidated material:								
Cemented gravel	*				*	*	*	
Sandstone					*	*	*	
Limestone					*	*	*	
Shale					*	*	*	
Igneous and metamorphic rocks					*	*	*	

2.8 Aquifer tests

2.8.1 Introduction

Osborne (1993) suggested that the interest has grown tremendously in groundwater as a resource and to develop it for public and domestic use. Therefore impact which other industries might have on groundwater quality such as mining and agriculture provided a need for pertinent studies to be conducted in order to understand these groundwater systems. One of the most reliable type of aquifer tests are a pump test which provide estimates of hydraulic properties and an aquifer. Slug tests are also used in certain site studies to provide initial estimates of hydraulic properties.

According to Kruseman and De Ridder (1994) an aquifer test is performed to ascertain one or more of the hydraulic properties of an aquifer. These aquifer

properties are one of the fundamental components that contribute to a more detailed conceptual site model (Kresic, 2007). The principle of a single-well aquifer test is that a well is pumped and the effect of this pumping or slug displacement on the aquifer's hydraulic head is measured in the well itself. The change in water level induced by the pumping is known as the drawdown. In such a test, a well that has been discharging for some time is shut down, and thereafter the recovery of the aquifer's hydraulic head is measured in the well and/or in nearby piezometers.

In order to ensure a successful aquifer test certain requirements have to be met (see Figure 2.8);

- Determination of the pre-pumping water level trend; and
- Controlled pumping rate and accurate water level measurements at precisely known times during both drawdown and recovery periods.

In the case of a slug displacement of the water level (falling hydraulic head), this can be seen as the drawdown phase of a pump test and once reaching its maximum displacement volume the water level will start to recover (Kresic, 2007).

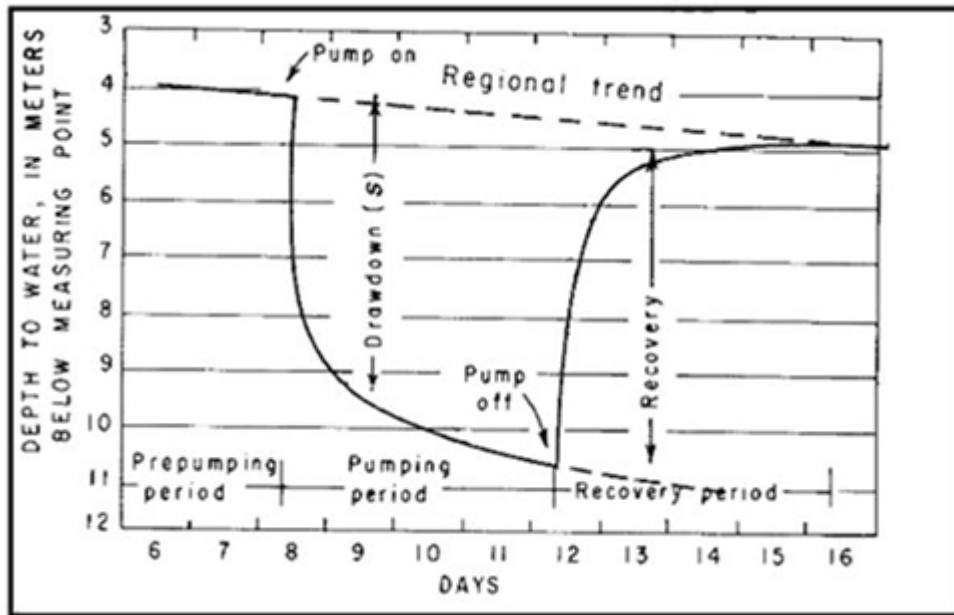


Figure 2.8 Trends in water level obtained during a pump test (Heath, 1983).

2.8.2 Single borehole pump out tests

A single borehole test (see Figure 2.9) can be conducted if the borehole yield is sufficient to endure drawdown conditions of at least 2 hours and occur within a single borehole with no measurements of nearby piezometers (Kruseman and De Ridder, 1994). Single borehole aquifer tests provide estimates of transmissivity values where cost and access preclude multi well aquifer tests (Halford et al., 2006), and it is commonly analysed with analytical solutions such as the Cooper - Jacob (1946) method because of its computational simplicity (Kresic, 2007). It's known that numerous factors influence the outcome of these hydrogeological tests and therefore the apparent ones can be incorporated into the analytical models to ensure relative simplicity (Ratej and Brencic, 2005).

2.8.3 Slug borehole tests

A slug test involves the displacement of a volume of water in a borehole. This typically occurs with the lowering down of a cylinder into the borehole which would cause an increase in head (Van Tonder and Vermeulen, 2005). This method serves as a good compromise for boreholes that do not yield sufficient water or a pump out test. Therefore if the rate of recovery or recession of the water level

is measured, the transmissivity or hydraulic conductivity of the borehole can be determined (Kruseman and De Ridder, 1994). Slug tests are usually conducted to estimate the hydraulic conductivity of a borehole or to determine the initial estimate of a borehole yield (Van Tonder and Vermeulen, 2005). Usually the Cooper method (Cooper and Jacob 1946) or the Bouwer and Rice method (1976) is used to estimate the hydraulic conductivity (K-value) or transmissivity (T-value) in the case of a slug test (Van Tonder and Vermeulen, 2005).

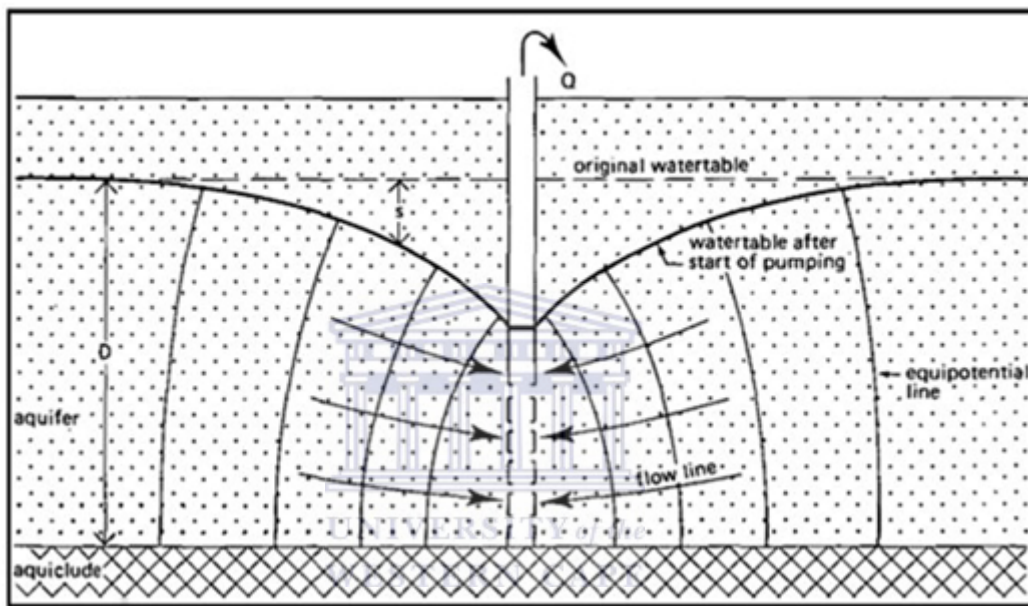


Figure 2.9 Schematic cross section of a single pumped borehole (Kruseman and De Ridder, 1994). D: Aquifer saturated thickness, S: Drawdown, Q: Discharge.

2.9 Analysis of aquifer test solutions

Most of the solutions used for the analysis of pump test data are usually based on derivatives of the steady state solution derived by Thiem in 1906 and transient solution developed by Theis in 1936 (Kresic, 2007). Although both of these solutions are based on various simplified assumptions and are only applicable to fully confined homogeneous aquifers, they are still used in unconfined aquifers because of computational simplicity and because of traditional inertia (Kresic, 2007).

These solutions provide the basis for other analytical solutions such as Cooper and Jacob (1946), Hantush (1962) and Bouwer and Rice (1976) which devise parameters such as transmissivity and storativity values of an aquifer. The assumptions of the analytical solutions are all based on the saturated thickness remaining constant over the area influenced by the aquifer test (Heath, 1983; Kruseman and De Ridder, 1994). However these parameters are known to be spatially highly variable within crystalline basement complex aquifers (Wright, 1992).

The method for analysing residual drawdown (pump test) data is often straight line methods which calculate the transmissivity from the slope of a semi-log straight line, i.e. from differences in residual drawdown (Kruseman and De Ridder, 1994). The Cooper-Jacob analytical solution is devised for confined aquifer system and could be used for unconfined aquifer systems provided the pump test drawdown does not exceed 25% of the unconfined aquifer saturated thickness (Kresic, 2007). A correction factor of the data is required should the drawdown of 25% be exceeded.

In wedge shaped aquifers the Theis/Cooper-Jacob assumption is not satisfied and other solutions needed to be used. The Hantush solution is devised for aquifer tests in wedge-shaped confined aquifers whereby the saturated thickness does not remain constant over the area influenced by pump test.

The analysis of slug test is based on the Bouwer and Rice (1976) solution whereby the transmissivity parameters of a borehole could be estimated.

2.9.1 Theis Equation (Kruseman and De Ridder, 1994)

The Theis equation which was derived from the analogy between the flow of groundwater and conduction of heat could be written as:

$$s = \frac{Q}{4\pi KD} \int_u^{\infty} \frac{e^{-y}}{y} dy = \frac{Q}{4\pi KD} W(u) \quad \text{Equation 2.4}$$

Where:

- s = the drawdown in meters measured in a piezometer

at a distance r in meters from the well

- Q = the constant well discharge in m^3/day
- KD = the transmissivity of the aquifer in m^2/day
- U = $r^2S/4KDt$ and consequently $S = 4KDtu/r^2$
- S = the dimensionless storativity of the aquifer
- t = the time in days since the pump started
- $W(u)$ = the exponential integral is written symbolically as $W(u)$, which in this usage is generally read 'well function of u ' or 'Theis well function'

From Equation 2.4 it can be seen that, if Drawdown (s) can be measured for one or more distances from the borehole (r) and for several values of Time (t), and if the well discharge Q is known, S and KD can be determined.

2.9.2 Cooper – Jacob Equation (Kruseman and De Ridder, 1994)

The Jacob method (Cooper and Jacob, 1946) is based on the Theis equation. After being rewritten and changed into decimal logarithms, the equation is reduced to:

$$S = \frac{2.30Q}{4\pi KD} \log \frac{2.25KDt}{r^2S} \quad \text{Equation 2.5}$$

Because Q , KD , and S are constant, the use of drawdown observations at a short distance r from the well, a plot of drawdown s versus the logarithm of t forms a straight line from which KD and S values could be estimated.

2.9.3 Pump test drawdown correction factor

The use of the Theis or Cooper-Jacob solutions are limited to confined conditions. A drawdown correction factor could be applied to a confined aquifer analytical solution used for an unconfined aquifer pump test on condition the total drawdown exceeds 25 percent of the saturated thickness of an unconfined aquifer (Jacob, 1944).

$$Sc(r, t) = S(r, t) - \frac{S^2(r, t)}{2D} \quad \text{Equation 2.6}$$

- $Sc(r, t)$ = corrected drawdown in meters

- $S(r,t)$ = observed drawdown in meters
- $2D$ = saturated thickness in meters prior to pumping

2.9.4 Hantush equation (Kruseman and De Ridder, 1994):

According to Hantush (1962) if the thickness of a confined aquifer varies exponentially in the flow direction (x-direction) while remaining constant in the y-direction the drawdown equation for unsteady-state flow takes the form and is written as follows:.

$$s = \left[\frac{Q}{4\pi K D_w t} \exp\left(\frac{r}{a} \cos\theta\right) \right] W\left(u, \left|\frac{r}{a}\right|\right) \quad \text{Equation 2.7}$$

- D_w = thickness of the aquifer at the location of the borehole
- Θ = the angle between the x-direction and a line through the borehole and a piezometer, in radius
- a = constant defining the exponential variation of the aquifer
- u = $\frac{r^2 S}{4KD t}$

2.9.5 Bouwer and Rice Equation (Kruseman and De Ridder, 1994):

To determine the hydraulic conductivity (K) and transmissivity (T) from a slug test, Bouwer and Rice (1976) presented a method that is based on Thiem's equation and written as follows:

$$Q = 2\pi K D \frac{h_t}{\ln\left(\frac{R_e}{r_w}\right)} \quad \text{Equation 2.8}$$

the hydraulic head subsequent rate of rise of dh/dt can be expressed as

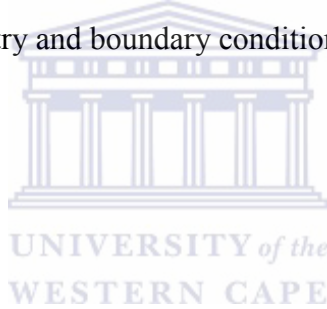
$$\frac{dh}{dt} = -\frac{Q}{\pi r_c^2} \quad \text{Equation 2.9}$$

therefore when integrating equation 6 and 7, K can be solved by means of the following equation

$$K = \frac{r_c^2 \ln \left(\frac{R_e}{r_w} \right)}{2d} \frac{l}{t} \ln \frac{h_o}{h_t} \quad \text{Equation 2.10}$$

- r_e = radius of the unscreened part of the well where the head is rising
- r_w = horizontal distance from well centre to undisturbed aquifer
- R_e = radial distance over which the difference in head h_o is dissipated in the flow system of the aquifer
- d = length of the well screen
- h_o = head in the well at time $t_o = 0$
- h_t = head in the well at time $t > t_o$

The geometrical parameters r_c , r_w , and d were used to derive empirical equations to relate R_e to the geometry and boundary conditions of the groundwater system.



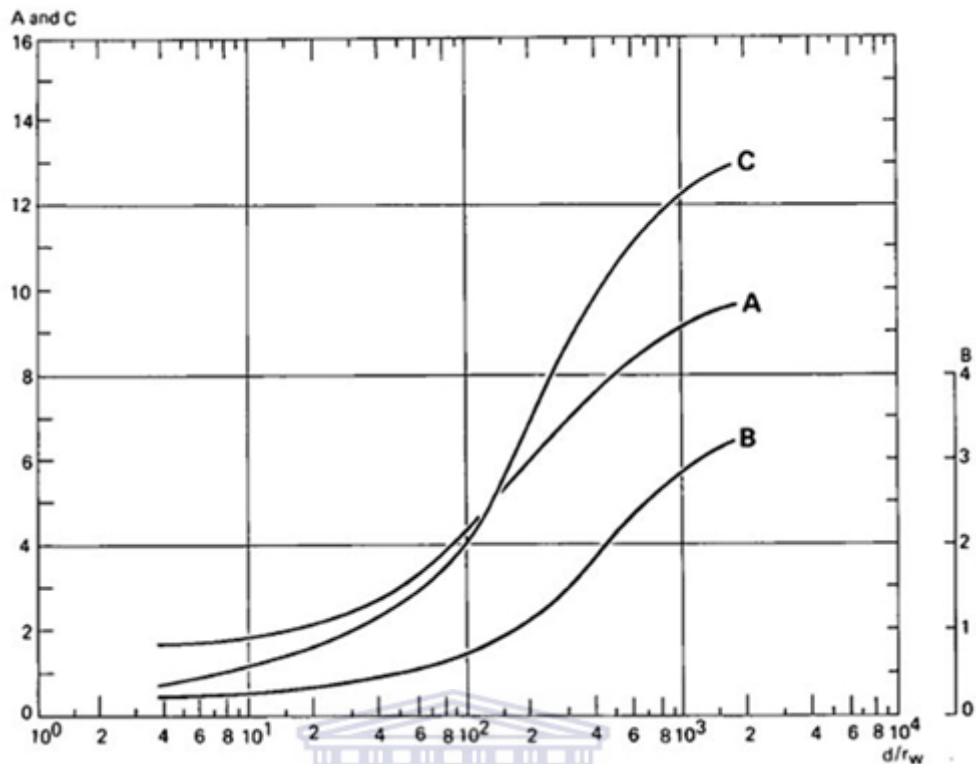


Figure 2.10 A graph devised by Bouwer and Rice (1976) to estimate a value for the R_e / r_w relationship.

2.10 Fluid logging

The relatively inexpensive specific conductance and temperature probes available for down borehole fluid logging makes it a valuable tool to investigate individual fractures, fracture zones, temporal changes in important in-situ hydrochemical parameters (i.e. specific conductance and temperature) to enhance the understanding of groundwater movement or permeable layers intersecting a borehole (Michalski, 1989; Doughty and Tsang, 2005). It is also known when employing this technique in deeper boreholes the change in temperature can be significant due to groundwater circulations in surrounding formations (Michalski, 1989).

2.10.1 Fluid Logging application techniques

The general application for fluid logging involves leaving a borehole undisturbed for at least a week before commencement of logging (Michalski, 1989). Fluid

logging may be performed under ambient (unstressed) conditions to identify the locations where water is flowing into (or out of) the borehole under natural gradients (possibly influenced by the borehole itself), or under stressed conditions with an induced high gradient into the borehole (Beauheim and Pedler 2009).

The use of fluid logging parameters such as temperature can infer fracture or flow zones whereby temperature profiles exhibit anomalies or sharp changes in the temperature profiles gradients (Anderson, 2005). A technique has been discussed by Maurice et al (2011) whereby a tracer solution was displaced throughout the borehole followed by logging the displaced solution with an in-situ multi-parameter sampler that was able to detect the solution. This method provided an indication as to where inflows and outflows of fractures are situated in the borehole. However, this method should not be carried out in low permeable formations due to the risk of the aquifer being contaminated or altering the ambient conditions of the groundwater system.

However there are sometimes misleading interpretation encountered from fluid logging such as thermal instabilities in low permeable boreholes and the contrast in specific conductance values between the open hole or screened section. The stagnant solid casing section is sometimes so distinct that the depth of the solid casing can be deduced from the specific conductance profile (Michalski, 1989).

Chapter 3

Site description

3.1 Introduction

The Kruger National Park is located within the Lowveld of north-east South Africa. The Lowveld boundaries consist of the footslopes of the Drakensberg Great Escarpment to the west and Lebombo Mountain/coastal plains of Mozambique to the east. It was estimated that more than 80% of KNP consists either of granitic or basaltic formations and the associated hillslope catenas host unique ecological assemblages at these scales. Granitic areas are often characterized by catenas consisting of sandy soils at the crest and clayey soils at foot slopes (Du Toit et al., 2003). These catenal elements are separated by a band of grey hydromorphic soils also known as the seepline (Du Toit et al., 2003). Granitic landscapes characteristically contain steep, short low order hillslopes and regular, long high order hillslopes (Cullum and Rogers, 2011).

3.2 Location

The study site is located within a 3rd order sub-catchment namely the southern granite (Stevenson Hamilton) supersite of the N'waswitshaka basin (see figure 3.1). The supersite sub-catchment has an area of 1.48km² and covers one of four newly delineated research supersites (Smit et al., 2013), within the Kruger National Park.

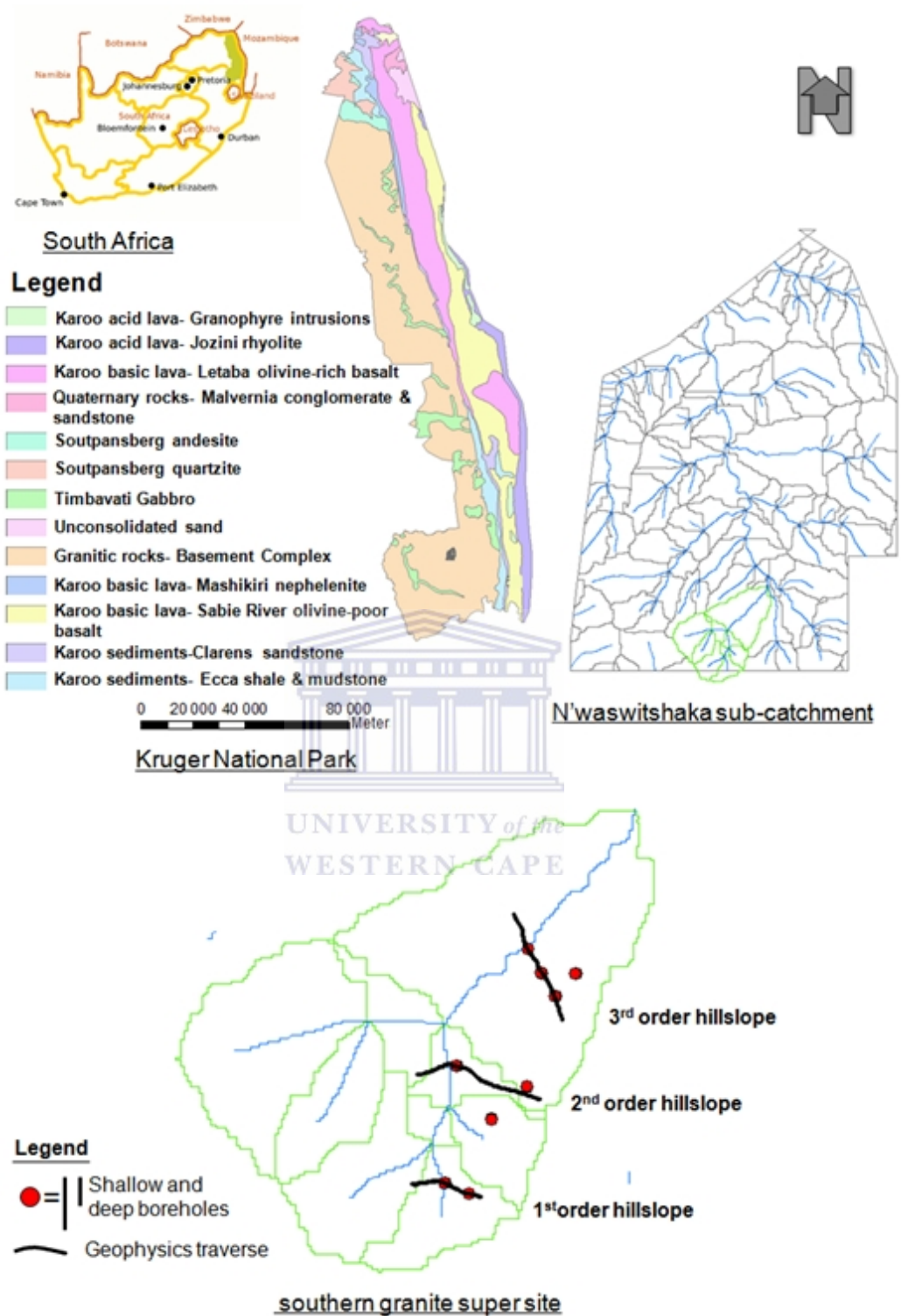


Figure 3.1 Location of the southern granite supersite with respect to the N'waswitshaka basin, Kruger National Park and north eastern South Africa.

3.3 Hillslope soil and vegetation

According to Van Zijl et al. (2011) the slope gradients of the hillslopes decrease from the headwater to higher order streams. The catchment of the first order hillslope has a poorly defined stream bed. The higher hillslope orders have footslopes that increase in prominence downstream. The crests and midslopes are convex straight and covered by soils of the Mispah (Ms), Glenrosa (Gs) and Cartref (Cf) forms in the catchments of 1st, 2nd and 3rd order hillslopes (see figure 3.2). The typical vegetation covering the crest and mid-slopes are broad leaved, moderately dense *Compretum apriculatum*, *Compretum zeyheri* bush veld and *Terminalia sericia* (mid-slopes) Occasionally soils of the Kroonstad form (2% of crest) and Sterkspruit form (1% of midslope) is recorded. Crest and midslope soils are of the Clovelly form and much deeper in higher hillslope orders. The footslope in the higher hillslope order catchments is longer and chemically weathered saprolite occasionally occurs under the prisma-cutanic B horizons. The footslopes are small (<5%) and has soils of the Sterkspruit (Ss), Milkwood (Mw), Bonhiem (Bo) and Mayo (My) soils with fine leaved, open *Arcacia gerrardii* and *Euclea divinorum* shrubveld, . The A horizon of the Sterkspruit soils is severely eroded (>90% of the area).

The Mispah (Ms), Glenrosa (Gs) and Cartref (Cf) soils of the lower order stream catchments are shallow with bleached A horizons. Darker coloured, non-bleached A horizons occur between the bleached soils where trees form small patches. Brighter coloured A horizons occur in patches of 3m diameter. The A horizons have coarse sand with 5% clay. Soils of the Sterkspruit form occur in straight concave shapes of the midslopes and in local depressions on the crest. The clay content of the prisma-cutanic B horizon is 15% to 40%. The soils of the lower order catchments are extremely hard setting. It is covered with grass and scattered patches of trees. Burrows of large animals 300 mm deep are localized. Thin clayey saprolite is recorded in some observations. Gley and redoximorphic features are extremely scarce and only recorded in a few localities in the valley bottom of the 3rd order hillslope.

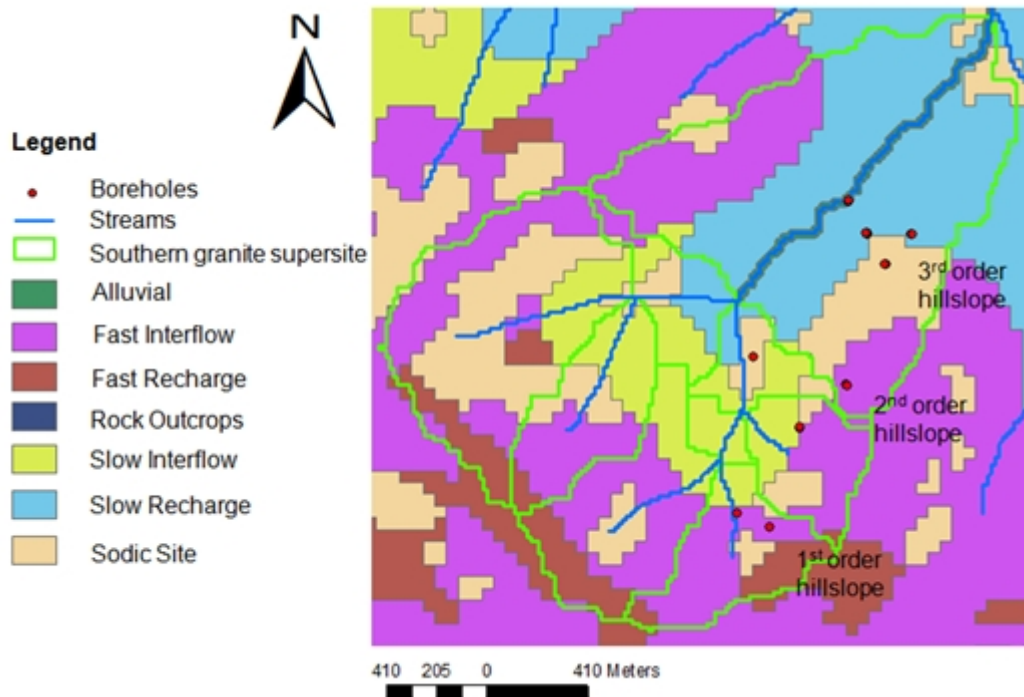
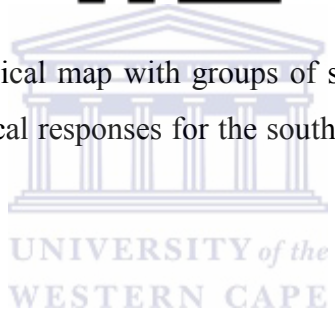


Figure 3.2 Soil hydrological map with groups of soils discussed above based on their expected hydrological responses for the southern granite supersite (Van Zijl, 2013).



3.4 Topography

The southern granite supersite falls within the greater Skukuza land system which consists of moderately undulating plains (Venter et al., 2003). The topography for the supersite ranges from 338-384mamsl with the highest elevated part of the catchment being the 1st order hillslope and decreases towards the 3rd order hillslope (see Figure 3.3). It will be discussed later in chapter 6 that the general groundwater level flow direction tends to mimic the topography of the supersite catchment, following the typical assumptions of groundwater flow direction on a regional scale (Kresic and Mikszewski, 2013).

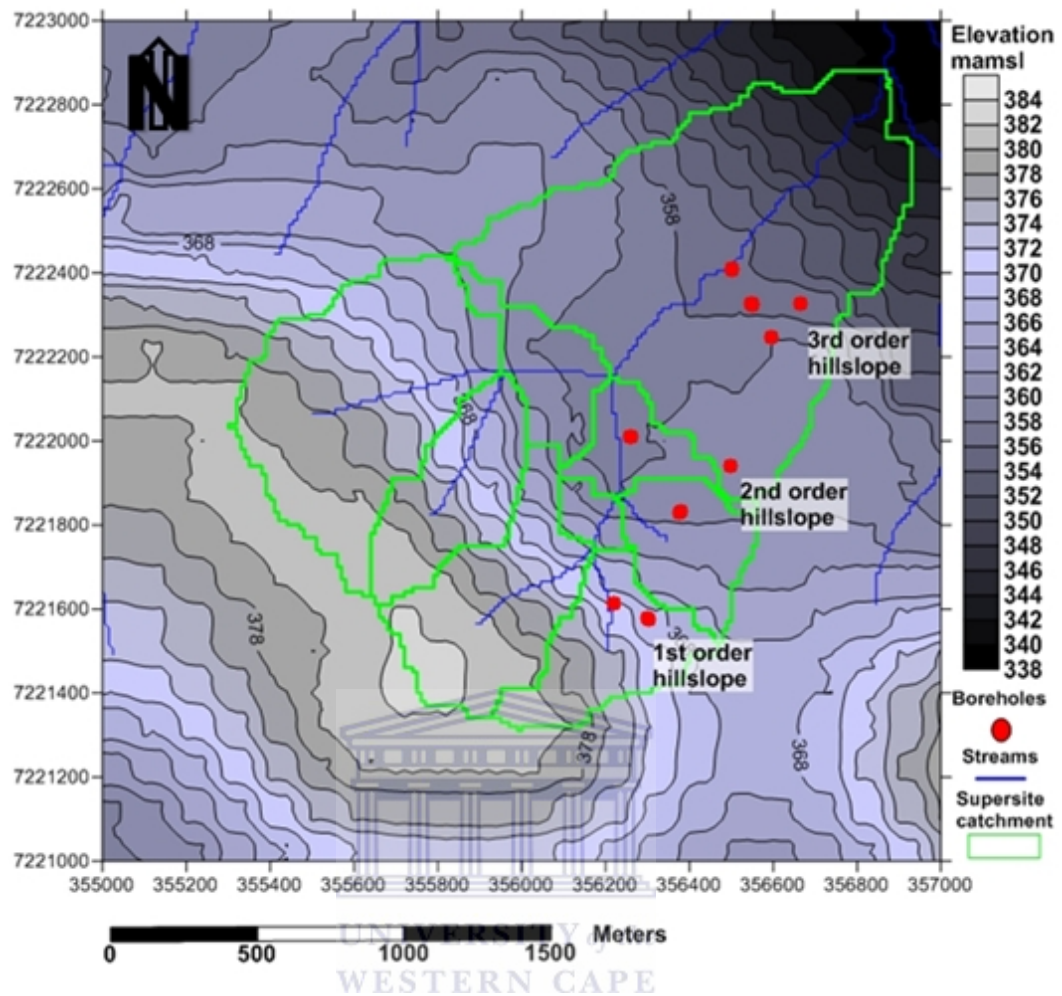


Figure 3.3 Topography across the southern granite supersite catchment.

3.5 Climate and rainfall

The Köppen climate classification BSh class (Kottek et al., 2006) correlates with KNP consisting of two climatic zones (Venter et al., 2003). The south and central part containing the southern granite supersite fall within the lowveld bushveld zone which estimates an average annual rainfall of between 500-700mm (Venter et al., 2003). This annual range roughly correlates to the range of annual rainfall distributed on the southern granite supersite given it was quite a wet hydrological season. There is a strong rainfall gradient which decreases from west to east and south to north concentrated between October to April (Venter et al., 2003, Gertenbach, 1980). For site specific perspective on rainfall, a daily rainfall graph for the southern granite supersite hydrological season of September 2012 to September 2013 has been plotted. Three main rainfall sequences or depth of

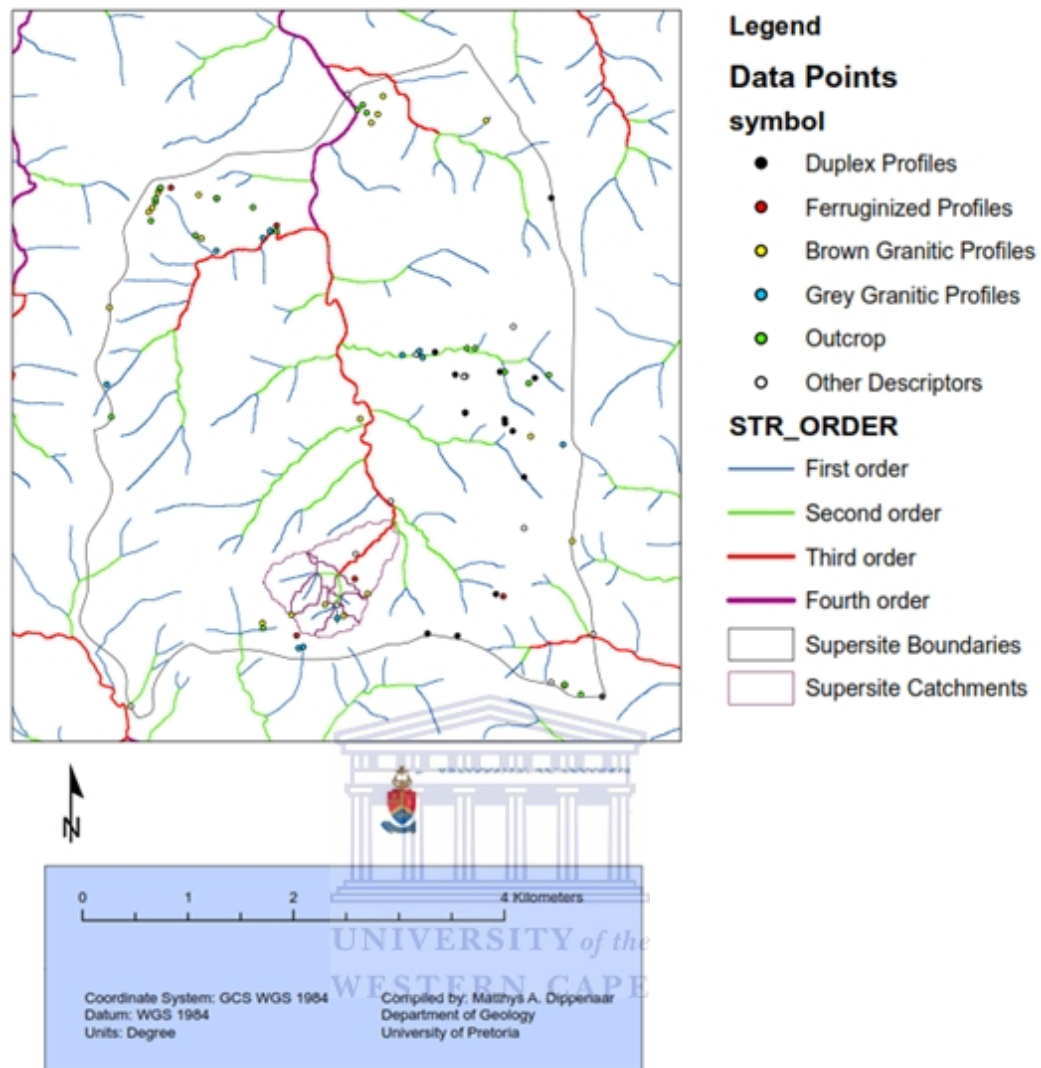


Figure 3.5 Locations of survey samples taken for the geological characterisation of the southern granite supersite (Dippenaar, 2013).

Chapter 4

Materials and Methods

4.1 Introduction

The selected study site has no record of available groundwater, surface water and vadose zone data. Therefore, a reconnaissance study was done in order to develop an initial hydrogeological conceptual model upon which favourable borehole drilling targets on the supersite was established. To achieve the study objectives, specific methodologies were carried out to determine groundwater distribution within the southern granite supersite catchment. A catchment scale map of relevant instrumentation positions could be seen in Figure 4.10 and a naming table of the boreholes and stream level loggers are shown in Table 4.1.

4.2 Site or transect selection for Electrical Resistivity Tomography (ERT) surveys

In order to spatially conceptualize subsurface geological characteristics, ERT surveys were conducted during the dry season (2 June-2 July 2011) in the southern granite supersite. This information was used to identify prospective positions to explore for groundwater along the 1st, 2nd and 3rd order hillslopes. These transects/traverses were preselected based on desktop analysis of evident geological features from aerial imagery using Google Earth © and relative ease of access from tourist and management roads within the KNP, for both geophysics equipment and groundwater-surface instrumentation installation and maintenance. However due to logistical challenges the ERT surveys were only conducted in June 2013 for the triangulation boreholes. This was done after the drilling of these boreholes to provide consistency in the investigative method of the groundwater system.

4.3 ERT survey method

Firstly, a protocol would be determined using the ABEM SAS 1000/4000 software to provide insight as to which electrode spacing should be used. This provides information on the depth at which resolution 2D resistivity profiles would be visible. The electrode spacing of 2m for the short protocol and 4m for the long protocol was chosen as it would accommodate both shallow and deep subsurface visualization for southern granite supersite. The ERT setup was then placed on either side of a 1st, 2nd and 3rd order stream, and extended towards the crest of the hillslope of interest using the Schlumberger array as it provides slightly more data points and a greater subsurface visualization both vertically and horizontally than the other arrays (see Figure 2.5). Upon installation of the ERT equipment (see Figure 4.1) an electrical current was transmitted into the ground through two current electrodes and measuring the resulting voltage difference at two potential electrodes (Loke, 1999). The apparent resistivity was then converted to a modelled true resistivity plotted in a 2D pseudo-section using the RES2DINV software (Loke, 2004).

The modelling software requires the following procedure: Firstly the raw data file from the SAS 1000/4000(.s4k file) would be converted to a data file compatible for the inversion process in RES2DINV (.dat file). The data file would be imported for smoothing to produce a robust modelled 2D inversion resistivity profile or pseudo-section. The pseudo-section would then be topographically corrected using elevation data obtained using a Trimble differential GPS system to provide detail of the hillslopes.

The model discretization involved an inversion procedure whereby bad data points or noisy data would be removed to reduce the RMS error (Loke, 2004). An inversion software coupled with the resistivity technique of choice would process data using the Jacobian matrix and forward modelling procedures to produce true geo-electrical 2D models of the subsurface lithological characterization (Loke, 2004).

The interpretation involved an informed estimation of at which depth the weathering/hard rock interface and groundwater level could be encountered. This consisted of assigning resistivity values to a specific subsurface material or mineral (refer to Figure 2.6 in Chapter 2 for resistivity values for various materials or minerals) and at the same time taking into consideration at which depth these resistivity values are encountered. Based on previous relevant studies, ground truthing and the theory behind electrical resistivity surveys for these particular geologies, possible water levels would be associated with a continuation or sharp change in low resistivity values relatively close to the surface. The high resistivity values would be associated with low permeable material, possibly hard rock. This information was then used to infer the development of an initial hydrogeological conceptual model consisting of estimated subsurface lithological descriptions i.e. depth to weathering and hard rock, depth to groundwater level and piezometric borehole positions targeting specific hillslope components i.e. crest, midslope or riparian zone.



Figure 4.1 An Abem Signal Averaging System (SAS) 1000/4000 Terrameter and switching unit powered by a 12 volt battery with 64 steel probes and clips to connect to four 100m cables with 21 take outs on each to form electrodes.

4.4 Air Percussion drilling

Air percussive drilling (Figure 4.2) is employed in hard rock such as granite, basalt and for extremely abrasive softer rock such as sandstone (ICRC, 2010; Vagins and Simons, 1964). Therefore given the environmental setting at hand air percussion drilling was favourable in that it permitted a collection of detailed information on each subsurface material when penetrated such as depth to weathering, hard rock, water strikes. This provided a lithological characterization of the boreholes.



Figure 4.2 Super rock 5000 air percussion rig on a 10 ton 6x6 truck with 24 bar 900CFM compressor used for drilling the southern granite supersite boreholes.

4.4.1 Air percussion drilling method

Nineteen (19) borehole positions were drilled along the geophysics traverses which was intended to explore the shallow (weathered) and deep (hard rock) subsurface of the riparian, mid-slope, crest and triangulation position of each hillslope (see Figure 4.3 for shallow and deep borehole construction). Due to a mechanical failure which resulted in the burning down of the drilling rig on the 3rd order hillslope and several technical failures with the replacement drilling rig resulted in only priority boreholes being drilled. Other limitation was that the drilling was confined to operations during the dry season. Therefore only the riparian, crest and triangulation position boreholes of the 1st and 2nd order hillslopes were drilled.

The Department of Water Affairs (DWA) Polokwane drilling division procedure would include ensuring that the rig was correctly positioned since the drilling rig was dependent on hydraulic support. Once the rig was levelled a hammer head of 1m in length and drill bit of 250mm diameter was drilled into the subsurface. This could be seen as a pre-drilling procedure which was done in order to insert a starting casing of 250mm diameter to ensure the prevention of the shallow subsurface material from caving in.

Upon installation of the starting casing a 165mm diameter drill bit would be attached to the hammer with which the remainder borehole depth was drilled. 6m steel rod extensions were attached to the hammer head to enable drilling of boreholes at various depths. When the boreholes were drilled to the desired depth a 250mm drill bit was attached to the hammer head whereby the borehole would be reamed to a particular depth depending on the weathered/hard rock interface, to enable the insertion of steel casing of 6m in length and 165mm in diameter to case off the unconsolidated/weathered material for the deep borehole construction. The shallow borehole construction was drilling only into the unconsolidated/weathered material and cased off with 165mm solid and perforated casing. Once the casing has been installed a standard cement sanitation seal of 1m diameter and 0.5m depth would be placed around the borehole.

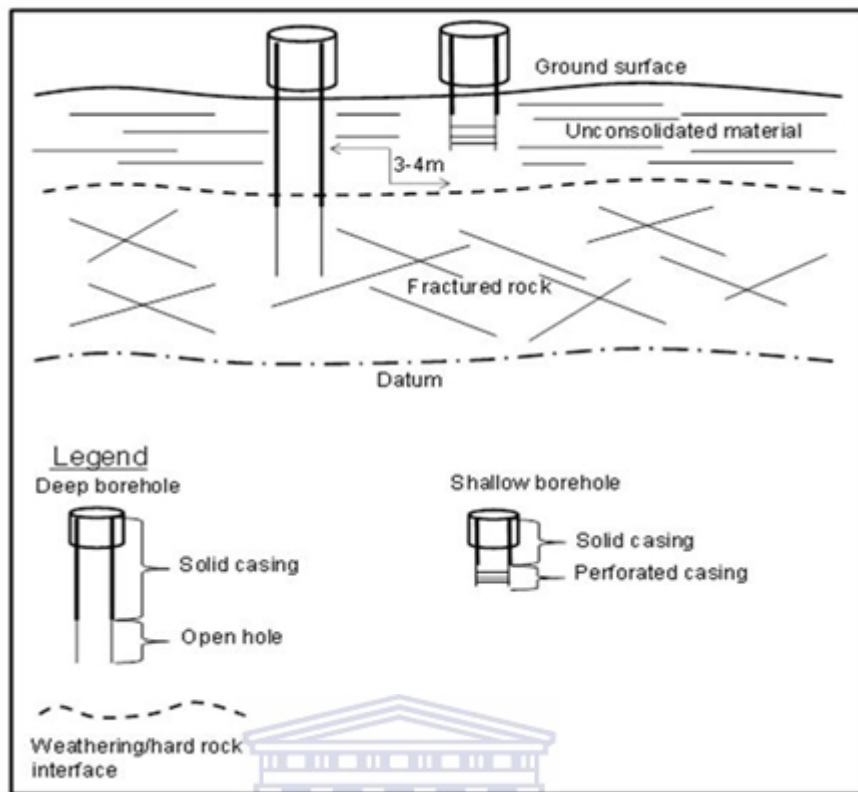


Figure 4.3 Schematic diagram of the piezometric or shallow and deep borehole construction.

UNIVERSITY of the
WESTERN CAPE

4.4.2 Borehole lithology logs

To understand the lithological description of boreholes drilled using the percussion method, a classification of the subsurface material was required. The subsurface material was drilled every meter and brought to the surface by means of compressed air and placed in rows seen in Figure 4.4.

Once the drilled logs were brought to the surface, grab sub-samples were collected and transported to the Geology department laboratory at the University of Pretoria for identification analysis. The analysis involved using the Guidelines for Soil and Rock Logging in South Africa which apply methodology set out in the South African National Standard (SANS) 633 profiling and percussion and core borehole logging in South Africa for engineering purposes (Brink and Bruin, 1990). These guidelines took into account properties such as texture, colour,

mineral composition of the lithology log samples in order to categorize weathered and hard rock material.

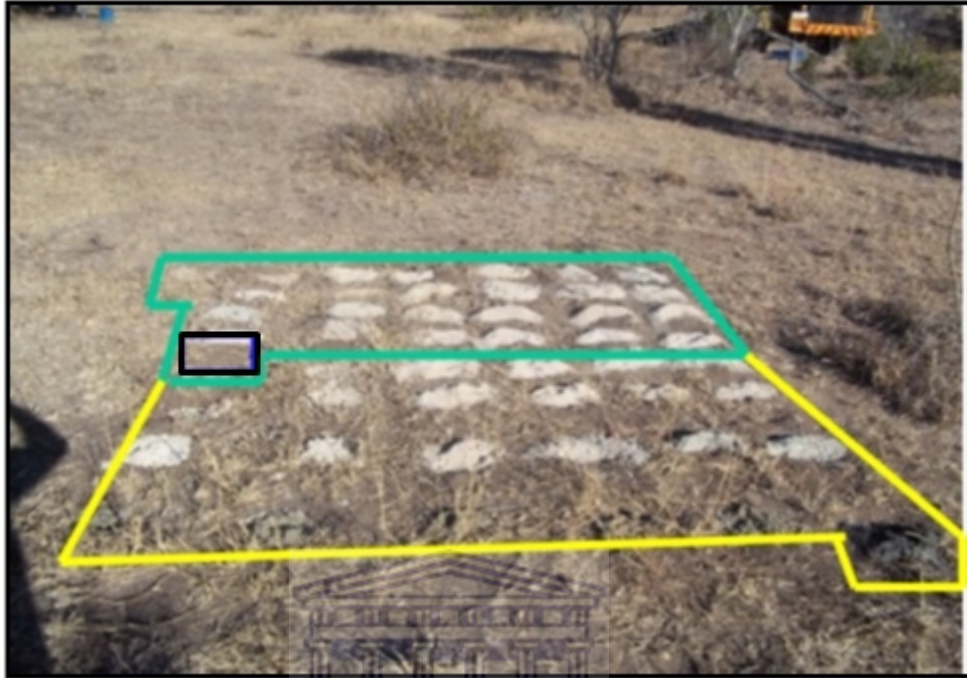


Figure 4.4 Borehole lithology log of weathered material (green highlighted section) and hard rock material (yellow highlighted section). The black highlighted section indicates the depth at which a water strike was encountered.

4.5 Monitoring

4.5.1 Groundwater level trends

The groundwater flow gradient is dependent on the difference in groundwater hydraulic head divided by the distance (L) between the hydraulic heads as illustrated in Figure 4.5. The schematic demonstrates the hydraulic gradient (I) from BH2 towards BH1 as groundwater always flows from a higher hydraulic head ($H1$) towards a lower hydraulic head ($H2$). In order to determine hydraulic gradients, groundwater levels were measured using a Solinst water level meter seen in Figure 4.6 for time series observations in water level response to daily rainfall. These water levels were then differentially corrected above sea level using a Trimble GPS in order to interpolate between the actual hydraulic head of

boreholes, hence the drilling of triangulation boreholes which was primarily used to provide the groundwater flow direction.

The water levels were also used to plot hydraulic heads between the boreholes and barometric pressure corrected stream level loggers (Figure 4.7) with the use of a geo-statistical method kriging. This was done in Surfer version 9 which takes into consideration spatial variance, location and sample distribution to produce a spatial groundwater level flow distribution map. These gradients were then used to infer potential recharge (generally shallower water levels) and discharge/surface water interaction processes. The water levels were measured in both the shallow and deep boreholes to determine the possibility of two aquifers interacting (hard rock and weathered) and whether they have differences in flow distribution and responses within the catchment. The water levels were taken on a bi-weekly basis during the generally higher rainfall period (October 2012 – February 2013) and on a monthly basis during the generally lower rainfall to dry periods (June 2012 – September 2012) and (March 2013 – September 2013)

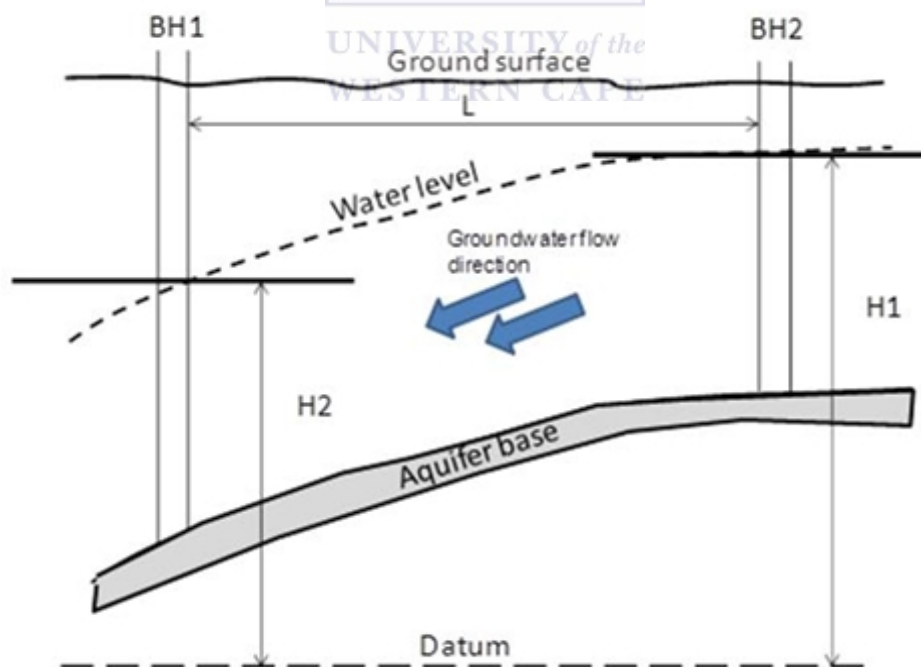


Figure 4.5 Schematic representation of groundwater hydraulic heads ($H1$ and $H2$) and gradient (Kresic, 2007).



Figure 4.6 Use of a SolinstTM water level meter to measure groundwater level at an error of ± 0.02 m.

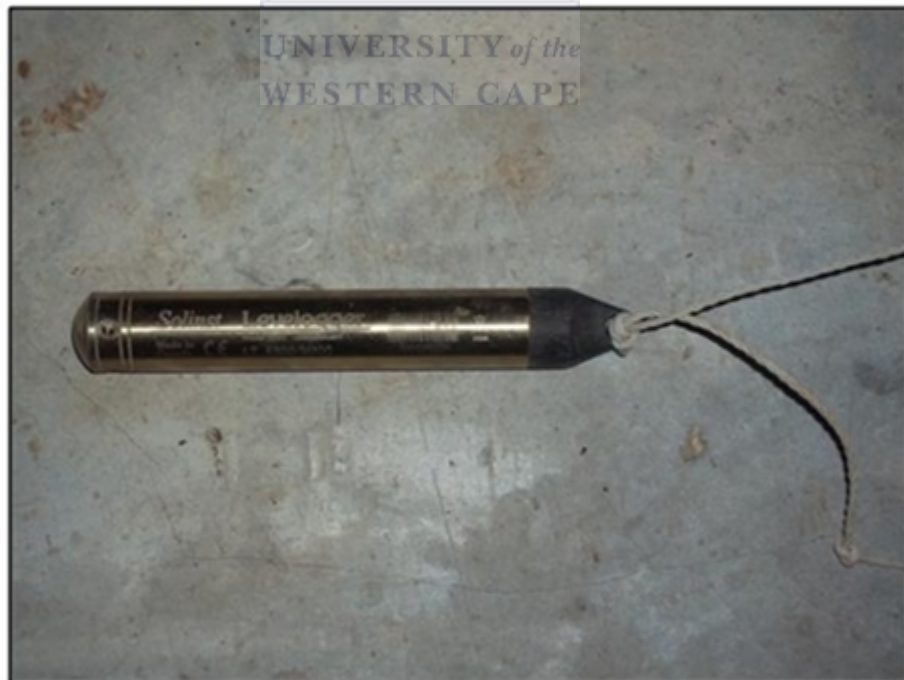


Figure 4.7 A SolinstTM level logger used to measure water level changes in the streams.

4.5.2 Fluid logging

The primary objective of the fluid logging was to provide in-situ borehole parameters of specific conductance (SC) and temperature with depth which would serve as spatial baseline data across the catchment. The secondary objective of the fluid logging was to log the boreholes under ambient conditions over different seasons to observe possible changes in the parameters. Change in parameters could infer active groundwater flow zones, flow direction and possible changes in the flow rate within fracture zones for borehole characterisation. This technique involved lowering a YSI (Yellow Spring Incorporated) 600XLMD sonde multi-parameter in-situ monitoring device into the boreholes (see Figure 4.8). The device logged at 2 second intervals in order to record these parameters approximately 0.25m with every drop. These in-situ parameters provided an additional layer of information to the groundwater conceptualization when referring to these parameters spatially across all boreholes such as possible changes in the trend over different seasons. The SC and temperature in-situ parameters were plotted spatially using a geo-statistical method of kriging within the software package Surfer version 9.

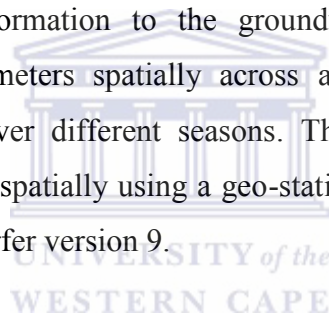




Figure 4.8 Yellow Spring Incorporated (YSI) 600XLMD sonde multi-parameter in-situ monitoring device.

4.5.3 Meteorologic data

This data was collected by a Davis weather station during the hydrological year of September 2012-September 2013. This station stored variables in the following SI units:

- Rainfall (mm): using a Davis vantage pro2 tipping bucket rain gauge calibrated to 0.1mm
- Temperature ($^{\circ}\text{C}$) and Relative Humidity (%): using a Davis vantage pro2 temperature sensor (PN Junction Silicon Diode) and relative humidity sensor (Film capacitor element).
- Wind Speed (m/s): using a Davis vantage pro2 solid state magnetic sensor.
- Solar Radiation (W/m^2): was also collected with an integrated pyranometer, all data were recorded on a 15min time step.

The Integrated Sensor Suite (ISS) houses these sensors and communicates with a console which provides a display of the logging variables. The console is interfaced with an Asus laptop using Weatherlink™ software to download the logging variables.

The rainfall data was manipulated into a combination daily rainfall intensity totals, cumulative rainfall and Antecedent Precipitation Index (API) to observe which rainfall sequences or depth of rainfall over a particular time period contributed to groundwater level responses across the catchment. Furthermore, this data provided additional understanding of the groundwater conceptual site model such as recharge.

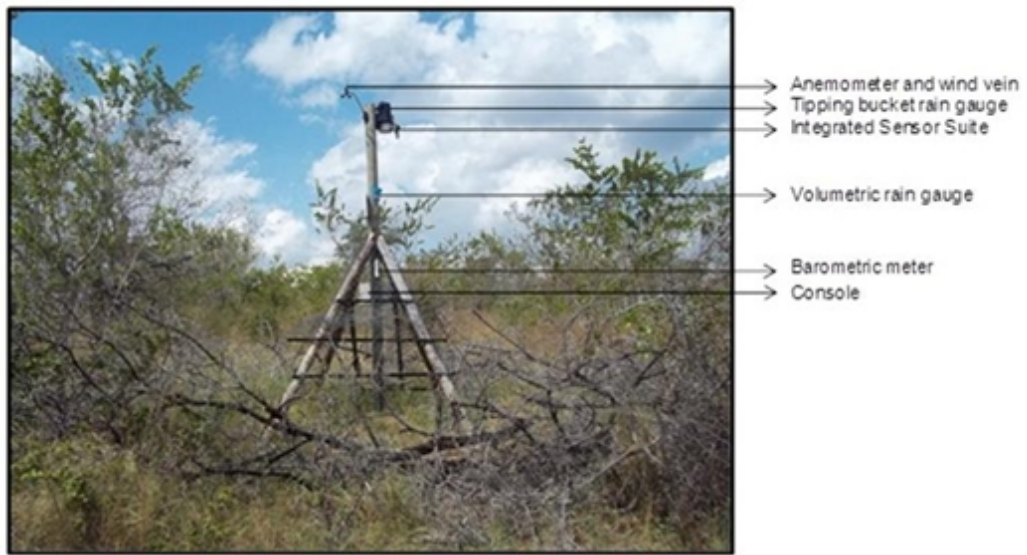


Figure 4.9 Southern granite supersite weather station.

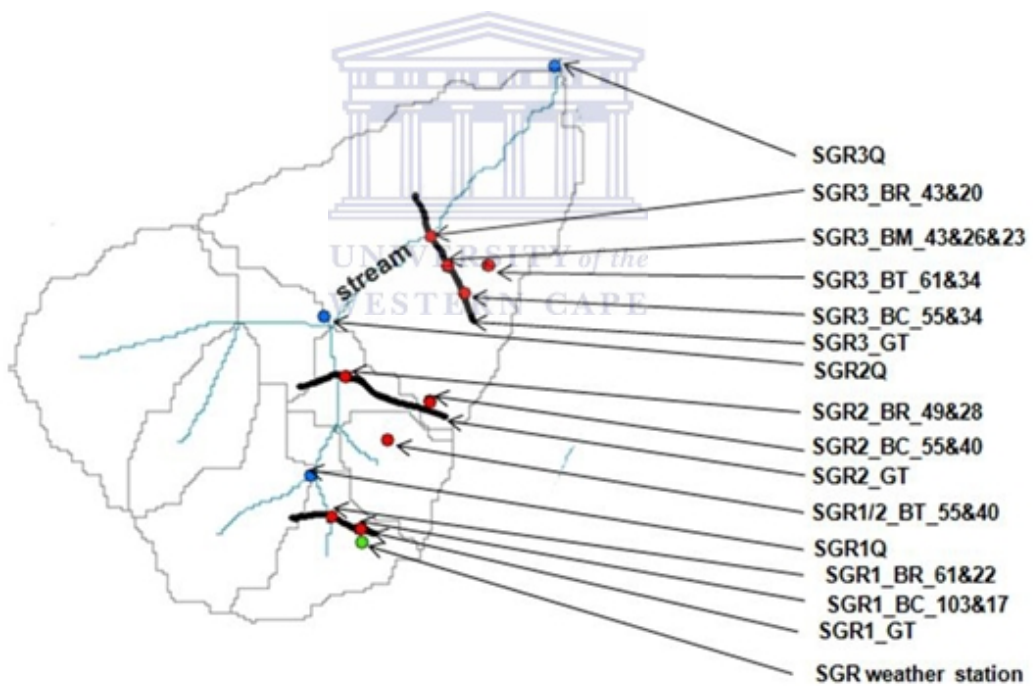


Figure 4.10 Location of site instrumentation (and black lines represent ERT traverses).

Table 4.1 Site names and their respective hillslope/stream order positions within the southern granite supersite.

Borehole Name	DWA Code	Site Description
SGR3_BR_43	MP190001	Southern Granite 3rd order riparian borehole 43m
SGR3_BR_20	MP190002	Southern Granite 3rd order riparian borehole 20m
SGR3_BM_49	MP190003	Southern Granite 3rd order midslope borehole 49m
SGR3_BM_26	MP190004	Southern Granite 3rd order midslope borehole 26m
SGR3_BM_23	MP190005	Southern Granite 3rd order midslope borehole 23m
SGR3_BT_61	MP190006	Southern Granite 3rd order triangulation borehole 61m
SGR3_BT_34	MP190007	Southern Granite 3rd order triangulation borehole 34m
SGR3_BC_55	MP190008	Southern Granite 3rd order crest borehole 55m
SGR3_BC_34	MP190009	Southern Granite 3rd order crest borehole 34m
SGR2_BR_49	MP190010	Southern Granite 2nd order riparian borehole 49m
SGR2_BR_28	MP190011	Southern Granite 2nd order riparian borehole 28m
SGR2_BC_55	MP190012	Southern Granite 2nd order crest borehole 55m
SGR2_BC_40	MP190013	Southern Granite 2nd order crest borehole 40m
SGR1_BR_61	MP190014	Southern Granite 1st order riparian borehole 61m
SGR1_BR_22	MP190015	Southern Granite 1st order riparian borehole 22m
SGR1_BC_103	MP190016	Southern Granite 1st order crest borehole 103m
SGR1_BC_17	MP190017	Southern Granite 1st order crest borehole 17m
SGR1-2_BT_61	MP190018	Southern Granite 1st and 2nd order triangulation borehole 61m
SGR1-2_BT_36	MP190019	Southern Granite 1st and 2nd order triangulation borehole 36m

Stream level logger name	Site Description
SGRQ1	Southern Granite 1st order streamflow level logger
SGRQ2	Southern Granite 2nd order streamflow level logger
SGRQ3	Southern Granite 3rd order streamflow level logger

4.6 Aquifer properties characterisation

4.6.1 Pump test

A single-borehole pump test was conducted in an effect to lower the water level or hydraulic head in the borehole. During pumping the water level is measured in the borehole itself. The change in water level induced by the pumping is known as the drawdown. The pumping from the borehole is shut down after completion of the drawdown phase, to record the recovery of the boreholes hydraulic head. Refer to Figure 2.8 in chapter 2 for a schematic of a pump test process.



Figure 4.11 Equipment used during a pump test.

4.6.2 Slug test

In performing a slug test, the static water level in a borehole was suddenly lowered or raised. This was done by rapid displacement of borehole water by lowering a closed cylinder/slug into a borehole. When the cylinder was lowered it replaced its own volume of water within the borehole, thus increasing the pressure in the borehole. Once the water level has dropped to its reference point, the slug would be removed and as a result the water level would drop and the rate of recovery or recession of the water level was measured. The (T) or (K) of the borehole was then determined by using the displacement measurements of the water level over time and boreholes construction detail.



Figure 4.12 Equipment required to perform a slug test.

4.7 Data analysis

4.7.1 Pump test

Once the drawdown data, recovery data and constant pump rate has been collected the borehole T would be calculated. The Cooper-Jacob (1946) equation (Eq 2.5) which was selected provided that the correction factor (Eq 2.6) discussed in chapter 2 was applied for the determination of transmissivity (T) values for a pump test. These pump test were restricted to the boreholes that could satisfy the assumptions of a pump test and the Cooper-Jacob or Hantush solution. If the assumptions were not met for a pump test, for example a minimum pump drawdown test of >2 hours, and/or a constant pump rate achieved then slug tests would be performed. The Cooper-Jacob (1946) or Hantush (1962) T would be calculated by entering data such as the drawdown, recovery, pump rate and

borehole construction details into an MS Excel macro devised by Van Tonder et al., (2001) or the software package devised by Duffield (1996-2007).

4.7.2 Slug test

Once the drop or recession in water level was measured over time, the data was then analysed using the Bouwer and Rice (1976) method for determining T or K. This was calculated in a MS Excel macro by Halford and Kunainsky (2005). The Bouwer and Rice (1976) equation also included the boreholes construction details such as depth to initial water level, final borehole depth, borehole radius and length of screen section.



Chapter 5

Results and discussion: Spatial characterisation

5.1 Introduction

In order to understand the role of groundwater within the southern granite supersite, a spatial characterisation of the hydrogeological regime will be discussed in detail. This would comprise developing an initial conceptual model at the hillslope scale of each order. Electrical Resistivity Tomography (ERT) surveys were used as a scoping tool to provide insight into the deep and shallow groundwater systems such as estimated to groundwater level and lithological distribution. The initial conceptual model which was drawn from these reconnaissance studies. These ERT surveys were then revised to represent the actual environmental setting on completion of the following activities:

- borehole log samples of the subsurface to provide a lithological description at each hillslope order,
- blow out yields for an initial estimate of aquifer properties,
- pump and slug tests for a more refined estimate of the aquifers properties such as transmissivity and/or hydraulic conductivity,
- hydraulic head of groundwater and surface water levels which would infer the flow path distribution and potential interaction between the groundwater and surface water regimes.

5.2 Geophysical and borehole lithology log characterisation

To characterize the groundwater component, electrical resistivity tomography (ERT) surveys were conducted during the dry season (June- July 2011) on the southern granite (Stevenson Hamilton) supersite to assess the potential groundwater regime. The traverses described in the following sections provided a basis for which piezometrical (different depths) boreholes were drilled. These borehole locations and depths were based on initial interpretation of depth to the saturated zone within the hard rock and weathered aquifer as well as the different hillslope component. These are depicted in the plotted pseudosections including

interpretations of distinct crest, midslope and riparian zones A Google Earth © aerial image and catchment map has been included for site specific orientation at each of the pseudosection interpretations.

The boreholes were drilled by the Department of Water Affairs drilling rigs from May -October 2012. Added value of the boreholes was that a more refined hydrogeological characterisation was obtained, including aquifer properties, in-situ hydrochemistry and subsurface lithological descriptions. The latter were useful for updating the initial ERT surveys. To this end, actual depths to groundwater levels, depth to the weathering/hard rock interface and water strikes, and other potential geological features i.e. clay lenses were identified. Blow out yields were also useful to give an initial estimate of the aquifer properties.

In general the highly weathered, jointed and fractured lithologies would tend to have a slightly higher transmissivity than the slightly weathered or un-fractured lithologies.

5.2.1 Southern granite first order transect

Figure 5.1 initial interpretation: The unsaturated zone across the profile of the 1st order hillslope was interpreted at a depth of 8 m at the crest and increasing in depth towards the riparian zone with variable moisture contents due to the changes in low resistivity (3-75 Ωm) values across the profile at shallow depths. Therefore the estimated groundwater level is expected to be approximately 8-12m across the profile. The riparian zone was estimated to have deep weathering which then decreases in depth towards the crest due to shallower depths of high (1875-5484 Ωm) resistivity values seen at the crest. These high resistivity values are consistent with low porous material which is likely to be hard rock. Two boreholes were proposed to be drilled at the riparian zone as saturated condition might occur at two distinctive depths namely the weathered/unsaturated zone and hard rock/ saturated zone given the difference in resistivity in the shallow (3-75 Ωm) and deep (1875-5484 Ωm) subsurface. The close banding of resistivity 219-641 Ωm at 20-25m depth across the hillslope suggests a possible interface zone between the weathered and hard rock granite. The crest has two proposed

boreholes as it was estimated that two zones occur such as the high resistivity values (1875-5484 Ωm) of hard rock/saturated zone and low resistivity values (7-75 Ωm) of weathered/unsaturated zone annotated on the profile.

Figure 5.1 final interpretation: The 1st order hillslope boreholes provided data on the positions of weathered and hard rock zones. The borehole data showed that the riparian zone has a deeper weathering profile of 25m compared to the crest weathering depth of 21m (Figure 5.2). The 1st order hillslope exhibits a low permeability weathered granite aquifer and relatively high permeability hard rock granite aquifer at the crest. This is based on the shallow 17m borehole being drilled dry and the deep 103m borehole having two water strikes generating a blow out yield of 1.25 L/s (see Appendix IV figure IV p and q). This suggests that the hard rock aquifer is more permeable and is likely to be an active groundwater flow system at this point. The weathered aquifer at this point has a perched water table due to the 17m borehole having a water level later on in the season. Therefore the weathered aquifer can be seen as an 'unsaturated reservoir' owing to its low permeability and this would temporary store groundwater. The deep 61m riparian position borehole had only one water strike which generated a blow out yield of 0.07 L/s (see Appendix IV figure IV n) which infers a relatively low permeable hard rock aquifer groundwater flow system at this point. The shallow 22m riparian borehole was drilled dry suggesting a low permeable weathered aquifer at this point.

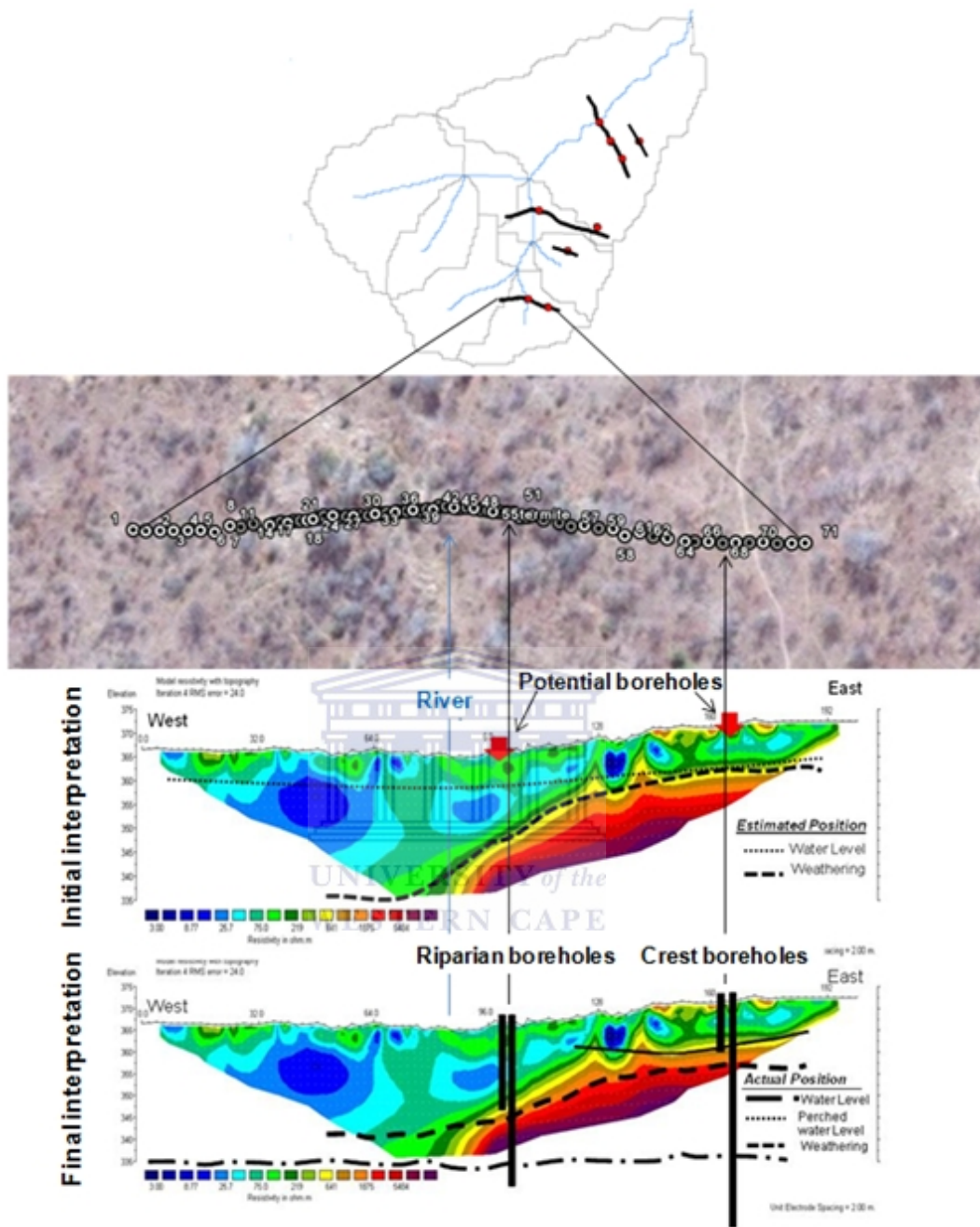


Figure 5.1 Initial and final interpretation of 2D ERT traverses coupled with topography data, satellite imagery and estimated and actual positions of groundwater level and weathering.

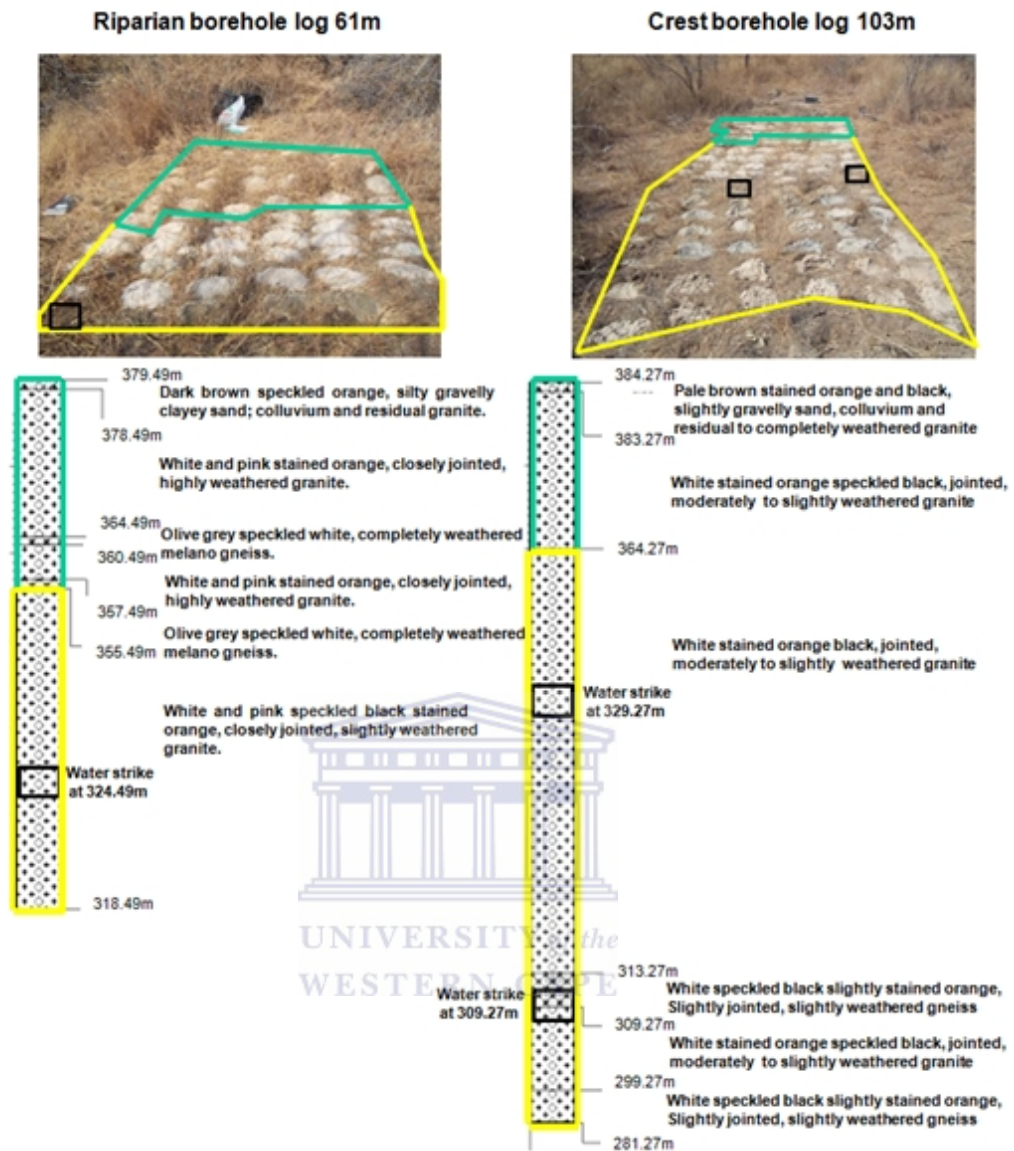
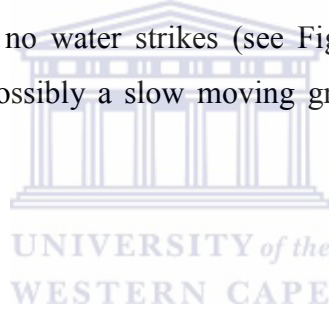


Figure 5.2 Borehole lithology log of the southern granite first order riparian 61m and crest 103m boreholes, the green highlighted section indicates weathered material, the yellow highlighted section indicates hard rock material and the black blocks indicate water strike positions.

5.2.2 Southern granite first/second order triangulation transect

The first/second order triangulation geophysics traverse does not extend to depths of actual weathering which can be seen in Figure 5.3. However the low resistivity values (3-75 Ωm) seen within the first 13m could be interpreted as the highly weathered, silty, clayey material observed in the borehole samples (Figure 5.4.). The high resistivity values (1875-5484 Ωm) seen at >24m depth is like to be hard rock material. However, the borehole log has a highly weathered granite and clay layer from >24m-36m which does not support the geophysics interpretation (Figure 5.4). It is possible that the highly weathered clay feature that exists in the borehole log is creating a discontinuity and therefore generating misleading resistivity values perpendicular to its depth.

The borehole log for the 1st/2nd order triangulation borehole illustrates deep weathering of 41m and no water strikes (see Figure 5.4). This suggests a low yielding borehole and possibly a slow moving groundwater flow system at this point.



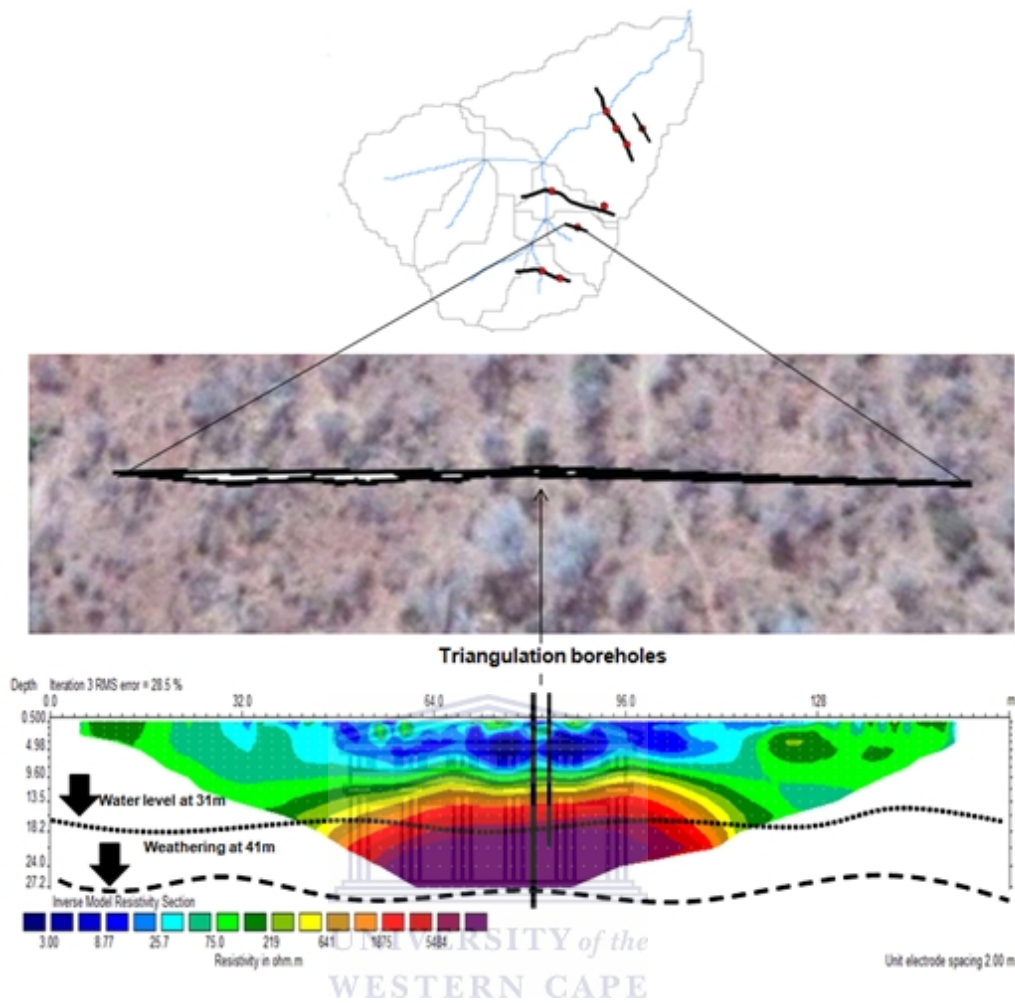


Figure 5.3 2D ERT traverse coupled with actual groundwater level and weathering positions (Topographic detail excluded) of the first/second order triangulation borehole position.

Triangulation borehole log 61m

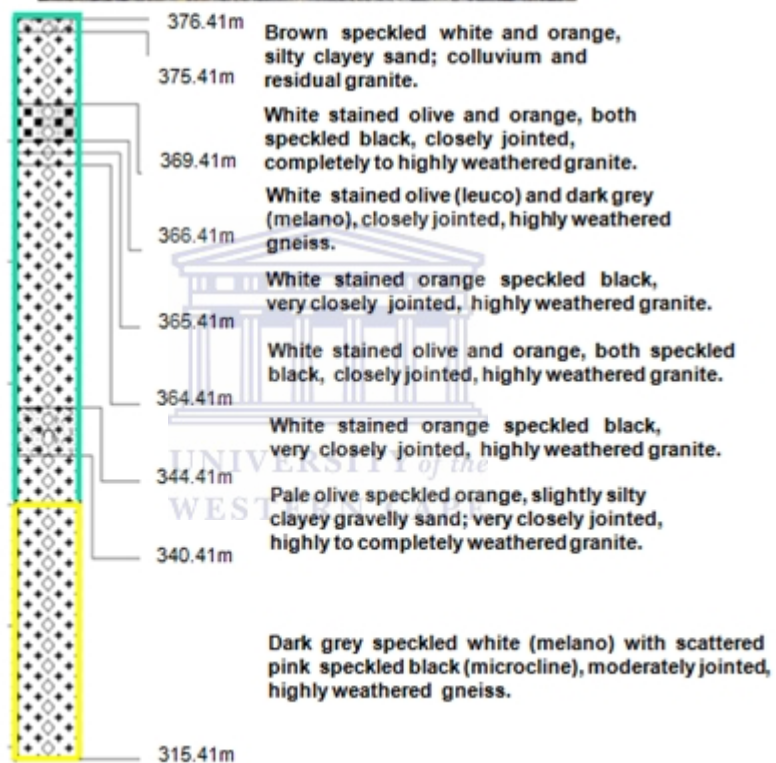


Figure 5.4 Borehole lithology log of the southern granite first/second order triangulation 61m borehole, the green highlighted section indicates weathered material and the yellow highlighted section indicates weathered gneiss material.

5.2.3 Southern granite second order transect

Figure 5.5 initial interpretation: It was estimated that the riparian zone of the 2nd order hillslope would exhibit an 8 meter unsaturated zone with shallow groundwater levels at 10m due to the low resistivity values (3-75 Ωm) across the profile within 8-10m below the subsurface. The riparian zone was expected to have deep weathering and decreases toward the crest due to high (1875-5484 Ωm) resistivity values occurring at a shallower depth at the crest. Two boreholes were proposed to be drilled at the riparian zone as saturated condition might occur at two distinctive depths namely the weathered/unsaturated zone and hard rock/saturated zone given the difference in resistivity in the shallow (3-75 Ωm) and deep (1875-5484 Ωm) subsurface. Across the profile the groundwater level was expected to be relatively flat due to a consistency with depth in low resistivity values (3-75 Ωm) across the profile. The clumping together of resistivity values 219-641 Ωm suggests an interface between the weathered and hard rock zones. The resistivity values suggest a low (3-75 Ωm) and high (1875-5484 Ωm) resistivity zone which could be interpreted as weathered and hard rock zones respectively. Two boreholes were proposed at the crest as it was estimated to have weathered and hard rock zones.

Figure 5.5 final interpretation: The 2nd order hillslope boreholes provided data on the positions of the weathered and hard rock zones. The borehole data showed that the riparian boreholes of the 2nd order hillslope actually have shallower weathering profile of 29m compared to the crest of 41m (Figure 5.6). The shallow and deep boreholes of the 2nd order hillslope riparian zone and crest produced no blow out yields which suggest low permeable shallow and deep groundwater system at these points.

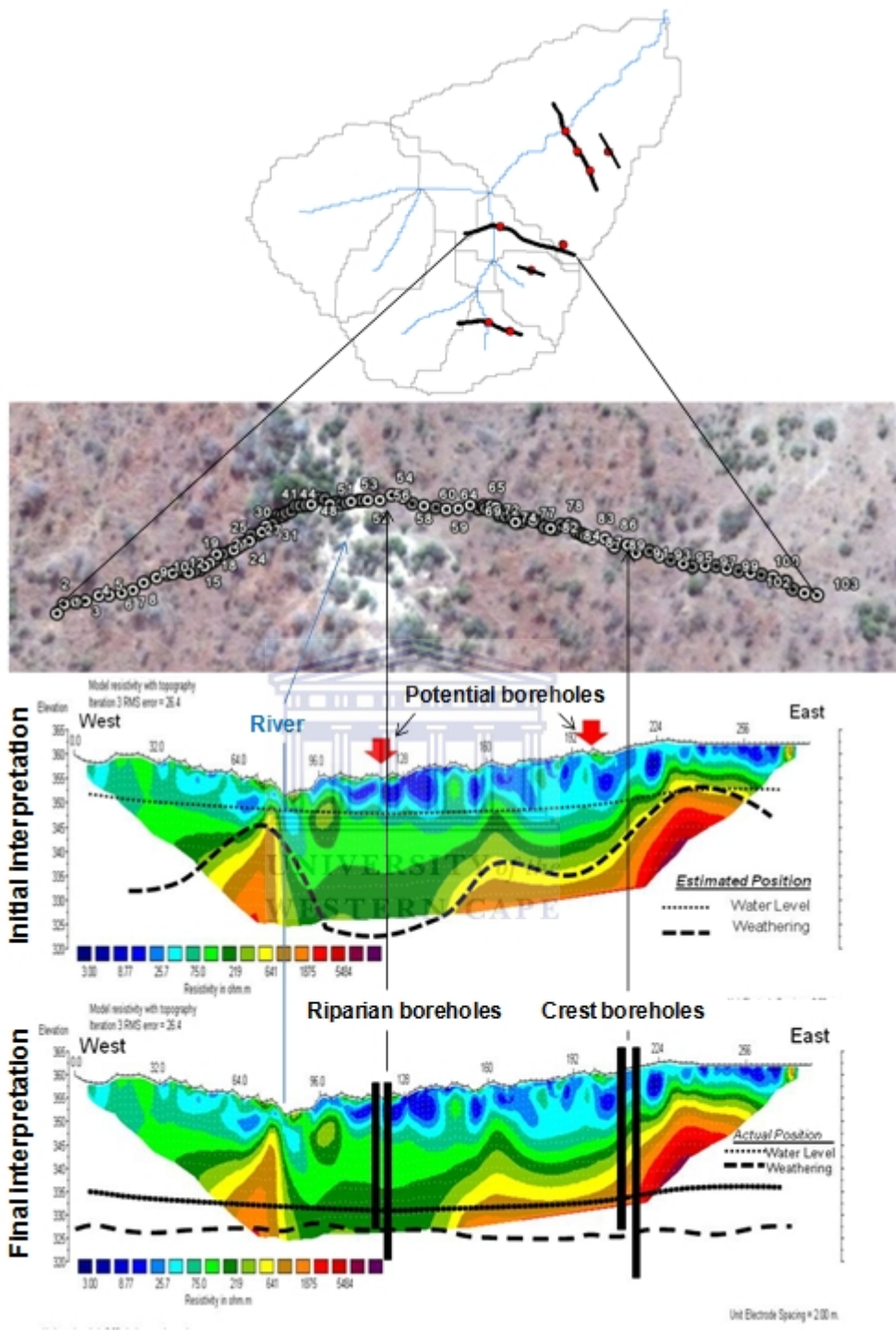


Figure 5.5 Initial and final interpretation of 2D ERT traverses coupled with topography data, satellite imagery and estimated and actual positions of groundwater level and weathering.

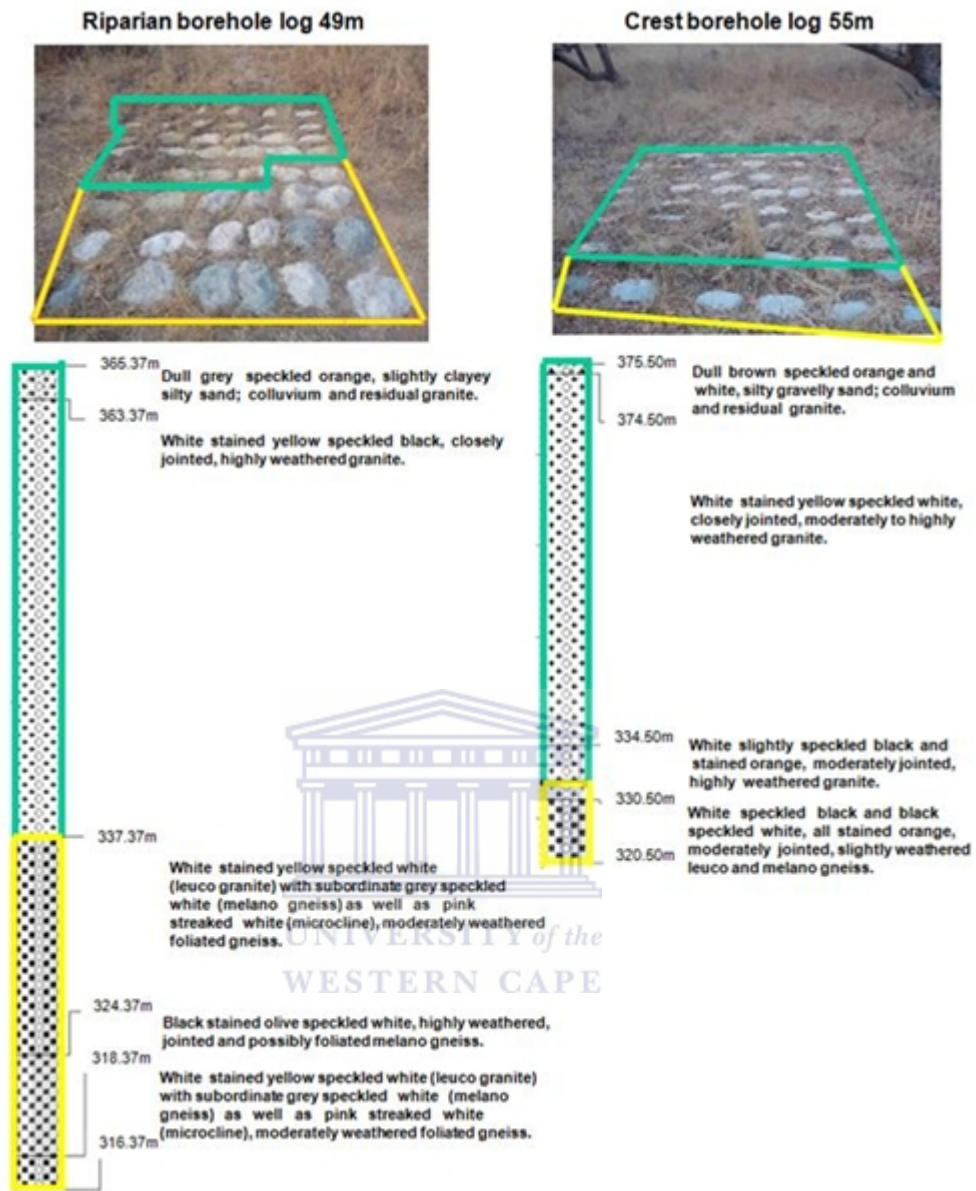


Figure 5.6 Borehole lithology logs of the southern granite second order riparian 49m and crest 55m borehole, the green highlighted section indicates weathered material and the yellow highlighted section indicates hard rock material.

5.2.4 Southern granite third order transect

Figure 5.7 initial interpretation: The low resistivity values (3-75 Ωm) at a shallow depth across the profile were interpreted to represent the unsaturated zone across the profile. A thickness of 8-12 m was estimated with a relatively flat groundwater levels across the profile. High resistivity values (1875-5484 Ωm) occur at a depth of approximately 25m within the riparian zone, 26m at the mid-slope and 30-35m at the crest. The mid-slope has a sodic site which could be explained by the low resistivity values (3-75 Ωm) occurring at the mid-slope towards the crest. These sodic sites are saline, porous and high in clay content hence the occurrence of low resistivity (high conductance) values. This illustration was validated by field observations i.e. herbaceous and sparse vegetation, grazed grass on duplex soil (see Figure 3.2).

Figure 5.7 final interpretation: Based on the borehole data the weathering occurs at a depth of 25m, 26 m and 38m at the riparian zone, mid-slope and crests respectively on the 3rd order hillslope. Across the profile there are distinct weathered and hard rock zones. The riparian boreholes produced a very low blow out yield of 0.01 L/s (see Appendix IV figure IV a and b) upon being drilled which suggests a low permeable shallow and deep groundwater system. The mid-slope and crest position boreholes produced higher blow out yields 0.16 and 0.33 L/s respectively (see Appendix IV figure IV c and d) which suggest permeable shallow and deep groundwater flow systems. The intensely fractured and highly weathered lithology description of the mid-slope position 49m borehole at a depth of 330-320 mamsl is likely to be a fractured or flow zone (see Figure 5.8).

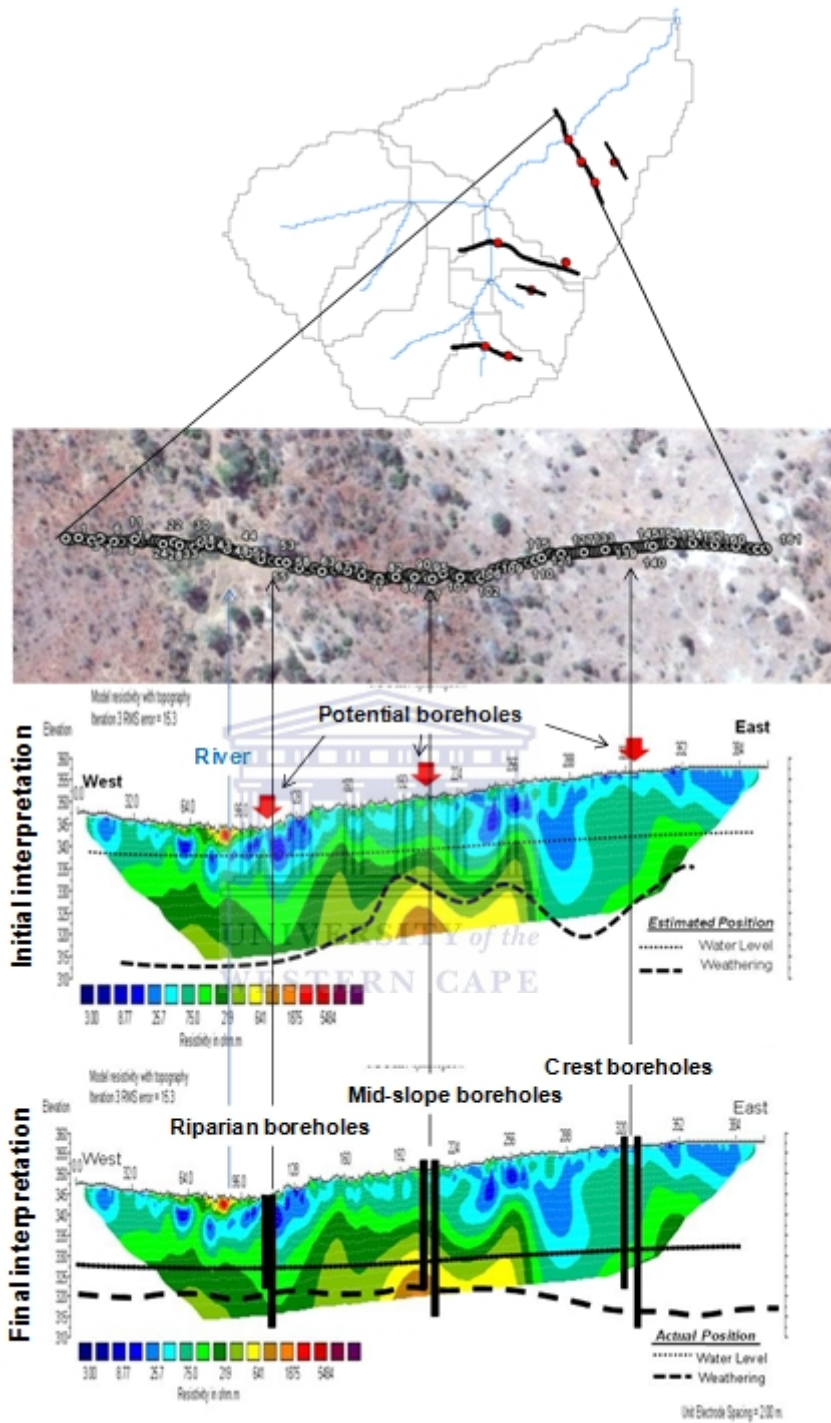


Figure 5.7 Initial and final interpretation of 2D ERT traverses coupled with topography data, satellite imagery and estimated and actual positions of groundwater level and weathering.

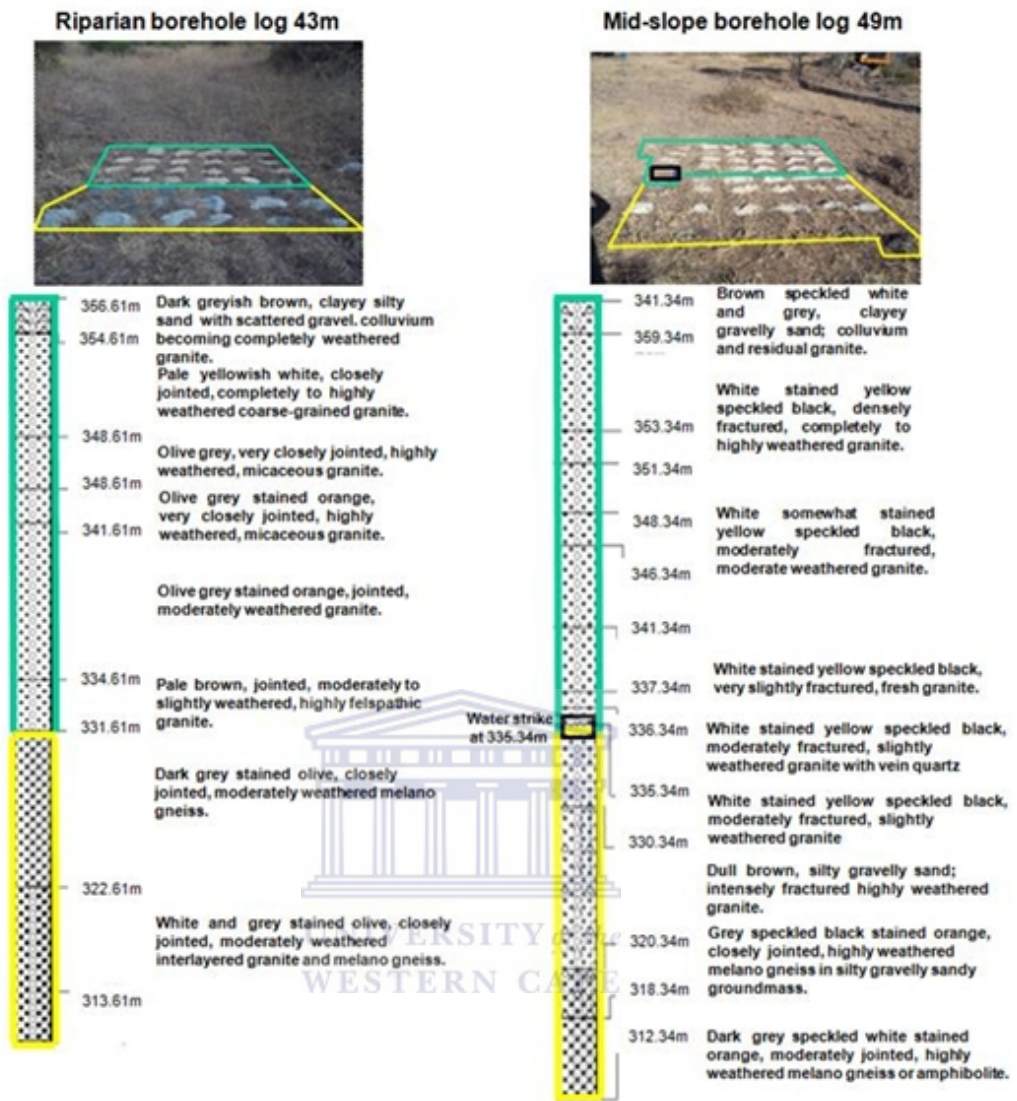


Figure 5.8 Borehole lithology log of the southern granite third order riparian 43m and mid-slope 49m boreholes, the green highlighted section indicates weathered material, the yellow highlighted section indicates hard rock material and the black block indicates the water strike position.

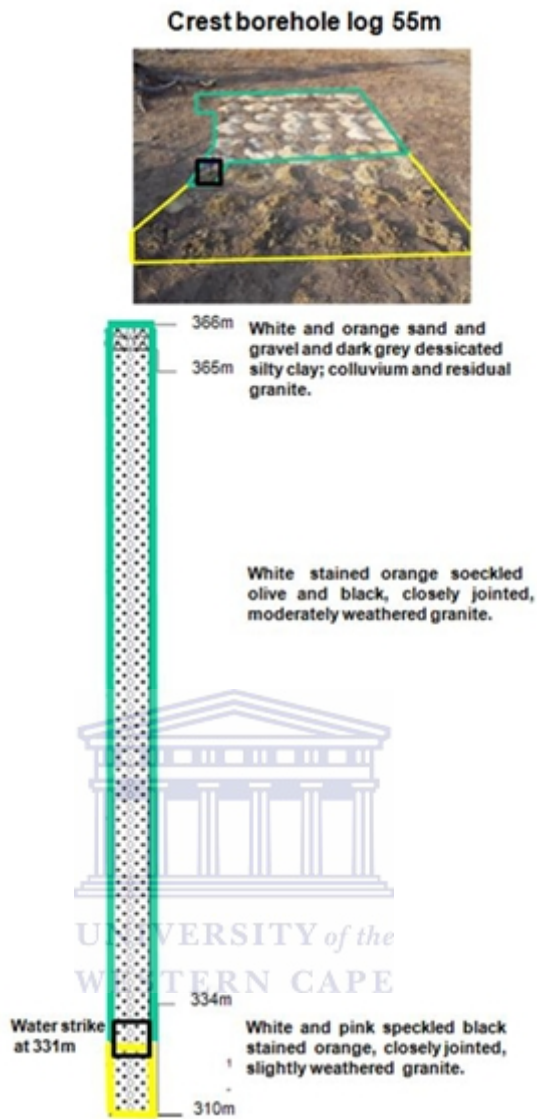


Figure 5.9 Borehole lithology log of the southern granite third order crest 55m borehole, the green highlighted section indicates weathered material, the yellow highlighted section indicates hard rock material and the black block indicates the water strike position.

5.2.5 Southern granite third order triangulation transect

The low resistivity values (3-75 Ωm) seen across the 3rd order triangulation geophysics traverse at an approximate depth of 18m could be interpreted as the very fine material or highly weathered granite seen in the borehole log in Figure 5.11. The profile indicates low resistivity to 38m at the borehole position which corresponds with the deep weathering displayed in the borehole log. The borehole had no blow out yields, suggesting a low permeable groundwater flow system at this point.

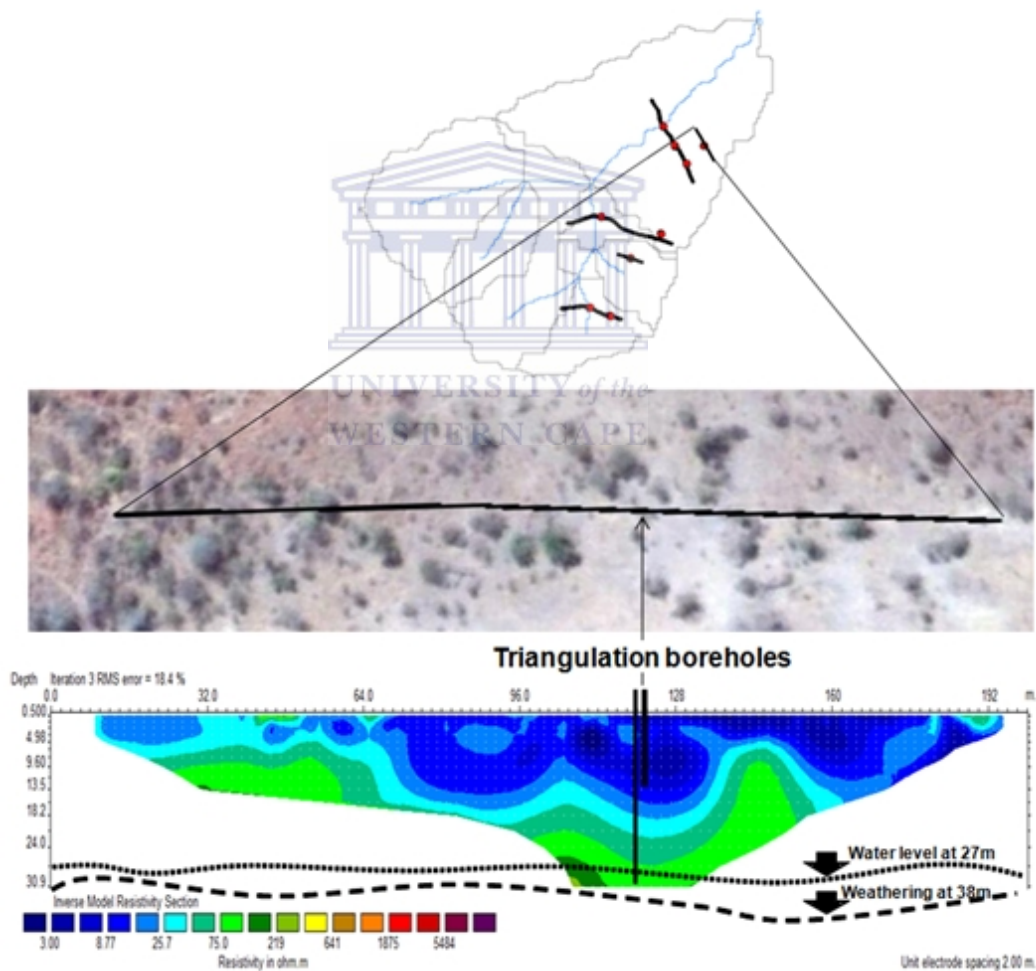


Figure 5.10 2D ERT traverse coupled with actual groundwater level and weathering positions (Topographic detail excluded) of the 3rd order triangulation borehole position.

Triangulation borehole log 61m

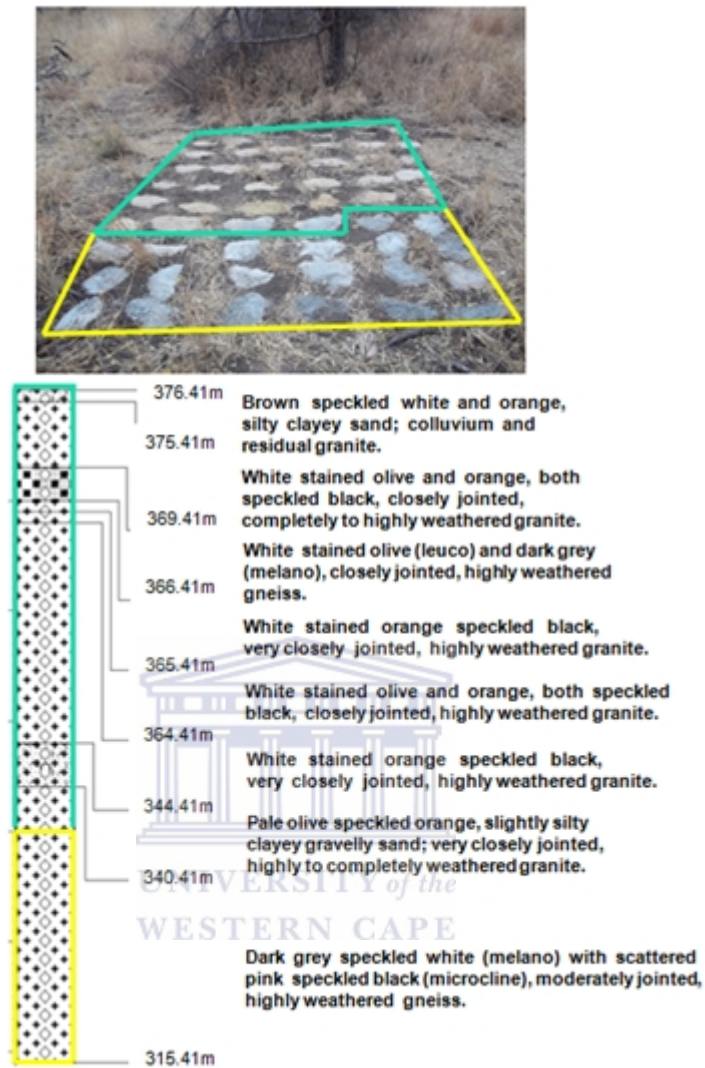


Figure 5.11 Borehole lithology log of the southern granite third order triangulation 61m borehole, the green highlighted section indicates weathered material, the yellow highlighted section indicates hard rock material.

5.3 Hydraulic characterisation for the southern granite supersite boreholes

To gain additional insight to the flow of groundwater and aquifer properties, aquifer tests were conducted to obtain transmissivity (T) values. These hydraulic properties were estimated using various analyses depending on a particular set of assumptions such as the blow out yield of boreholes, or the volume sustaining a given borehole pump rate during a pump test for at least 2 hours without drying out and assumptions set out by the analytical solutions used discussed in chapter 2.

Figure 5.12 and 5.13 provide examples of the pump test data and slug test data performed on the southern granite supersite (see Appendix I for the remainder of the pump and slug test data). In Figure 5.12 the drawdown and recovery data is illustrated in graph a and b respectively during a pump test. Graph c demonstrates the MS Excel macro based on Cooper-Jacob (1946) equation (Eq 2.5) used to determine the transmissivity values for the boreholes which could satisfy a pump test and the Cooper-Jacob analysis assumptions. However in the Figure 5.12 example for the 3rd order mid-slope position, the 26m borehole does not satisfy the Cooper-Jacob assumption of a constant saturated thickness under pumping conditions as it is drilled into the weathered aquifer whereby the wedge shape of the hillslope becomes a factor. An analysis was performed using software based on the Hantush (1962) equation (Eq 2.7). In boreholes that fail to satisfy pump test conditions the Bouwer and Rice (1976, Eq 2.10) method is used. An example of this is shown in Figure 5.13 where the recovery data is illustrated in graph a and the MS Excel macro in graph b. The Bouwer and Rice equation (Eq 2.10) then also uses borehole construction data (i.e. depth to initial water level, final borehole depth, borehole radius, length of screen section, etc) and recovery data to generate a T value.

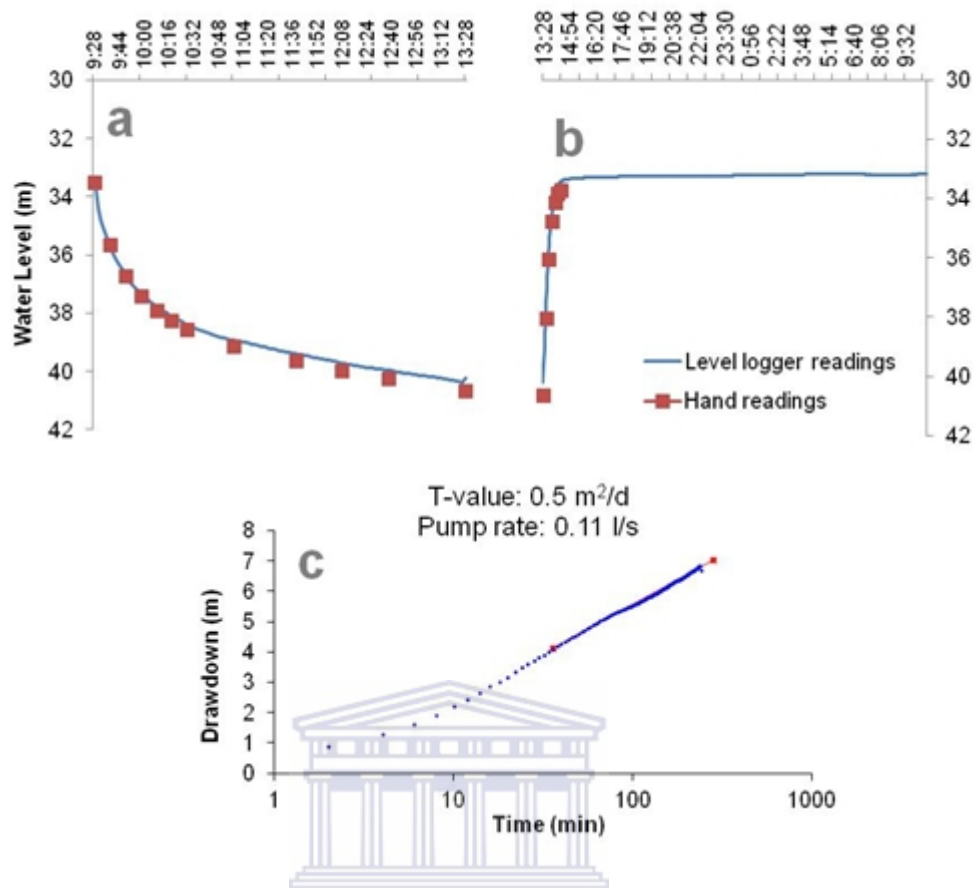


Figure 5.12 Data acquired during a pump test for the southern granite 1st order riparian position 61m borehole, a=drawdown, b=recovery and c=pump test Cooper - Jacob macro (Van Tonder et al., 2001).

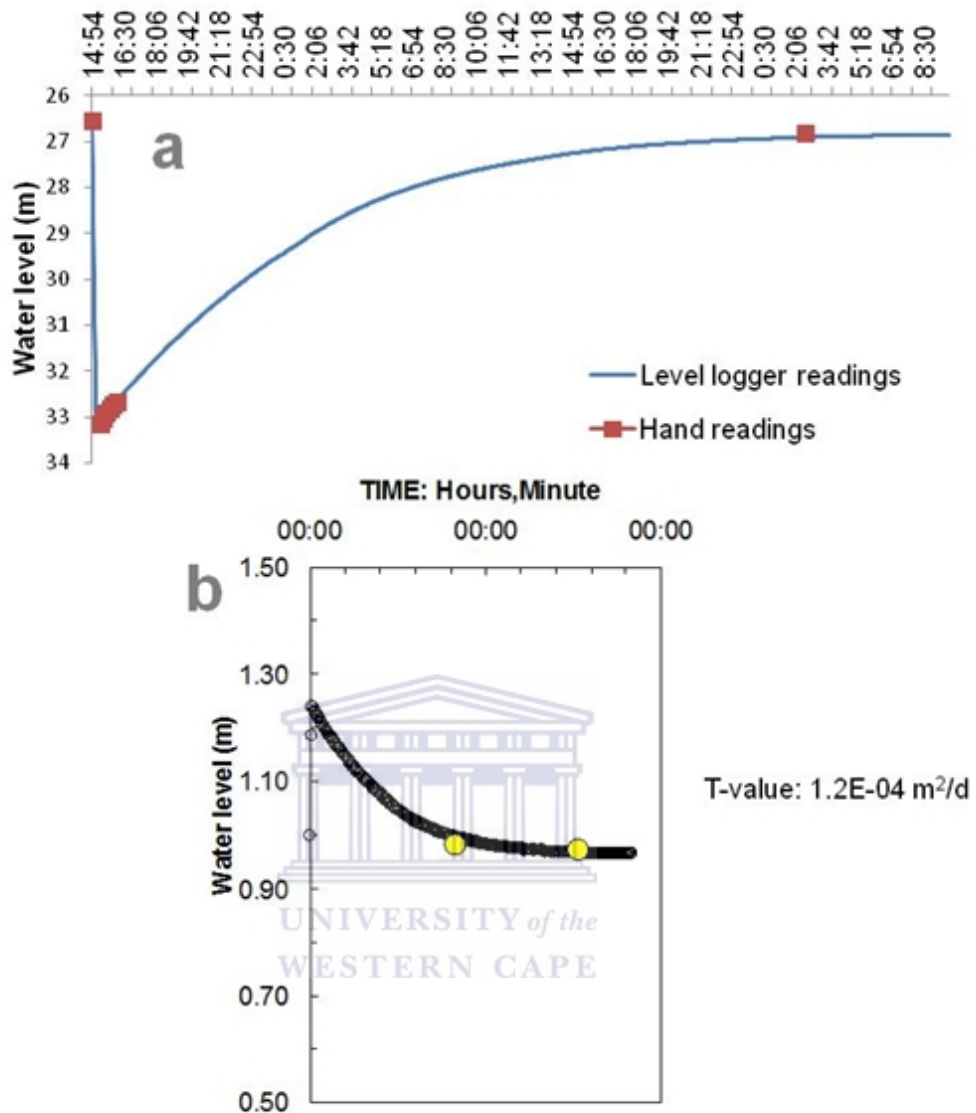


Figure 5.13 Data acquired during a slug test for the southern granite 3rd order crest position 34m borehole, a=recovery and b=slug test excel macro (Halford and Kuniansky, 2005).

5.3.1 Transmissivity

Figure 5.14 and 5.15 reveals that the majority of the 19 boreholes have a low transmissivity which is in agreement with Fischer et al (2009) which suggests that crystalline rocks are likely to be characterized by low T or K values. Only 5 boreholes comprise slightly higher transmissivity which are boreholes drilled into the hard rock granite/gneiss aquifer with only one borehole drilled into the

weathered aquifer (see Figure 5.14). These 5 higher yielding boreholes also consisted of blow out yields, water strikes/fracture zones discussed in section 5.2. Based on relatively low transmissivity values of these boreholes it is inferred that these characteristics do not conform to a densely inter-connected fractured groundwater flow system within the hard rock aquifer. The low transmissivity values estimated for the shallow boreholes (see Figure 5.15) drilled into the weathered granite aquifer suggest a possible porous but low permeable weathered aquifer.

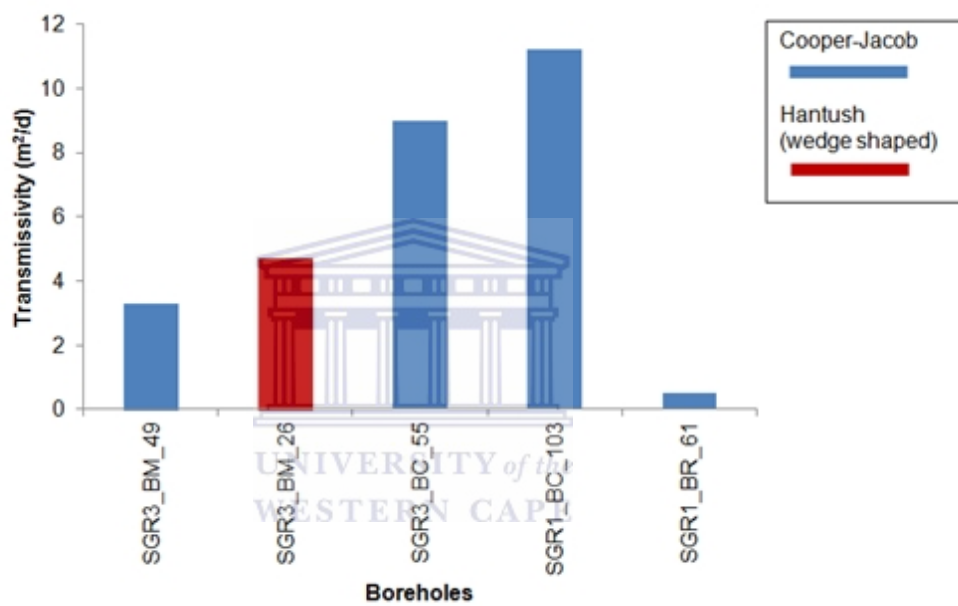


Figure 5.14 Transmissivity values for the southern granite supersite boreholes calculated using the Cooper-Jacob and Hantush (wedge shaped) solutions.

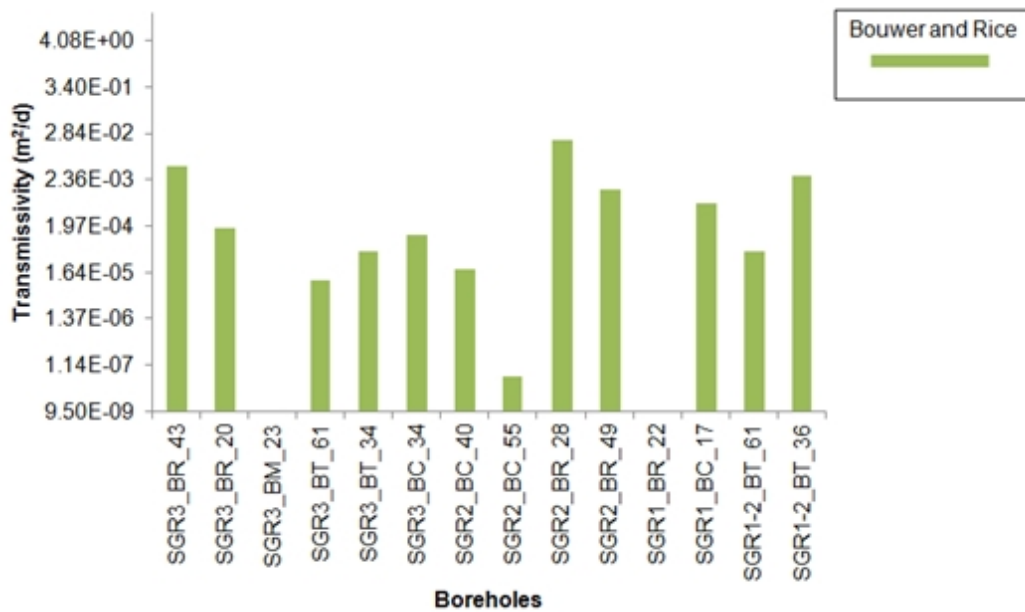


Figure 5.15 Transmissivity values for the southern granite supersite boreholes calculated using the Bouwer and Rice solution.

5.4 Groundwater flow direction and gradients

Upon completion of each installed borehole water levels were routinely monitored in order to determine the hydraulic heads (h) and gradients (i) of the groundwater in the catchment. Once (h) of two or more boreholes are known, the (i) or difference in (h) between them will be used to infer a general groundwater flow direction.

Figure 5.16-5.19 reveals spatial plots of groundwater and surface water levels. This is in order to plot a generalized spatial groundwater and surface water flow distribution at the 3rd order scale. The general dry season flow distribution maps (see Figure 5.16 and 5.17) illustrate quite flat groundwater levels with a gentle flow gradient from 1st order boreholes towards the 3rd order boreholes.

The general wet season groundwater flow direction (see Figure 5.18 and 5.19) also extends from the 1st order boreholes toward the third order boreholes, moving almost parallel to the stream. The water level of the deep boreholes are relatively flat with a slight hydraulic gradient extending from the 1st order boreholes towards the 3rd order boreholes; however a more pronounced gradient

is visible from the 1st order crest position 17m borehole (SGR1_BC_17) towards the 1st, 2nd and 3rd order stream level logger (SGR1Q/SGR2Q/SGR3Q) during the high intensity rainfall occurring during January 2013 (see Figure 5.18). The presence of this gradient suggests a potential groundwater discharge into the streams via interflow processes within the weathered aquifer. The deep groundwater water levels do not suggest potential discharge into the 1st, 2nd and 3rd order streams due to a negative gradient from the stream water levels towards the groundwater levels (see Appendix III). Since the weathered and hard rock aquifer groundwater levels flow toward the 3rd order hillslope it is possible that at higher stream orders (beyond the scale of this study) the deeper groundwater system could discharge in the stream. The general weathered and hard rock groundwater flow direction tends to mimic the surface topography which decreases in elevation from the first order hillslope towards the third order hillslope (see Figure 3.3). Therefore the general groundwater flow direction correlates with the typical groundwater flow direction from topographical highs or highest hydraulic head to topographical lows or lowest hydraulic head (Freeze and Cherry, 1979 and Winter et al., 1998)

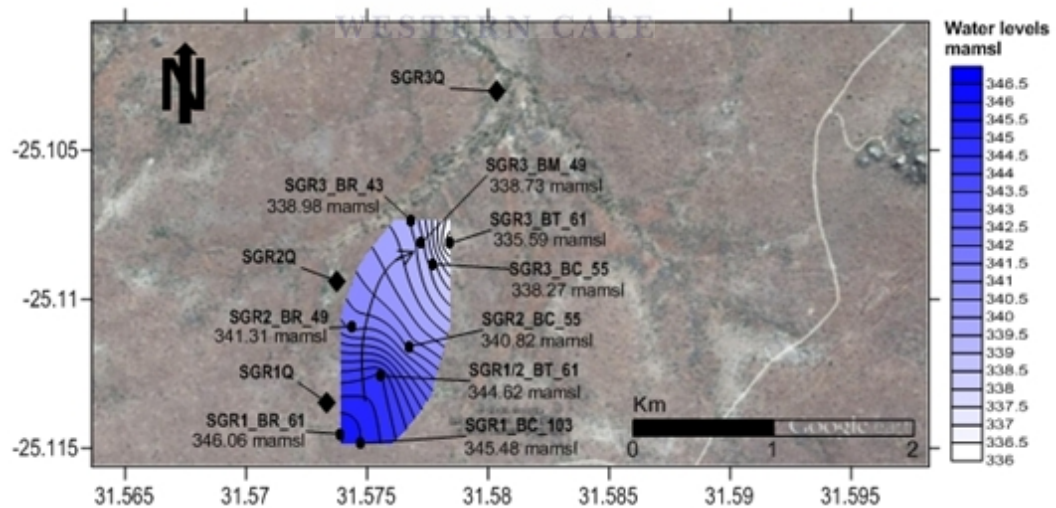


Figure 5.16 General groundwater flow direction of the boreholes drilled into the hard rock aquifer during the dry season (date of water level taken: 27-Sep-12).

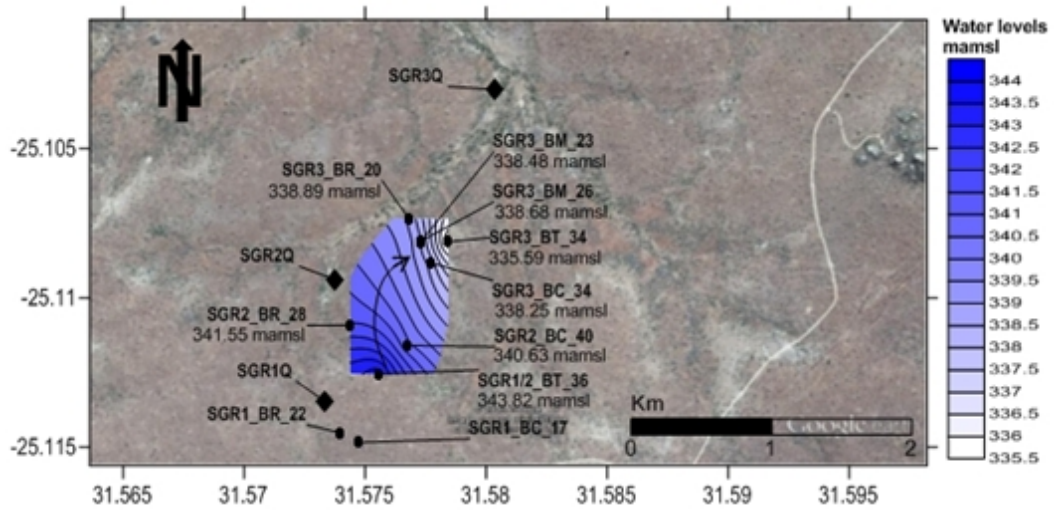


Figure 5.17 General groundwater flow direction of the boreholes drilled into the weathered aquifer during the dry season (date of water level taken: 27-Sep-12).

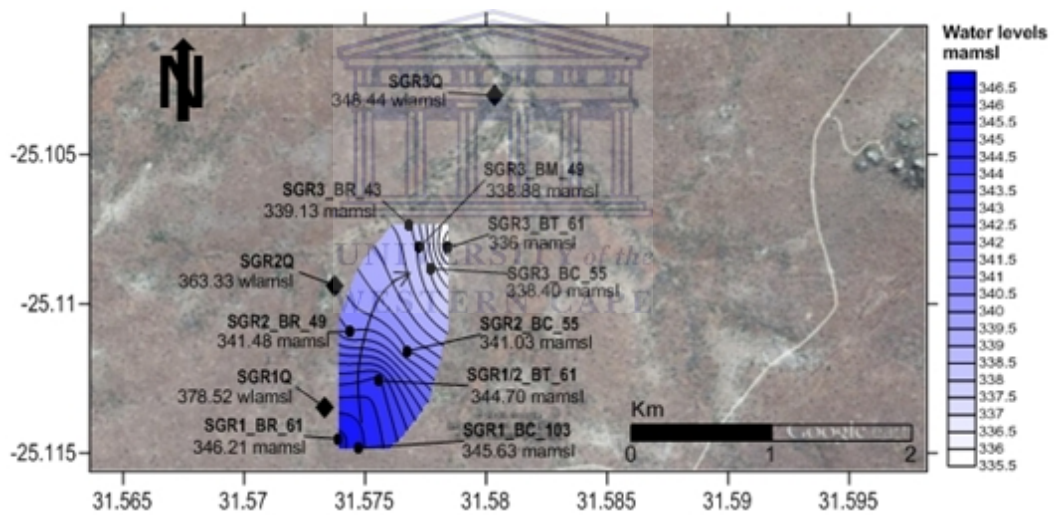


Figure 5.18 General groundwater flow direction of the boreholes drilled into the hard rock aquifer during the wet season (date of water level taken: 28-Jan-13).

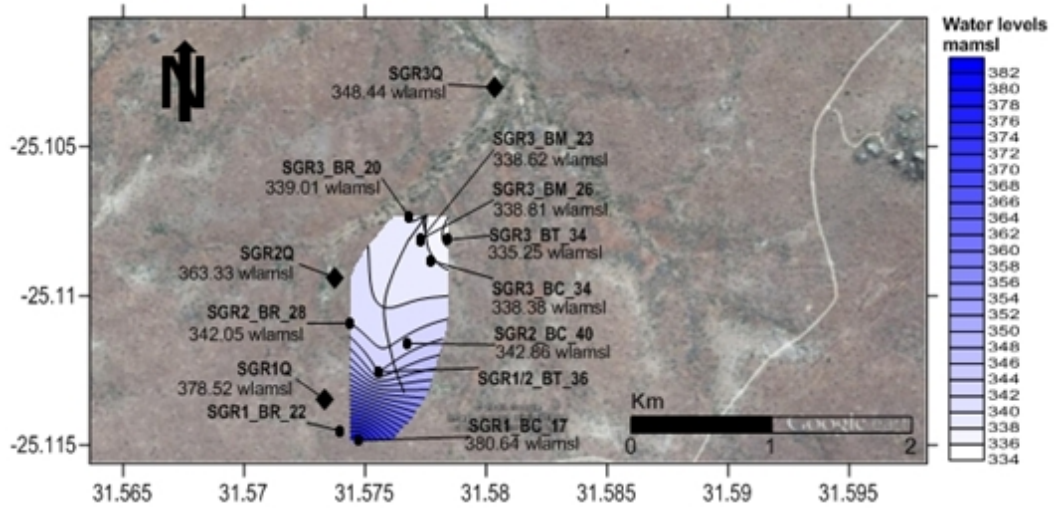


Figure 5.19 General groundwater flow direction of the boreholes drilled into the weathered aquifer during the wet season (date of water level taken: 28-Jan-13).



Chapter 6

Results and discussion: Spatial-Temporal characterisation

6.1 Introduction

This chapter discusses the spatial and temporal characterisation of groundwater levels verses rainfall and in-situ parameters/fluid logging. This information is used in the build up to the final hydrogeological conceptual model presented through this research.

6.2 Time series rainfall

The hydrological season for the southern granite supersite commenced on 4th September 2012 and thus the hydrological year used in this research is continued to September 2013. Rainfall is plotted in 3 ways and when viewed collectively it illustrates a broader perspective on the intensity, trend and sequence of the rainfall distribution over the southern granite supersite. Therefore firstly, Figure 6.1 illustrates the daily rainfall intensities of the particular sequences of rainfall events which occur September 2012, October 2012- December 2012 and December 2012 - February 2013. Secondly, in Figure 6.2 the cumulative rainfall provides the total rainfall for the hydrological season and for the particular sequences of rainfall events. It can be seen that the total rainfall for the hydrological year consisted of 773.8mm which was more than the range set out by Venter et al (2003) of 500-700mm per annum. This occurrence is due to the slightly above average rainfall occurring for this particular hydrological year or given the ranges set out by Venter et al (2003) covered a greater area. Lastly, the antecedent precipitation index (API) is used to organise the rainfall events into distinct sequences (see Figure 6.3) or depth of rainfall over a particular time period as it will be seen and discussed later that the borehole water levels respond to a sequence of rainfall events. It can be seen that 3 major types of rainfall sequences occur namely, September 2012, October 2012- December 2012 and December 2012 - February 2013 (see Figure 6.3). The September 2012 rainfall sequence 1 consisted dominantly of moderate rainfall ranging 5-31mm/day for 2 weeks with a total rainfall of 87.7mm, October 2012-December 2012 rainfall sequence 2 consisted

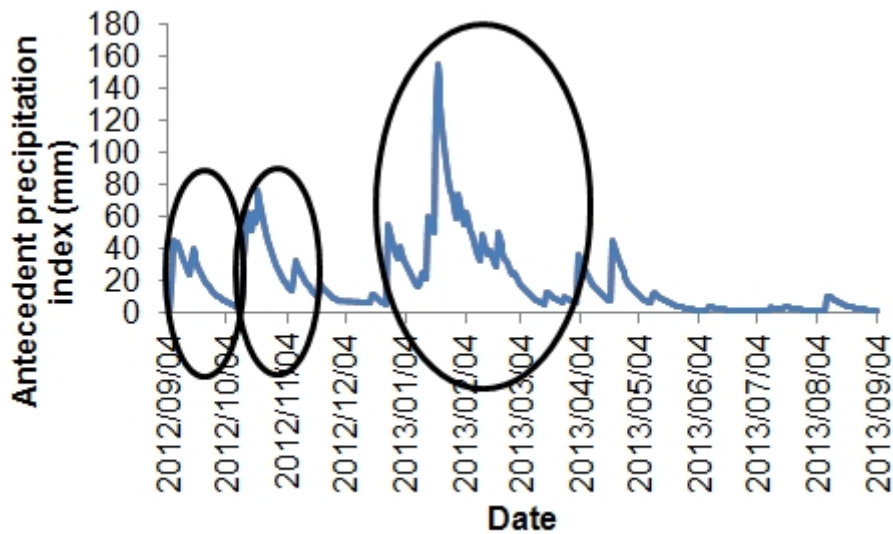


Figure 6.3 API for the southern granite supersite illustrating the 3 major rainfall sequences during September 2012 to September 2013.

6.3 Time series groundwater levels and rainfall

To gain understanding of the trend in groundwater levels in response to rainfall, each nested piezometric (shallow and deep) borehole water level within a particular catenal element or hillslope component was plotted against rainfall. In this way one would be able to infer flow gradients and possible processes identified such as groundwater recharge, discharge and interflow.

6.3.1 First order boreholes

The hard rock deep groundwater level can be seen in Figure 6.4 and the weathered shallow groundwater level can be seen in Figure 6.5. These two water levels have more than 20m difference in depth to water level suggesting the presence of a perched water level at the 1st order crest position 17m borehole.

The 1st order crest position 103m borehole has a 2 month lag in response to sequence 1 of 5-31mm/day of rainfall over 2 weeks in September 2012. The change in hydraulic head (dH) was 0.08m as a result of these sequences of rainfall. The presence of a change in hydraulic head with a change in time or gradient (dH/dT) was evident. The dH had a lag of 2 months and increased by 0.09m for sequence 2 of 5-35mm/day of rainfall over 3 weeks during October

2012-December 2012 with a slight decrease in dH/dT . The dH increase by 0.32 m over the rainfall period of December 2012-August 2013. The dH/dT has increased during this period. The dH/dT tends to increase more after the high intense rainfall that occurred during December 2012- February 2013 whereby sequence 3 of 5-95mm/day of rainfall for 4 weeks occurred. The rise in dH to the sequence 3 rainfall events has a response time of 2 months and then starts to follow a more gradual trend.

These trends in water level indicate a piston recharge process as a sequence of rainfall events is required for the water levels to rise. The time lag in response also suggests the recharge area is further away possibly on a regional groundwater scale. The 1st order riparian position 61m borehole responses to the major sequence of rainfall events are similar to the 1st order crest position 103m borehole. The only different is that the riparian borehole has a higher hydraulic head (see Figure 6.6). Therefore a slight upward gradient exists from the riparian zone to the crest.

The 1st order crest position 17m borehole dH has increased by 6.13m as a result of the moderate sequence 2 rainfall events (5-35mm/day) in October 2012 and then recedes after three months. The dH increases by 12.10m as a result of the high intensity sequence of rainfall events January 2013 (whereby 200mm of rainfall occurred over 6 days). The lag time for these responses were 2-3 weeks and given the required sequence 2 and 3 of rainfall events an increase in dH can be associated with a piston recharge process. The recharge appears to be localized to hillslope scale owing to the relatively shorter time lag in response to rainfall events than with the deep groundwater level.

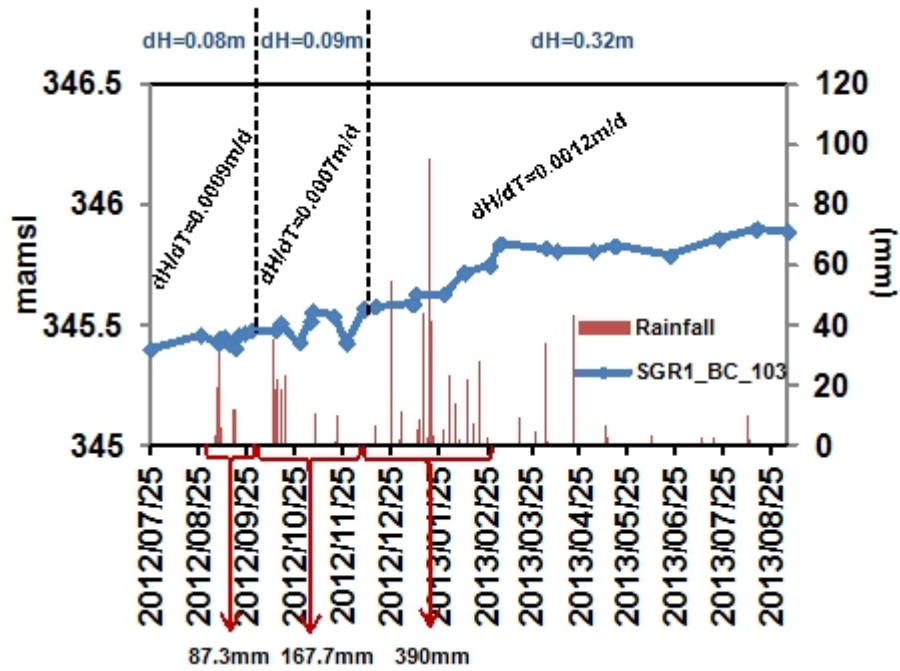


Figure 6.4 First order crest position 103m borehole water level response to rainfall over the hydrological season September 2012 to September 2013.

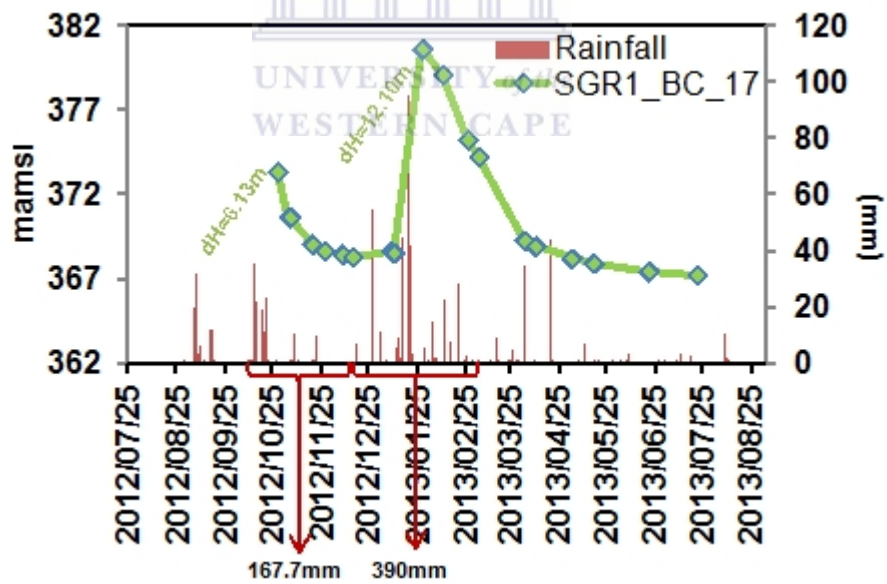


Figure 6.5 First order crest position 17m borehole water level response to rainfall over the hydrological season September 2012 to September 2013.

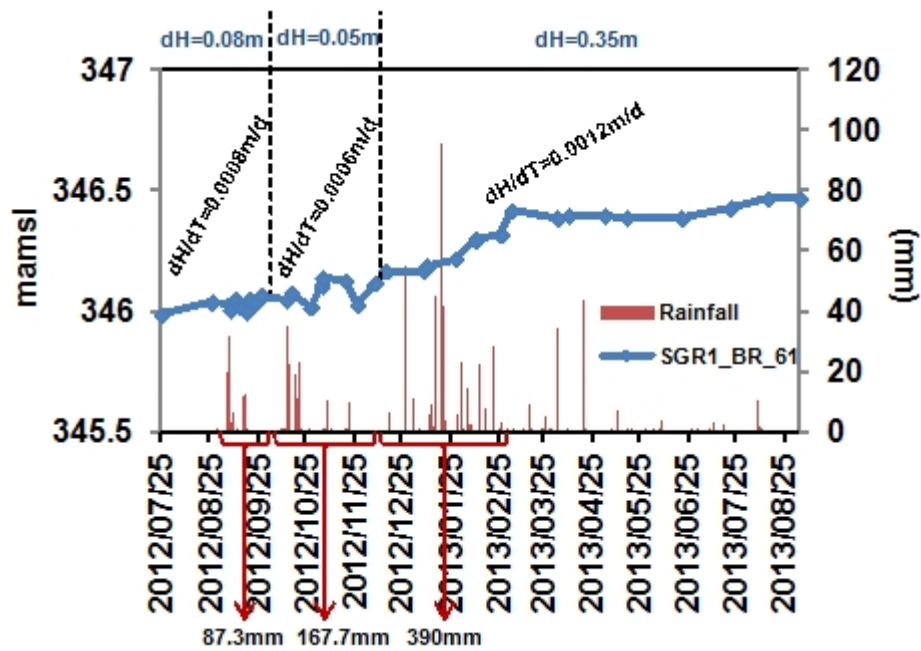


Figure 6.6 First order riparian position 61m borehole water level response to rainfall over the hydrological season September 2012 to September 2013.

6.3.2 First/Second order triangulation boreholes

The 1st/2nd order triangulation 36m and 61m boreholes follow the same trend to each other with similar water level depth (see Figure 6.7). The water level record only starts in October 2012 and the dH has increased by 0.09m in both the 1st /2nd order triangulation boreholes as a result of the moderate sequence 2 of rainfall events (5-35mm/day over 3 weeks) in October 2012-December 2012. The dH/dT increases as a result of the 3rd sequence of (390mm/day over 4 weeks) rainfall events occurring in December 2012- February 2013. The dH rises with a lag of roughly 2 ½ months after which it follows a more gradual gradient. In Both boreholes the dH increased by 0.33m subsequent to the December 2012-August 2013 rainfall events. The time lag in water level response to rainfall events are again indicative of possible recharge occurring from distant areas. This infers a recharge process occurring on a possible regional scale. The water levels dominantly responded to sequence 2 and 3 rainfall events inferring a possible piston recharge process.

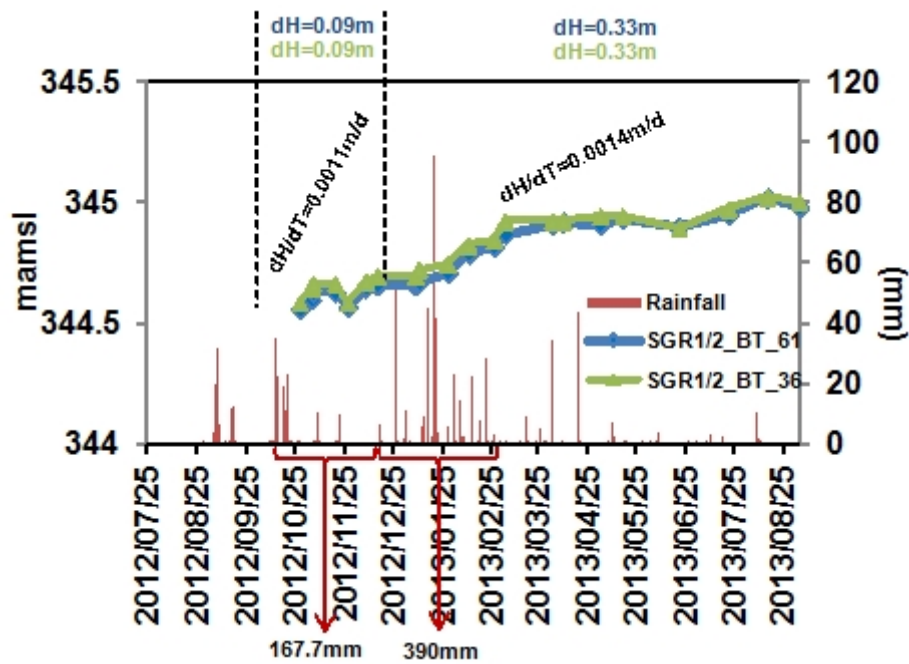


Figure 6.7 First/second order triangulation position 36m and 61m borehole water level response to rainfall over the hydrological season September 2012 to September 2013.

6.3.3 Second order boreholes

The 2nd order crest position 40m and 55m boreholes generally follow the same trend as each other with similar water level depth (see Figure 6.8). The dH and dH/dT for the water levels as a result of the September 2012 sequence of rainfall events has not been included. This was due to the water levels equilibrating consequent to aquifer tests being performed and would generate a negative gradient. The lengthy time taken for water levels to reach static would be a consequence of the low transmissivity values encountered in both the shallow and deep boreholes (see Figure 5.15). The 2nd order crest position 55m borehole dH raises by 0.20m during the October 2012-December 2012 sequence 2 of dominantly moderate (5-35mm/day over 3 weeks) rainfall events with a response time lag of 2 months. A steep dH/dT of 0.0041m/d exists during the period of October 2012-December 2012; this is explained by the water levels equilibrating as a result of aquifer tests.

The 2nd order crest position 40m borehole generally showed that dH had risen by 0.02m as a result of the sequence 2 rainfall events during October 2012 – December 2012. This rise in dH was measured outside the accuracy of the water level meter and is therefore not valid. However as a result of the moderate sequence of rainfall events (5-35mm/day over 2 weeks) during October 2012 caused the dH to increase by 4.38m and receded to the deep groundwater level roughly a month later. A rise in dH by 7.39m occurred as a result of the high intensity sequence of rainfall events (200mm over 6 days) during January 2013 and receded about 3 months later to the deep groundwater level. These abrupt changes in water level resulted from a borehole construction error whereby the gravel used to line the perforated section of the casing was filled to the ground surface creating a conduit for rainfall water. The general dH is 0.38m for the 40m borehole and 0.32m for the 55m borehole. The general rise in water level was mainly consequent of sequence 2 and 3 rainfall events, which infers a piston recharge process possibly on a regional scale due to the time lag response in water levels.

The 2nd order riparian position 28m and 49m boreholes generally follow the same trends as each other with similar water level depth (see Figure 6.9). The dH/dT during September 2012 sequence 1 rainfall events was relatively steep compared to the December 2012-September 2013 dH/dT due to the water levels reaching static as a result of aquifer tests. Therefore the rise in dH for the 28m and 49m borehole do not occur under ambient conditions during this period of rainfall. During the October 2012-December 2012 sequence 2 of moderate (5-35mm/day) intensity rainfall events, dH increased by 0.12m and 0.14m for the 49m and 28m borehole respectively with a response time lag of 2 months. The deep and shallow water levels tend to follow a more gradual gradient during the December 2012-August 2013 rainfall events. However the shallow borehole dH increased by 0.35m as a result of the high intensity (200mm over 6 days) sequence of rainfall events that occurred during January 2013. The response time lag and recession in water level was 2weeks. Due to the relatively rapid response and recession in water level suggests a possible localized indirect preferential recharge process from the 2nd order stream.

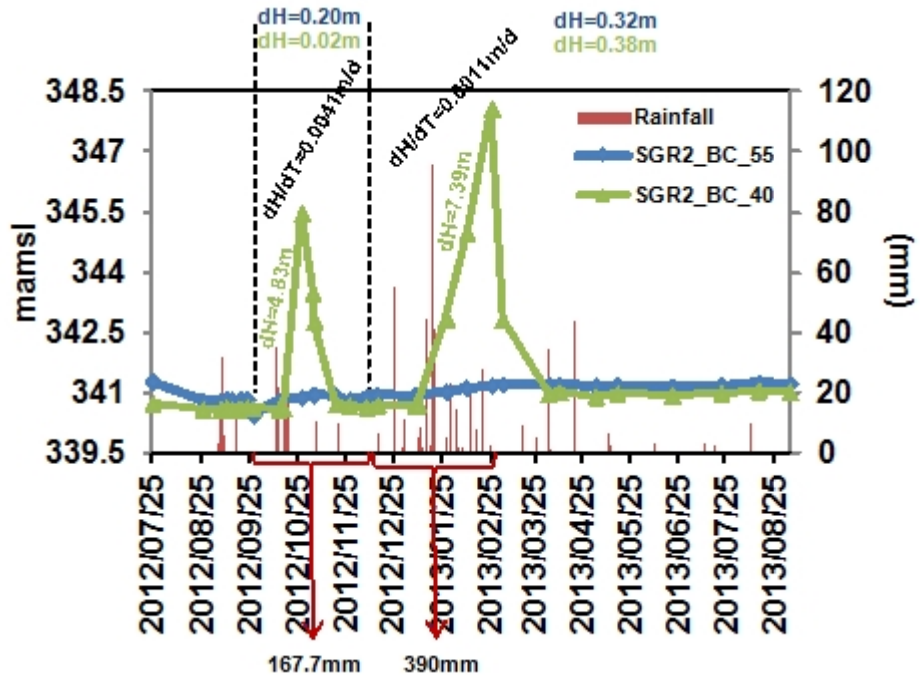
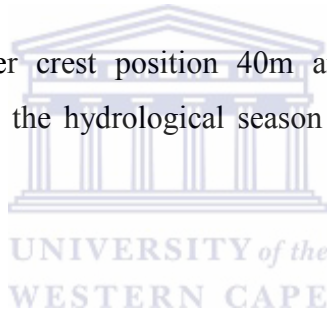


Figure 6.8 Second order crest position 40m and 55m borehole water level response to rainfall over the hydrological season September 2012 to September 2013.



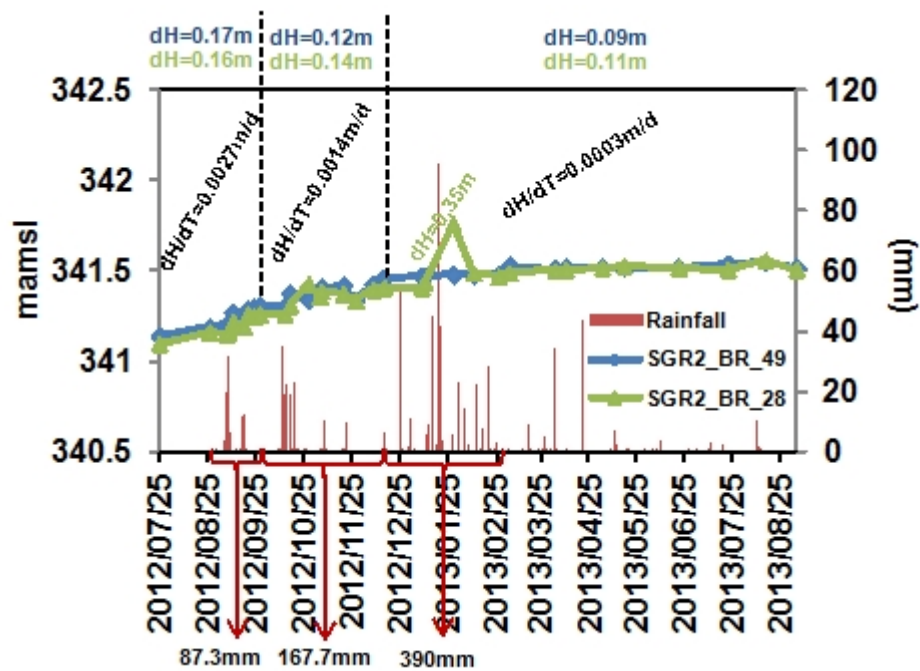


Figure 6.9 Second order riparian position 28m and 49m borehole water level response to rainfall over the hydrological season September 2012 to September 2013.

6.3.4 Third order boreholes

The 3rd order crest position 34m and 55m boreholes generally follow the same trend as each other and are at a similar water level depth (see Figure 6.10). The general gradient is relatively steep (0.0021m/d) during the September 2012 sequence 1 of rainfall events as a result of the water levels equilibrating after the completion of borehole installation. The dH increased by 0.16m and 0.06m for the 55m and 34m borehole respectively during the September 2012 sequence 1 rainfall events, these changes in hydraulic head are not representative of ambient conditions. The 55m and 34m borehole dH increased by 0.07m and 0.08m respectively during the October 2012-December 2012 sequence 2 rainfall events with dominantly moderate intensity rainfall occurring (5-35mm/day over 3 weeks). The gradient is quite gradual during this period. The 55m and 34m borehole dH increased by 0.28m and 0.29m respectively with a rather gradual gradient during the December 2012-August 2013 rainfall events. Both water levels tend to have an increased gradient after the high intensity (200mm over 6

days) rainfall events in January 2013 for roughly 2 months after which it follows a more gradual gradient. These lags in response time of water levels to the different sequences of rainfall events during the hydrological year suggest that the boreholes at this point co-incide with a regional groundwater flow system.

The 3rd order mid-slope position boreholes generally follow the same trend as each other; however the 49m borehole has a higher hydraulic head than the 23m and 26m boreholes which suggest the 43m borehole is flowing towards or contributing to the 23m and 26m boreholes (see Figure 6.11). This separation of hydraulic heads at the 3rd order hillslope possibly indicates that the deeper groundwater system possibly intersects or contributes to higher order streams. The dH increased by 0.12m, 0.13m and 0.11m in the 49m and 26m and 23m boreholes respectively during the September 2012 sequence 1 rainfall events which dominantly consisted of moderate intensity rainfall (5-31mm/day for 2 weeks). The gradient during this period was relatively steep due to the water levels equilibrating following borehole installation. These responses are not as a result of ambient conditions. The dH increased by 0.06m for the 55m and 0.02m for the 26m and 23m boreholes during the October 2012-December 2012 sequence 2 rainfall events with a decrease in gradient. This 0.02m rise in water level is invalid as it is measured outside the accuracy of the water level meter. The dH increased by 0.31m, 0.28m and 0.23m for the 55m, 26m and 23m boreholes respectively with an increase in gradient during the December 2012-August 2013 sequences of rainfall events.

The 3rd order riparian position boreholes generally follow the same trend as each other, however the 43m borehole has a higher hydraulic head than the 20m borehole which suggests the 43m borehole is flowing towards or contributing to the 20m borehole (see Figure 6.12). This separation of hydraulic heads at the 3rd order hillslope indicates that the deeper groundwater system possibly intersects or contributes to higher order streams. The dH increased by 0.12m and 0.09m for the 43m and 20m borehole respectively with a relatively steep gradient of 0.0016m/d during the September 2012 sequence 1 rainfall events. The steep gradient was likely due to the water levels equilibrating as a result of the borehole installation.

The increase in dH is therefore not under ambient conditions. The dH increased by 0.08m and 0.05m for the 43m and 20m boreholes respectively with a decrease in gradient during the October 2012-December 2012 sequence 2 rainfall events. These rainfall events consisted dominantly of moderate intensities (5-35mm/day for 3 weeks). The dH increased by 0.39m and 0.41m for the 43m and 20m boreholes respectively with an increase in gradient during the December 2012-August 2013 sequences of rainfall events. The 43m and 20m borehole water level tends to comprise of an increase in gradient for 2 months as a result of the high intensity (200mm over 6 days) rainfall sequences during January 2013 after which it follows a more gradual gradient.

The 3rd order triangulation position boreholes generally follow the same trend as each other; however the 61m borehole has a higher hydraulic head than the 34m borehole. This suggests the 61m borehole is flowing towards or contributing to the 34m borehole (see Figure 6.13). This separation of hydraulic heads at the 3rd order hillslope indicates that the deeper groundwater system is likely to intersect or contribute to higher order streams. The dH and dH/dT has not been calculated for the period August 2012-September 2012 due to the water level approaching equilibrium as a result of the borehole installations. The dH increased 0.78m and 0.37m for the 61m and 34m borehole respectively with a relatively steep gradient of 0.0091m/d during the October 2012-December 2012 rainfall period. These increases in dH and gradients are likely to occur as a result of the water levels recovering from the borehole installation phase. The low transmissivity seen in Figure 5.15 also contributes to the prolonged recovery of water levels at this point. These increases in dH are therefore not occurring as a result of ambient conditions. The dH increased to 0.37m and 0.32 m for the 61m and 34m borehole respectively with a gradual gradient present during the December 2012-August 2013 sequences of rainfall events. The 61m and 34m borehole water level gradient increased as a result of the high intensity sequence of rainfall events during January 2013 for 2 months after which it followed a gradual gradient. The drop in dH for the 34m borehole at 2013/04/25 was due to specific depth sampling which required the removal of groundwater for hydrochemical analysis of the larger WRC project discussed in chapter 1.

In general the hard rock aquifer water levels tend to respond to moderate (5-35mm/day) and high (45-95mm/day) intensity sequences of rainfall events. The responses are most notably seen during sequence 2 October 2012 – December 2012 and sequence 3 December 2012-February 2013 rainfall events. These responses are likely to be associated with piston recharge processes and likely on a regional scale due to the response time lags of roughly 2-3 months. Higher intensity sequence of rainfall events such as the 200mm of rainfall over 6 days occurring in January 2013 generate an increase in dH and ultimately recharge within the hard rock aquifer. The water levels of the boreholes drilled into the hard rock aquifer tend to have a higher hydraulic head than the boreholes drilled into the weathered aquifer at the 3rd order hillslope. This suggests given the general groundwater flow direction from the 1st order boreholes towards the 3rd order boreholes (see Figure 5.16 -5.19), the hard rock groundwater is likely to intersect or contribute to higher order streams. The general weathered aquifer water levels tend to respond to moderate (5-35mm/day) and high (45-95mm/day) intensity sequences of rainfall events. The responses are most notably seen during sequence 2 October 2012 – December 2012 and sequence 3 December 2012-February 2013 rainfall events. Given the shorter response time lag of roughly 2-3 weeks, these water level responses are likely to be associated with a localized piston recharge process. At the 2nd order riparian position 28m borehole, the rise in water level was relatively rapid during the high intensity rainfall events in January 2013. Given the position of this borehole its rise in water level is likely due to a direct loss from the 2nd order stream via indirect preferential flow recharge processes.

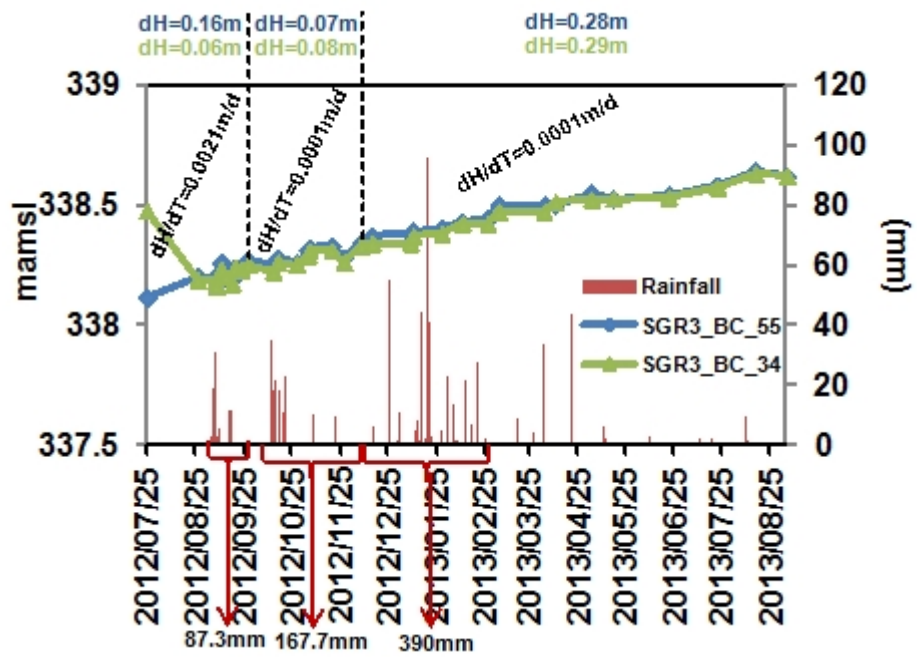
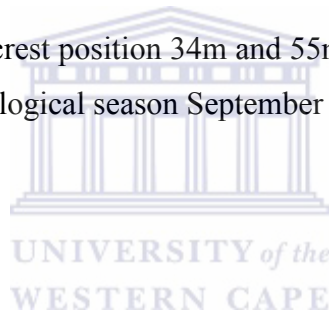


Figure 6.10 Third order crest position 34m and 55m borehole water level response to rainfall over the hydrological season September 2012 to September 2013.



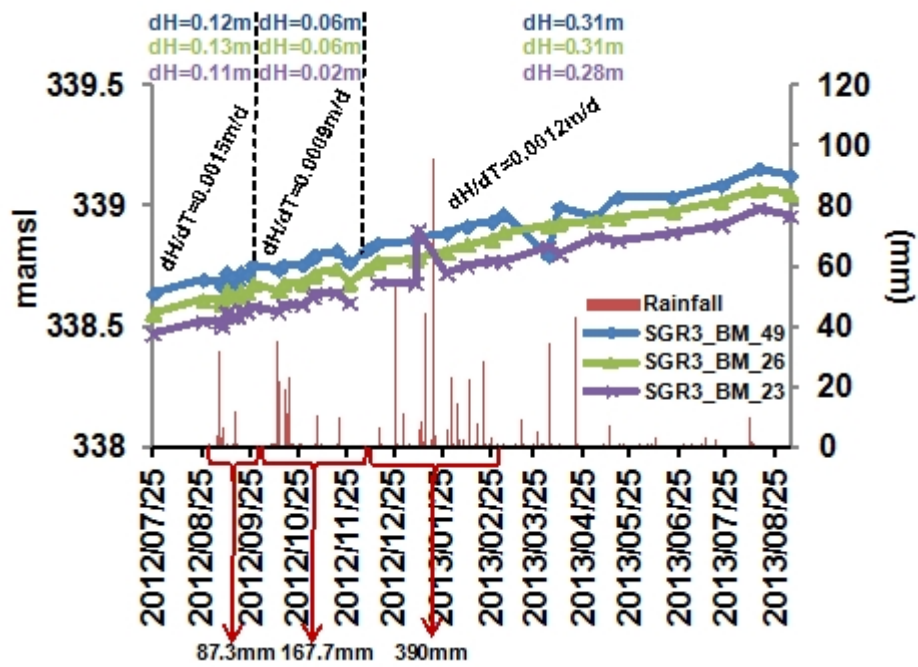


Figure 6.11 Third order mid-slope position 23m, 26m and 49m borehole water level response to rainfall over the hydrological season September 2012 to September 2013.

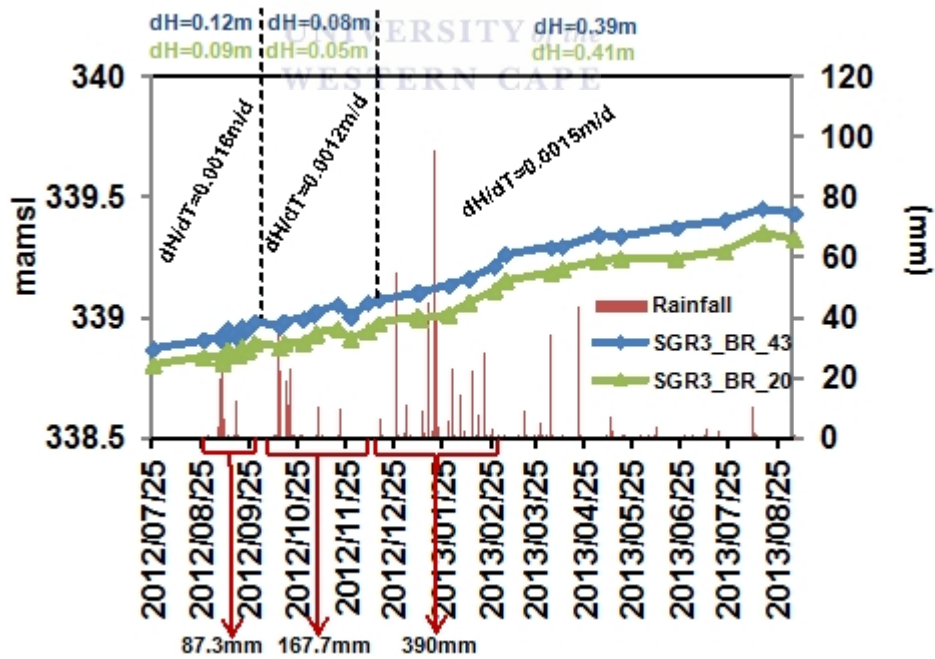


Figure 6.12 Third order riparian position 20m and 43m borehole water level response to rainfall over the hydrological season September 2012 to September 2013.

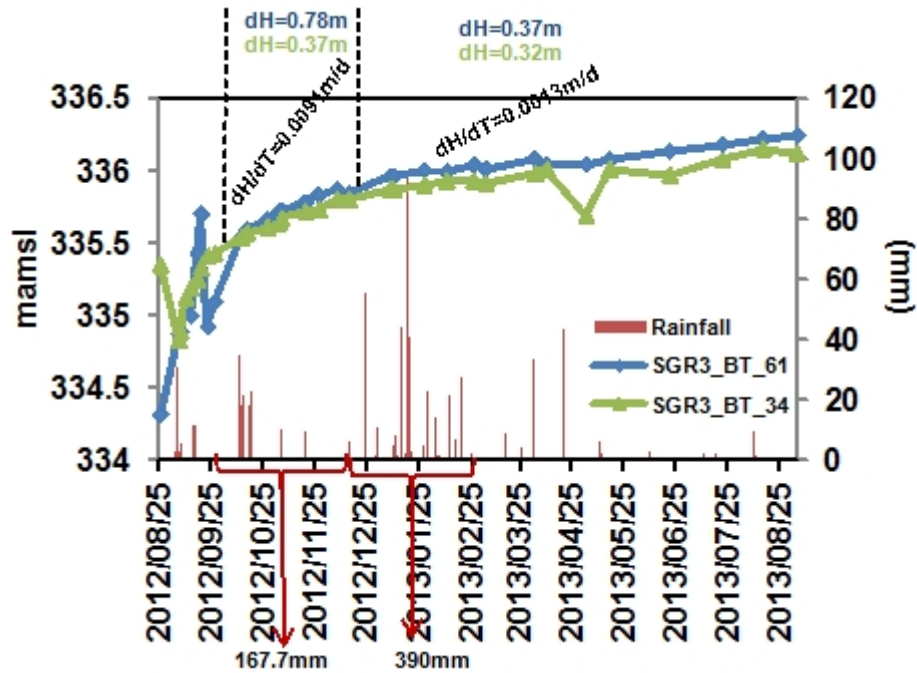


Figure 6.13 Third order triangulation position 34m and 61m borehole water level response to rainfall over the hydrological season September 2012 to September 2013.



6.4 General discussion:

It could be seen that specific sequence of rainfall cause a rise in water level and certain hydrological processes could be related to the manner in which these boreholes respond. In this study the data suggests a relationship between rainfall and water level responses require a particular sequence (see figure 6.3) of rainfall depth or high (45-95mm/day) intensity rainfall for the water levels to respond.

6.5 In-situ parameters/fluid logging

To gain an improved perspective of the spatial temporal distribution of groundwater within the catchment, in-situ parameters such as specific conductance (mS/cm) and temperature ($^{\circ}\text{C}$) were logged for each borehole every three months starting in September 2012-August 2013. The parameters serve as good indicators of groundwater movement and the vertical distribution of fractures. However, the fluid logs give no indication of any significant changes in the vertical distribution of temperature over the different seasons. (The

temperature fluid logs have been placed in Appendix II for the viewing of its variation in the vertical distribution of temperature and potential fracture characterisation of certain boreholes). Therefore the data here is potted spatially (see Figure 6.35 and 6.36). The purpose of the following discussion is to provide specific conductance fluid logs of the southern granite supersite boreholes on a quarterly basis to aid in the conceptualization of groundwater water movement.

6.5.1 First order boreholes

In the case of the 1st order crest position 103m borehole specific conductance values do not change significantly over the 3 successive monthly fluid logs (see Figure 6.14). This indicates that there is no active influx or mixing of fresh (low specific conductance) groundwater. Hence, there is no rapid response in water level to the moderate and high intensity sequence of rainfall events occurring in October 2012 and January 2013 respectively (see Figure 6.4).

The 1st order crest position 17m borehole shows low specific conductance (SC) values throughout the logs (see Figure 6.15). The low SC values suggest direct rainfall permeating into the weathered aquifer which is then slowly released into the hard rock aquifer possibly during high intensity (45-95mm/day) sequence of rainfall events. This can be seen by the decrease in SC values in the first 10m of the February 2013 fluid log (see Figure 6.14) in the 1st order crest position 103m borehole. The SC values do not show significant changes during the fluid logs of the 1st order riparian position 61m borehole (see Figure 6.16). This indicates that the stream is not likely to contribute or recharge the deep groundwater system at this point. The step seen at the depth of roughly 329,322, 309 and 298 mamsl is likely due to fractured zones as some of these changes in the vertical profile coincide with water strikes seen in Figure 5.2 and fracture zones depicted in Appendix II (Figure II a).

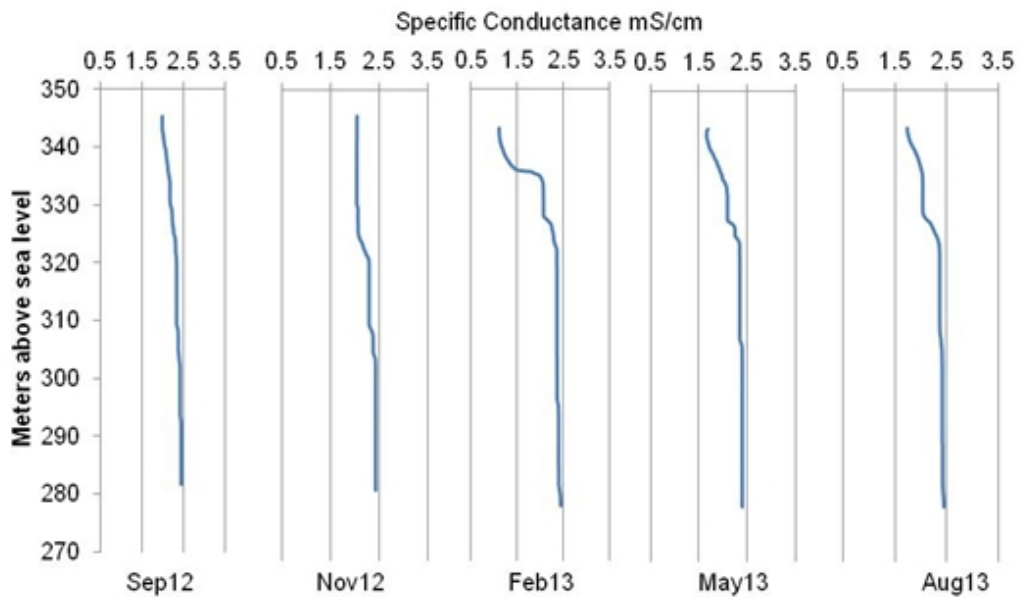


Figure 6.14 Specific conductance quarterly fluid log for the first order crest position 103m borehole.

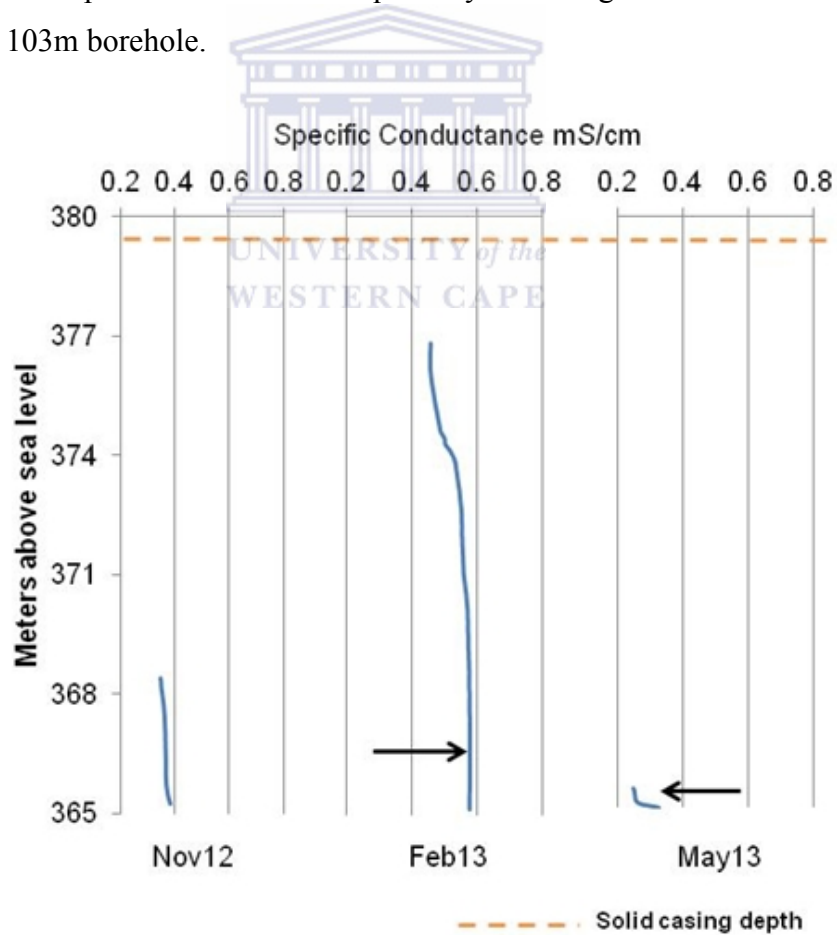


Figure 6.15 Specific conductance quarterly fluid log for the first order crest position 17m borehole.

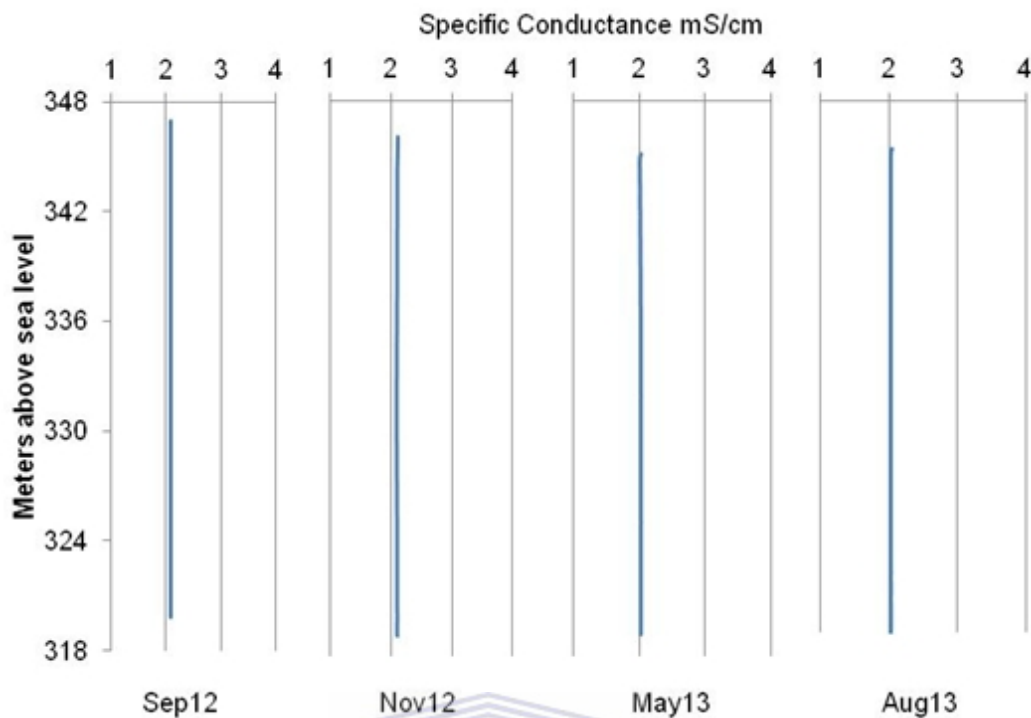
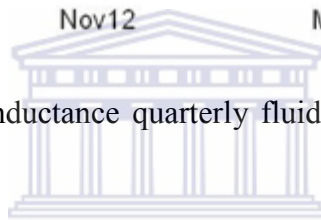


Figure 6.16 Specific conductance quarterly fluid log for the first order riparian position 61m borehole.



6.5.2 First/Second order triangulation boreholes

WESTERN CAPE

The 1st /2nd order triangulation position 61m borehole SC does not change significantly during the successive 3 monthly fluid logs (see Figure 6.17). This suggests no active influx of fresh groundwater (low SC) or rainfall into the deep groundwater system at this point. Hence, there is no rapid response in water level to the moderate (5-35mm/day) and high (45-95mm/day) intensity sequence of rainfall events occurring in October 2012 and January 2013 respectively (see Figure 6.7). The step seen at the depth of roughly 334 mamsl is likely to be due to the casing causing stagnant conditions within the borehole as discussed in Chapter 2 by Michalski (1989). However the 1st /2nd order triangulation position 36m borehole specific conductance changed significantly as seen in the February 2013 log (see Figure 6.18). Although the drop in SC cannot be correlated with a recharge event due to the delayed responses in water level seen in Figure 6.7, it is likely that an interflow contribution from the 1st order hillslope weathered aquifer produces the decrease in SC. This is possible based on the interpretation that in

general the shallow boreholes groundwater flow direction extends from the 1st order hillslope towards the 3rd order hillslope, as depicted in Figure 5.19.

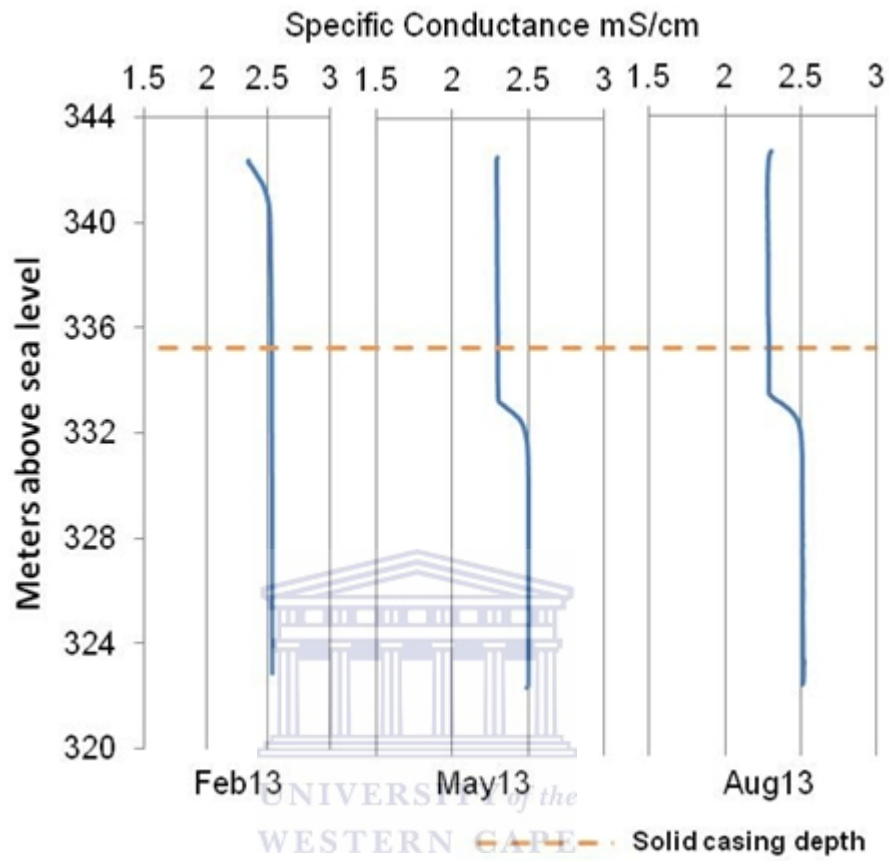


Figure 6.17 Specific conductance quarterly fluid log for the first/second order triangulation position 61m borehole.

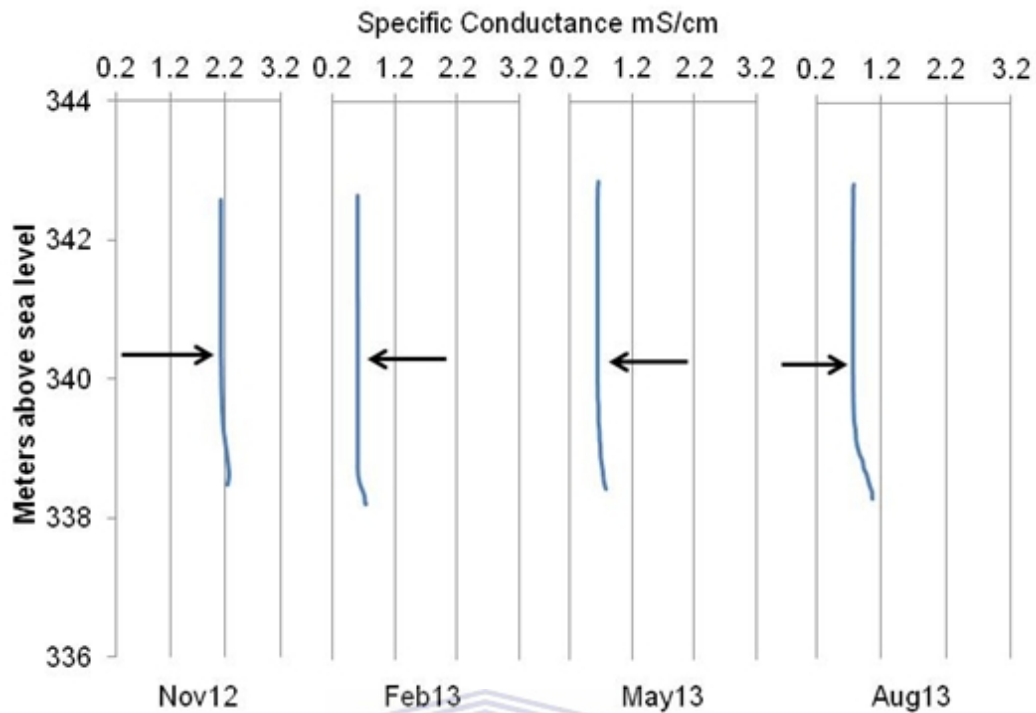


Figure 6.18 Specific conductance quarterly fluid log for the first/second order triangulation position 36m borehole.

6.5.3 Second order boreholes

The 2nd order crest position 55m and 40m borehole SC decreases significantly during the November 2012 fluid log (see Figure 6.19 and 6.20). This was during the moderate (5-35mm/day) intensity sequence of rainfall events during October 2012-December 2012 that caused the 40m borehole water level to rise by 4.83m seen in Figure 6.8. A 7.39m rise in the 40m borehole water level can be seen in Figure 6.8 as a result of the high (45-95mm/day) intensity sequence of rainfall events during January 2013. Therefore the decrease in SC is likely due to a flush of rainfall that infiltrated through the preferential conduit caused by the 40m borehole installation error. The step seen at the depth of roughly 332 mamsl in the 55m borehole fluid log is due to the casing causing stagnant conditions within the borehole. The SC of the 2nd order riparian position 49m borehole does not change significantly, an indication of no active influx of fresh groundwater into the hard rock groundwater system at this point (see Figure 6.21). Hence, there is

no rapid response in water level to the moderate and high intensity sequence of rainfall events occurring in October 2012 and January 2013 respectively.

The 2nd order riparian position 28m borehole SC decreased quite significantly during the November 2012 and consequent fluid logs (see Figure 6.22). This decrease in SC for the 28m borehole can be correlated with the rise in water level due to the October 2012 moderate (5-35mm/day) and January 2013 high (45-95mm/day) intensity sequence of rainfall events in Figure 6.9. It is likely that the 2nd order stream recharged the weathered aquifer due to the rapid response in the water level rise and recession of the 28m borehole. The drop in SC also infers the contribution of fresh (low SC) water in the vicinity, possibly from the 2nd order stream. The 2nd order riparian position 49m borehole SC fluid logs do not change over time, suggesting no active influx of fresh groundwater into the deep groundwater system at this point.

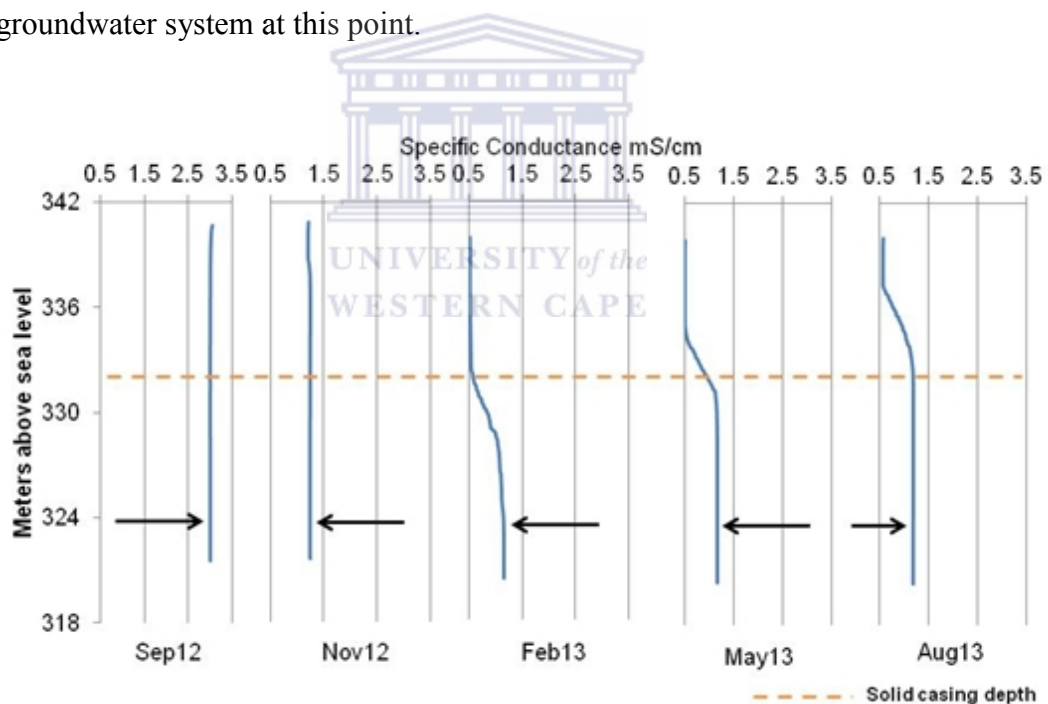


Figure 6.19 Specific conductance quarterly fluid log for the second order crest position 55m borehole.

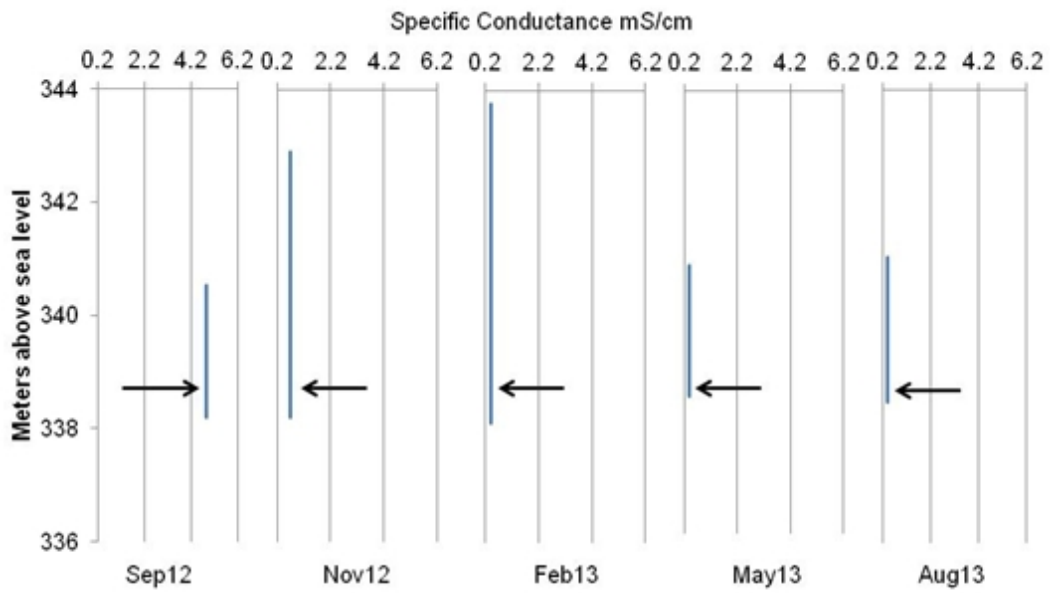


Figure 6.20 Specific conductance quarterly fluid log for the second order crest position 40m borehole.

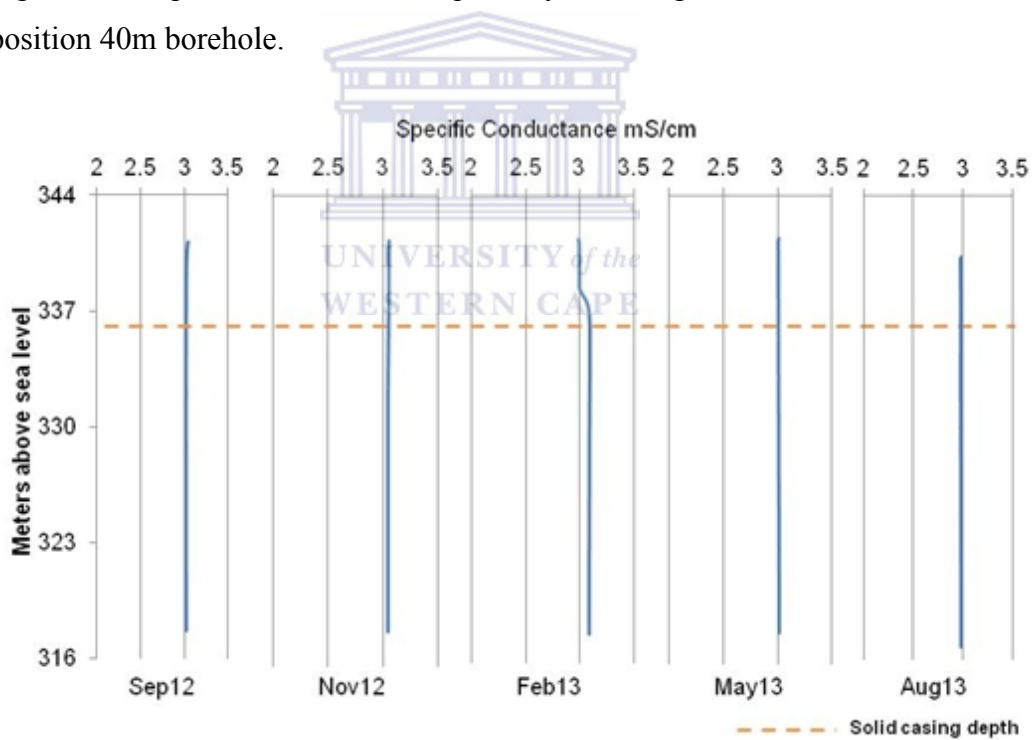


Figure 6.21 Specific conductance quarterly fluid log for the second order riparian position 49 m boreholes.

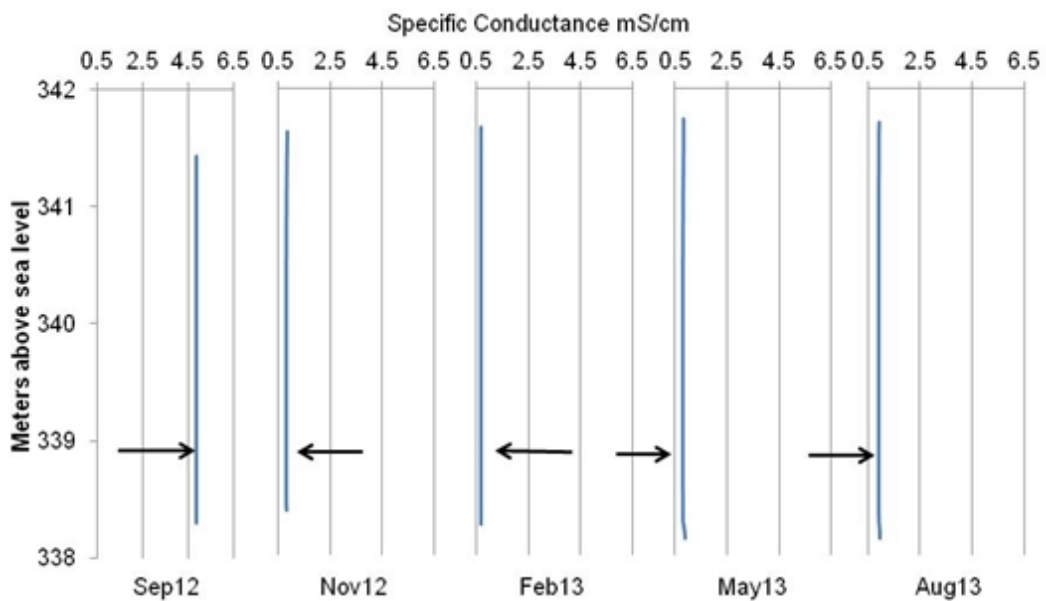


Figure 6.22 Specific conductance quarterly fluid log for the second order riparian position 28 m boreholes.

6.5.4 Third order boreholes

The 3rd order crest position 55m borehole SC does not change significantly during the fluid logs (see Figure 6.23). This suggests no active influx of fresh groundwater (low SC) or rainfall into the deep groundwater system at this point. The lengthy response time lag in water level to the moderate and high intensity sequence of rainfall events occurring in October 2012 and January 2013 also supports a non active groundwater flow system (see Figure 6.10). The 3rd order crest position 34m borehole SC slowly decreases at the November 2012 fluid log and continues to decrease with the consequent logs (see Figure 6.24). The water level response at this point does not correlate with a decrease in SC inferring a possible recharge event. However possible interflows from the lower order weathered aquifer hillslopes are likely to contribute active and therefore fresh (low SC) groundwater flow.

The 3rd order mid-slope position 49 m boreholes does not change significantly during the fluid logs (see Figure 6.25). This suggests no active influx of fresh groundwater (low SC) or rainfall into the deep groundwater system at this point. This correlates with the response in water level at this point which has a time lag

of 2 months to the moderate and high intensity rainfall events occurring in October 2012 and January 2013 (see Figure 6.11). Change in SC in the 49m borehole fluid log profile at 323 mamsl depth is likely to be a fractured zone as the lithology log describes highly weathered and fractured granite at this depth in Figure 5.8, (see Appendix II Figure II n for fracture characterisation). The 3rd order mid-slope position 26m borehole SC decreases quite significantly at the February 2013 fluid log. The water level response at this point does not correlate with the decrease in SC which is likely inferring a recharge event. It's possible that interflows from the lower order weathered aquifer hillslopes are contributing active and therefore fresh (low SC) groundwater flow to this point.

The 3rd order riparian position 43 m borehole SC does not change significantly during the fluid logs (see Figure 6.27). This suggests no active in-flux of fresh groundwater (low SC) or rainfall into the deep groundwater system at this point. This correlates with the water level response at this point which does not respond rapidly to the moderate and high intensity rainfall events seen in October 2012 January 2013 respectively (see Figure 6.12). The 3rd order riparian position 20 m borehole SC has a very slight decrease at the February 2013 fluid log and consequent fluid logs (see Figure 6.28). The no or slight changes in the groundwater flow system at the 43m and 20m boreholes suggests that the 3rd order stream is likely not to contribute to the shallow and deep groundwater flow system at this point.

The 3rd order triangulation position 61 m borehole SC does not change significantly during the fluid logs (see Figure 6.29). This suggests an in-active influx of fresh groundwater (low SC) or rainfall into the deep groundwater flow system at this point. This correlates with the lengthy lag time in water level response of about 3 months to the moderate to high intensity rainfall events of October 2012 and January 2013 at this point. The step seen at the depth of roughly 326 mamsl in the 61m borehole fluid logs is due to the casing causing stagnant conditions within the borehole (Michalski, 1989). The 3rd order triangulation position 34m borehole SC slowly decreases at the November 2012 fluid log and continues to decrease with the consequent logs (see Figure 6.30) This suggests

that possible interflows from the lower order weathered aquifer hillslopes are contributing active and therefore fresh (low SC) groundwater flow to the 34m borehole.

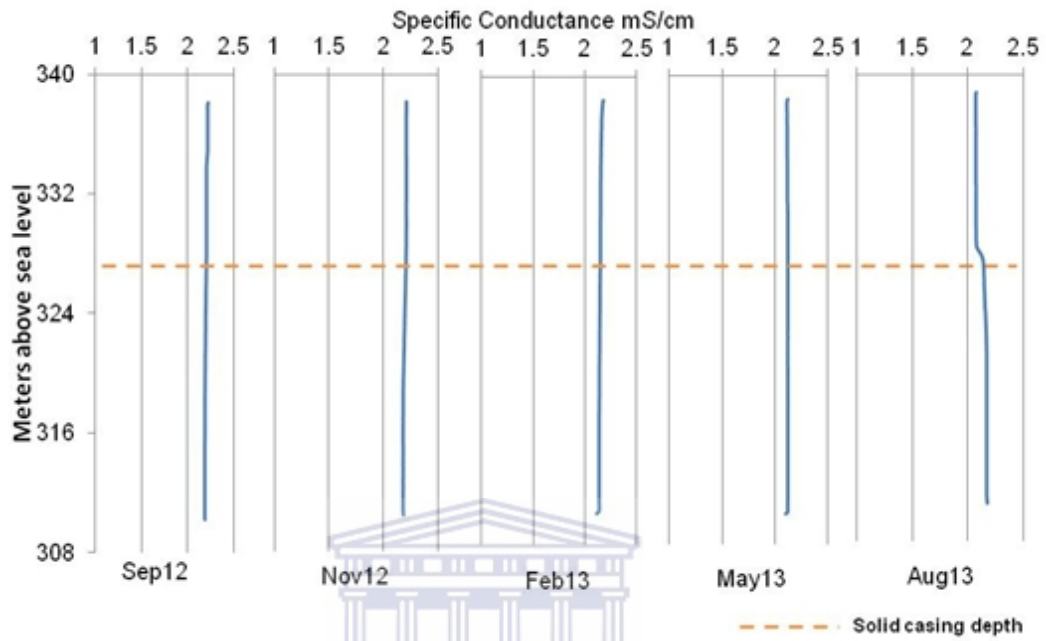
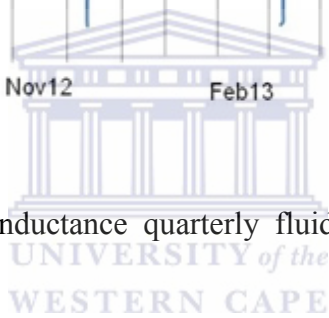


Figure 6.23 Specific conductance quarterly fluid log for the third order crest position 55m borehole.



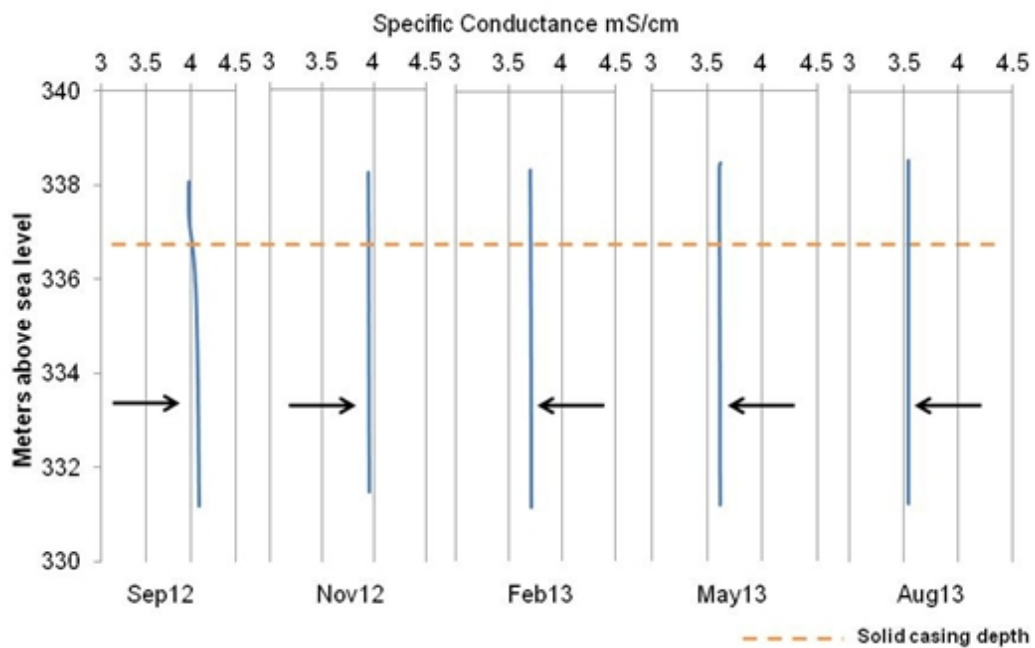


Figure 6.24 Specific conductance quarterly fluid log for the third order crest position 34m borehole.

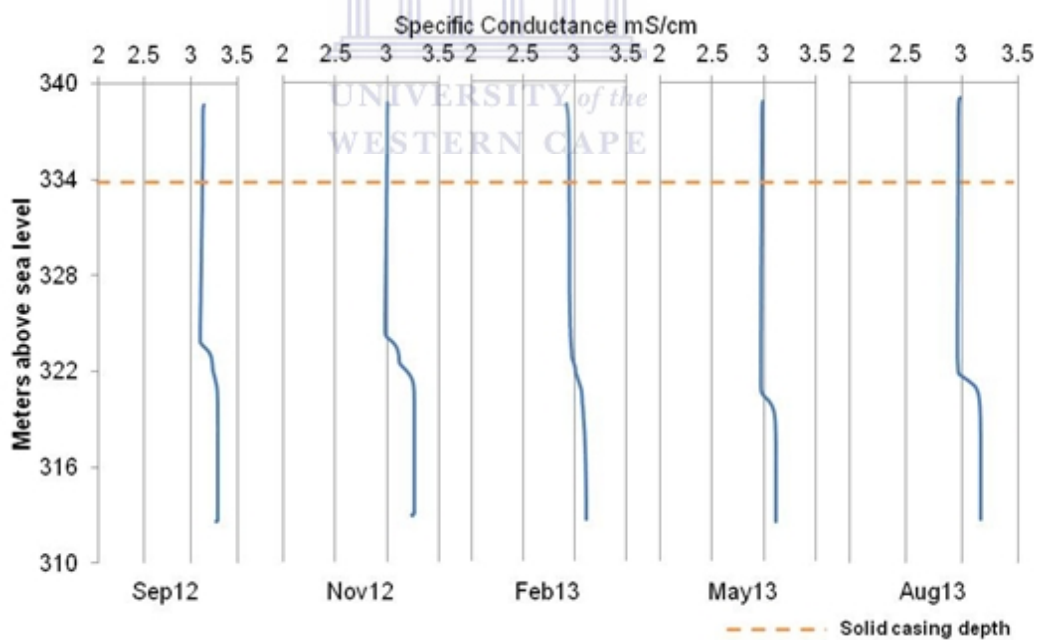


Figure 6.25 Specific conductance quarterly fluid log for the third order mid-slope position 49m borehole.

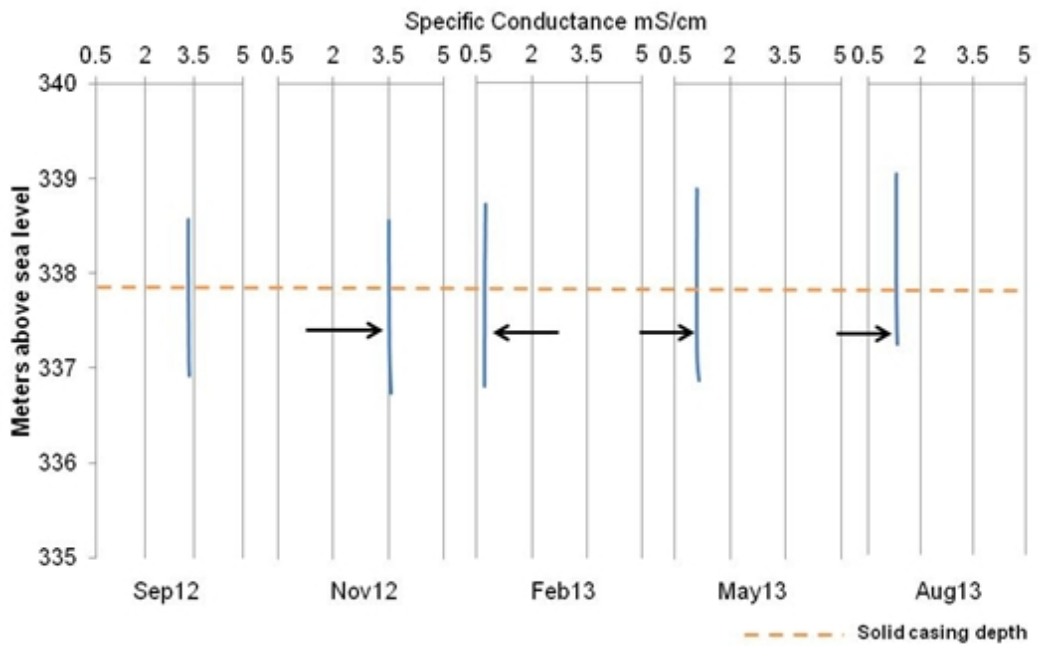


Figure 6.26 Specific conductance quarterly fluid log for the third order mid-slope position 26m borehole.

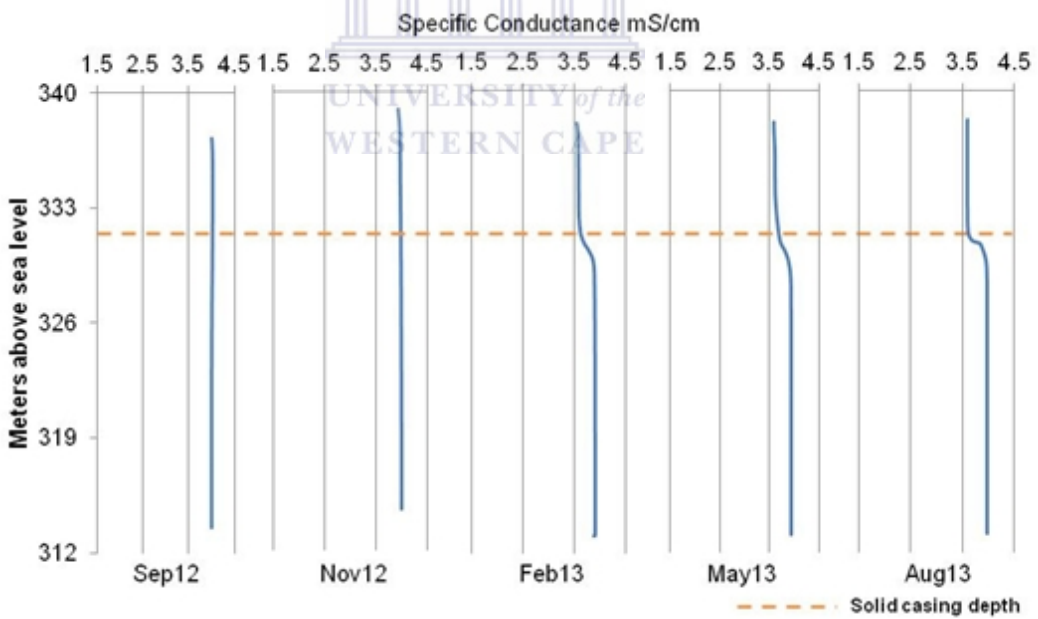


Figure 6.27 Specific conductance quarterly fluid log for the third order riparian position 43m borehole.

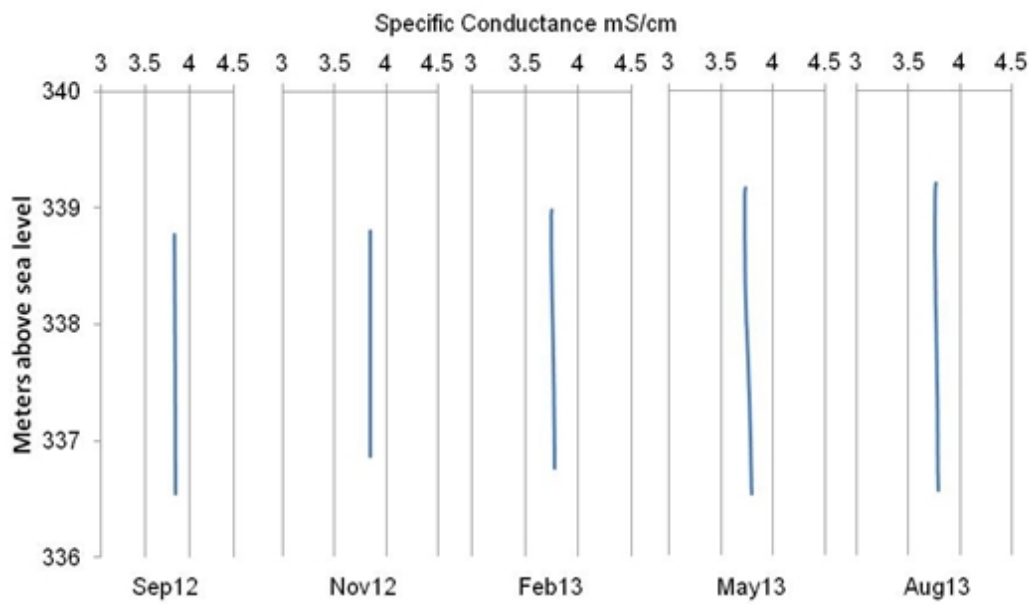


Figure 6.28 Specific conductance quarterly fluid log for the third order riparian position 20m borehole.

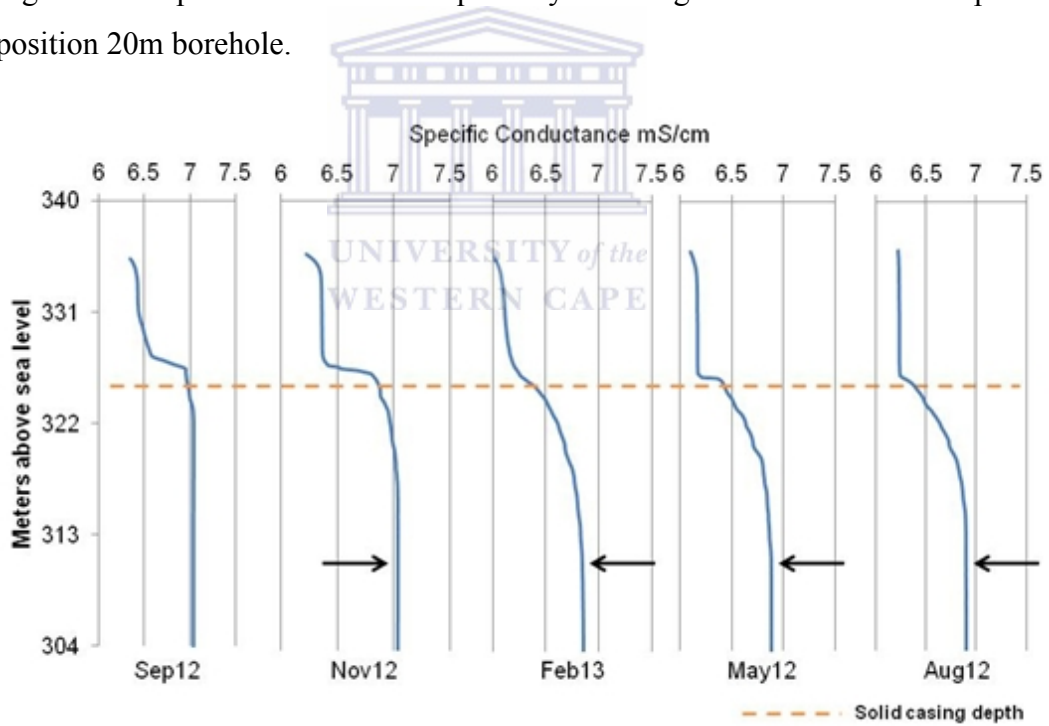


Figure 6.29 Specific conductance quarterly fluid log for the third order triangulation position 61 m borehole.

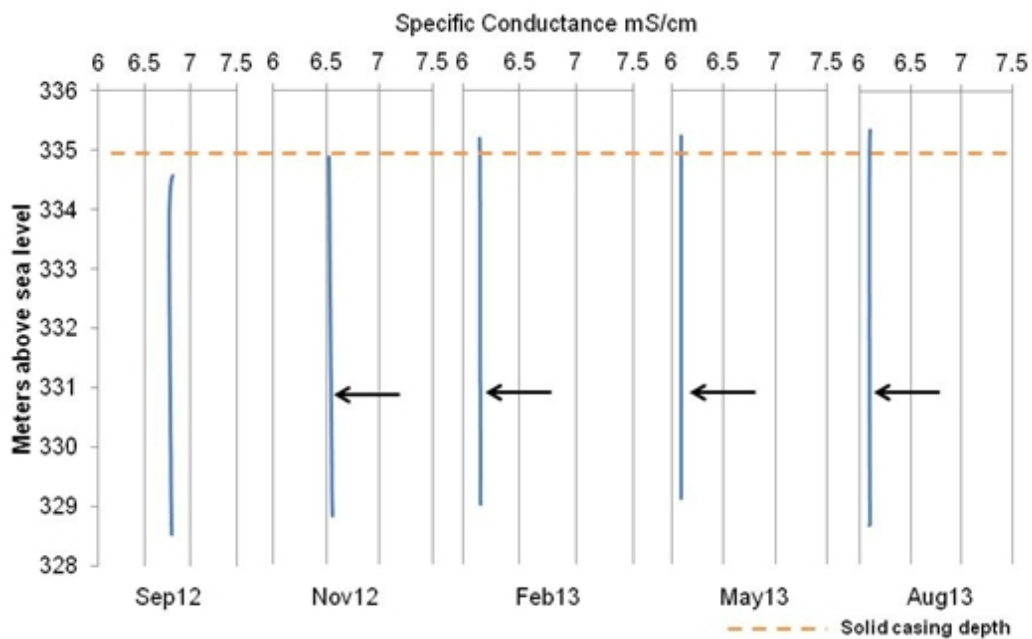
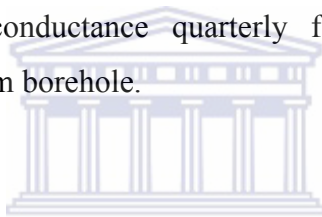


Figure 6.30 Specific conductance quarterly fluid log for the third order triangulation position 34m borehole.



6.5.5 Spatial distribution of average specific conductance for the southern granite supersite boreholes

The average specific conductance or SC for the dry (May 2013 and August 2013) and wet (November 2012 and February 2013) season fluid logs have been plotted to enable the spatial observation of the change in SC for the shallow and deep boreholes across the catchment. These spatial SC plots correlate with the groundwater flow direction seen in Figure 5.16-5.19 which moves from the 1st order hillslope boreholes with low SC towards the 3rd order hillslope boreholes with high SC (see Figure 6.31-6.34). Across the catchment the SC during the dry season fluid logs was slightly lower than the wet season fluid logs. This suggests that the generally low T values across the catchment resulted in the slow movement of fresh or low SC water through the shallow and deep groundwater flow system.

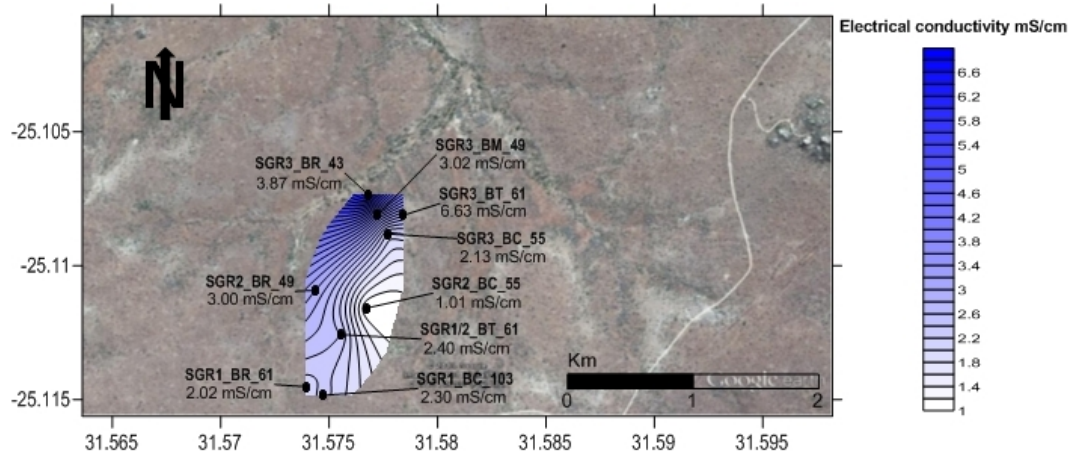


Figure 6.31 Spatial distribution of specific conductance for the southern granite supersite deep boreholes during the dry season combined averaged value fluid logs of May 2013 and August 2013.

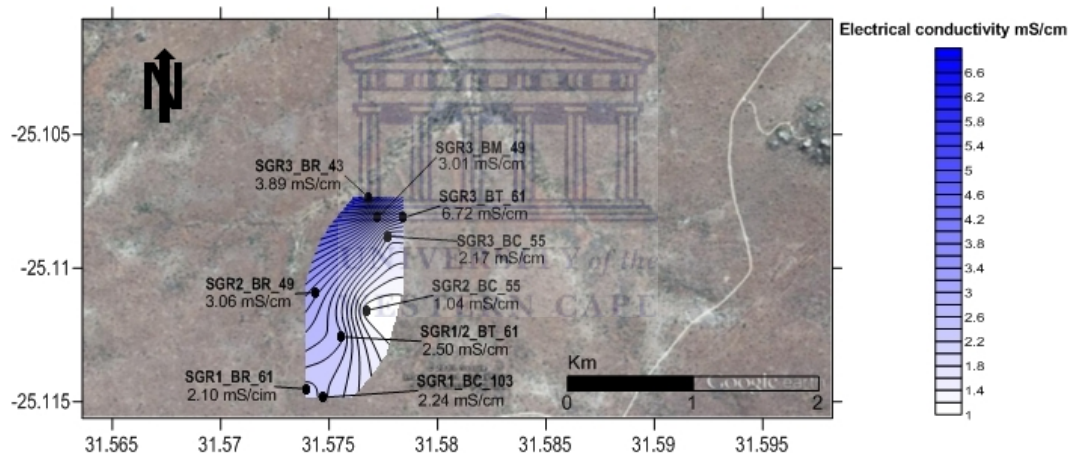


Figure 6.32 Spatial distribution of specific conductance for the southern granite supersite deep boreholes during the wet season combined averaged value fluid logs of November 2012 and February 2013.

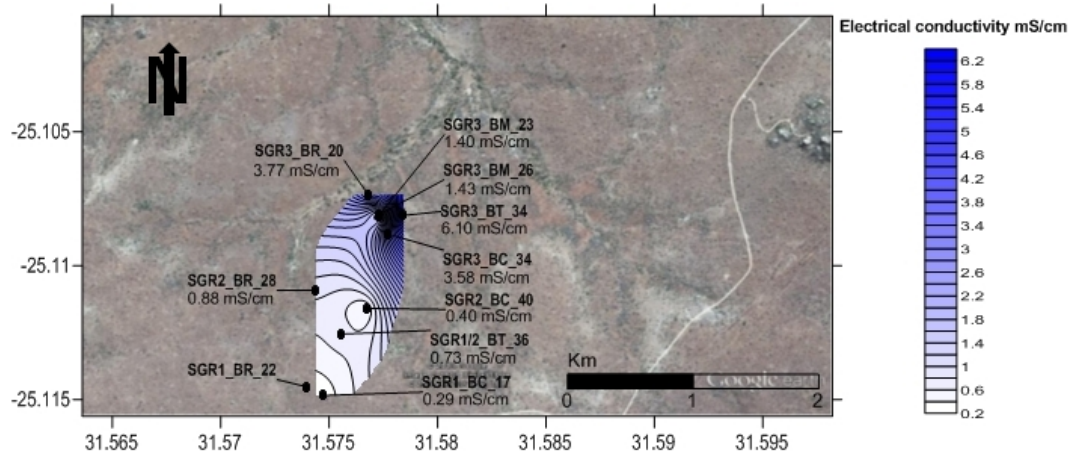


Figure 6.33 Spatial distribution of specific conductance for the southern granite supersite shallow boreholes during the dry season combined averaged value fluid logs of May 2013 and August 2013.

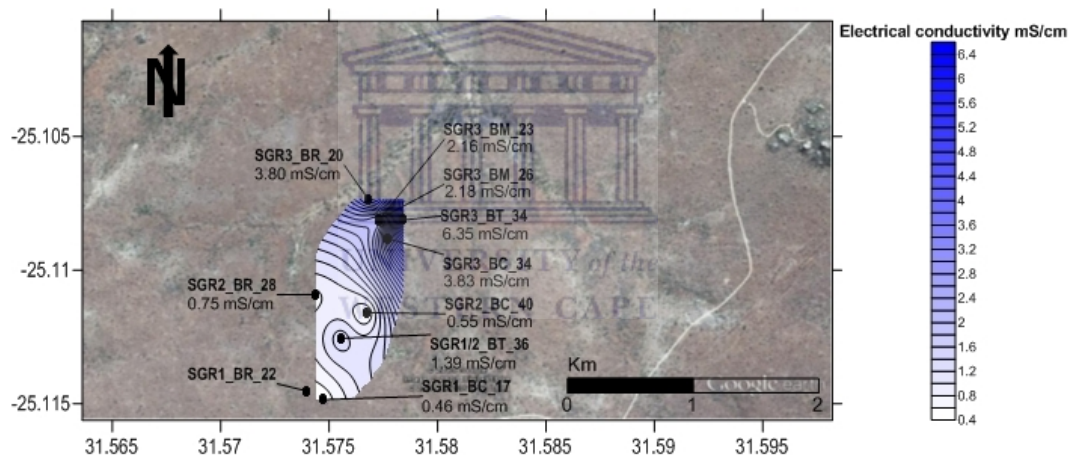


Figure 6.34 Spatial distribution of specific conductance for the southern granite supersite shallow boreholes during the wet season combined averaged value fluid logs of November 2012 and February 2013.

6.5.6 Spatial distribution of average temperatures for the southern granite supersite boreholes

The average temperatures for the dry (May 2013 and August 2013) and wet (November 2012 and February 2013) season fluid logs have been plotted to enable the spatial observation of the change in temperature for the shallow and deep boreholes across the catchment. The general temperature gradient correlates with the groundwater flow direction seen in Figure 5.16-5.19 moving from the

high temperatures at the 1st order hillslope boreholes towards the low temperatures on 3rd order hillslope boreholes (see Figure 6.35-6.36)

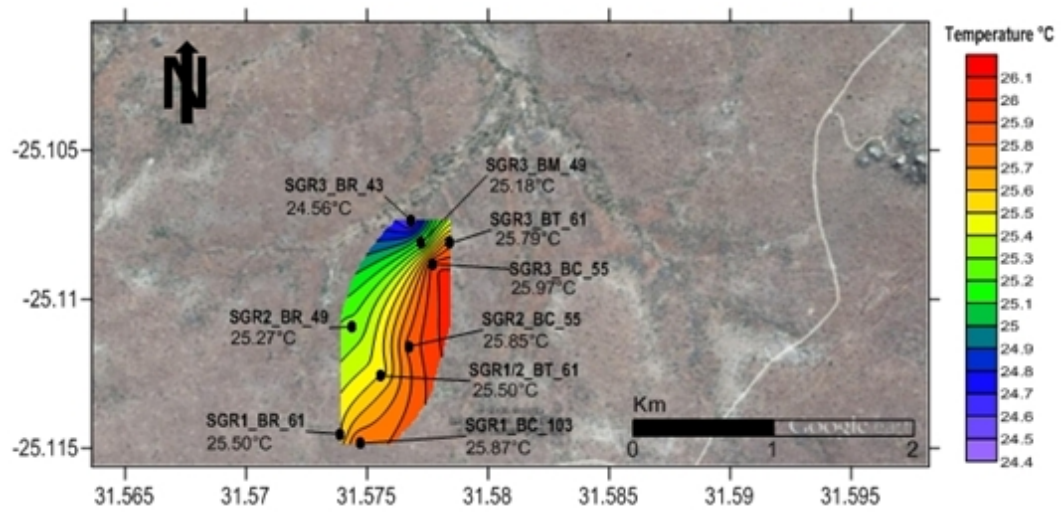


Figure 6.35 Spatial temperature distribution for the southern granite supersite deep boreholes during the hydrological season fluid logs of November 2012 to August 2013.

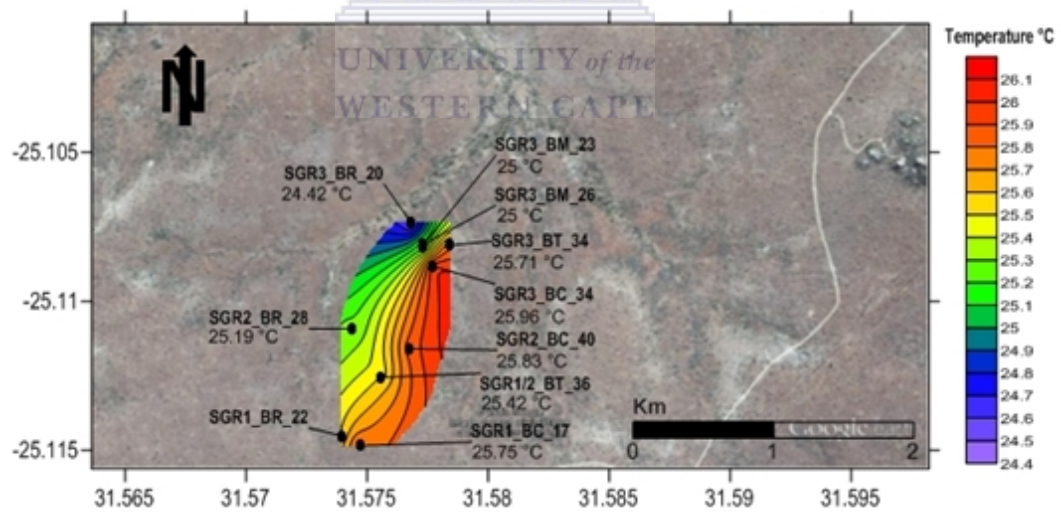


Figure 6.36 Spatial temperature distribution for the southern granite supersite shallow boreholes during the hydrological season fluid logs of November 2012 to August 2013.

Chapter 7

Synthesis: Hydrogeological conceptual site model

7.1 Introduction

This chapter consolidates the findings presented in chapters five and six to achieve a site specific conceptualization of the spatial – temporal groundwater water distribution of the southern granite supersite. In order to achieve this, a conceptual site model is represented schematically to portray the dominant hydrogeological processes within the catchment based on the findings of this research.

7.2 Discussion

7.2.1 First order hillslope

The 1st order crest position borehole observations and characterisations suggest that groundwater recharge occurs locally via a direct piston recharge process into the weathered aquifer (see green circled recharge area and yellow arrow a on Figure 7.1). The soils present on the 1st order crest also suggest a fast potential recharge pathway for rainfall reaching the groundwater level (see Figure 3.2). The weathered aquifer then acts as a retention layer and temporally retains the rainfall water and releases it slowly over time via a piston flow process due to the low transmissivity values seen in Figure 5.15, hence the perched water table. During the high intensity sequence of rainfall events during January 2013 where nearly 200mm fell over 6 days a 2m difference in hydraulic head between the perched water table and the 1st order stream occurred and increasing toward to the 2nd and 3rd order level loggers. It is likely that this gradient generated an interflow process, whereby the perched water table contributed to stream flow at the 1st order stream and possibly at higher stream orders. The soil hydrology also supports a fast interflow process from the crest towards the riparian zone at the 1st order hillslope (see Figure 3.2). The possibility of the perched water table leaching into the deep groundwater flow system is also likely during this time of the hydrological season due to the decrease in SC discussed in chapter 6. The

lengthy response time lags of roughly 2 months in the deep groundwater system at the 1st order crest and riparian suggest a piston recharge process that is driven by more regional scale hydrogeological processes (see blue arrows 1-5 on Figure 7.1). The 1st order riparian position 61m borehole fluid log observations suggest that the 1st order stream does not contribute to the deep groundwater system at that point due to no changes in the SC values. Throughout the hydrological season a constant negative hydraulic head (ranging 31.50-32.30m) from the stream towards the deep groundwater level (see Appendix III figure III a) at this point also suggest no contribution from the stream to the deep groundwater system.

7.2.2 Second order hillslope

The 2nd order crest position 40m borehole observations and characterisations suggest that due to a borehole construction error, localized groundwater recharge doesn't occur at this point. The rapid and high responses in the shallow borehole were due to a conduit created by the gravel lining the borehole casing. The lag in response time of the 55m borehole water level again supports the role of regional groundwater water fed system (see blue arrows 1-5 on Figure 7.1). The 2nd order riparian position 28m borehole observations and characterisations suggest local groundwater recharge in the weathered aquifer via indirect recharge from the 2nd order stream. This was seen by the rapid response of 2 weeks in the riparian position 28 m borehole water levels as a result of the moderate (10-35mm/day) and high (45-95mm/day) intensity sequence of rainfall events occurring in October 2012 and January 2013 respectively. The SC also decreased quite significantly during these periods of rainfall, suggesting a recent influx of fresh (low SC) water most likely to be relatively direct losses from the stream channel (see green circle recharge area on Figure 7.1). The lag in response time of roughly 2 months in 49m borehole water level at the riparian position suggests a regional groundwater flow system (see blue arrows 1-5 on Figure 7.1). The SC fluid logs did not significantly change during the hydrological season suggesting no recent influx of fresh water. Throughout the hydrological season a constant negative hydraulic head (ranging 21.55-21.90m) from the stream towards the deep groundwater level (see Appendix III figure III b) at this point suggests it is likely

that the deep groundwater system at this point does not receive contribution from the 2nd order stream.

7.2.3 Third order hillslope

The 3rd order hillslope borehole observations and characterisations suggest that groundwater recharge does not occur along this hillslope. This was due to the lengthy lag in response time of water levels of roughly 2 months to the 3 major sequences of rainfall events throughout the hydrological season. This suggests that the deep hard rock aquifer is connected to a regionally driven groundwater flow system (see blue arrows 1-5 on Figure 7.1). The drop in SC in the shallow crest, mid-slope and triangulation position borehole suggests that it is likely an influx of fresh groundwater via interflow from the weathered aquifer from the lower 1st and 2nd order catchments (see yellow arrows e, f and g on Figure 7.1). The presence of duplex soils (sodic site) along the 3rd order hillslope also supports the possibility of a shallow interflow process (see Figure 3.2). The possibility of the 3rd order stream contributing to the weathered or hard rock aquifer does not occur at the riparian zone. This is due to the water levels responding in a more regional trend to the 3 major sequences of rainfall. The unchanged SC values throughout the quarterly fluid logging at this point and negative hydraulic head (ranging from 8.90-9.75m) from the stream water levels towards the groundwater levels (see Appendix III figure III c) throughout the hydrological season suggests no contribution from the stream to the shallow or deep groundwater system.

7.2.4 General conclusion

The overall perspective of the southern granite supersite hydrogeology distribution is depicted in Figure 7.1. It reveals that two types of aquifers exist within the southern granite supersite catchment, namely the shallower weathered (orange) and deep hard rock granite/gneiss (grey) aquifer. Along the 1st, 2nd and 3rd hillslope weathering is generally deeper at the crest and shallower at the riparian zones. The general topographical slope is greatest at the 1st order hillslope and decreases towards the 3rd order hillslope. The general hard rock

aquifer (see blue arrows 6, 7 and 8) and weathered aquifer (see yellow arrows d, e, f and g) groundwater flow direction is from the 1st order towards the 3rd order running almost parallel to the streams. These complementary tools provided an improved conceptual understanding of the environmental setting and hydrogeological processes such as recharge mechanisms and interaction between groundwater, surface water and the vadose zone from a point along the hillslope to the overall 3rd order catchment.

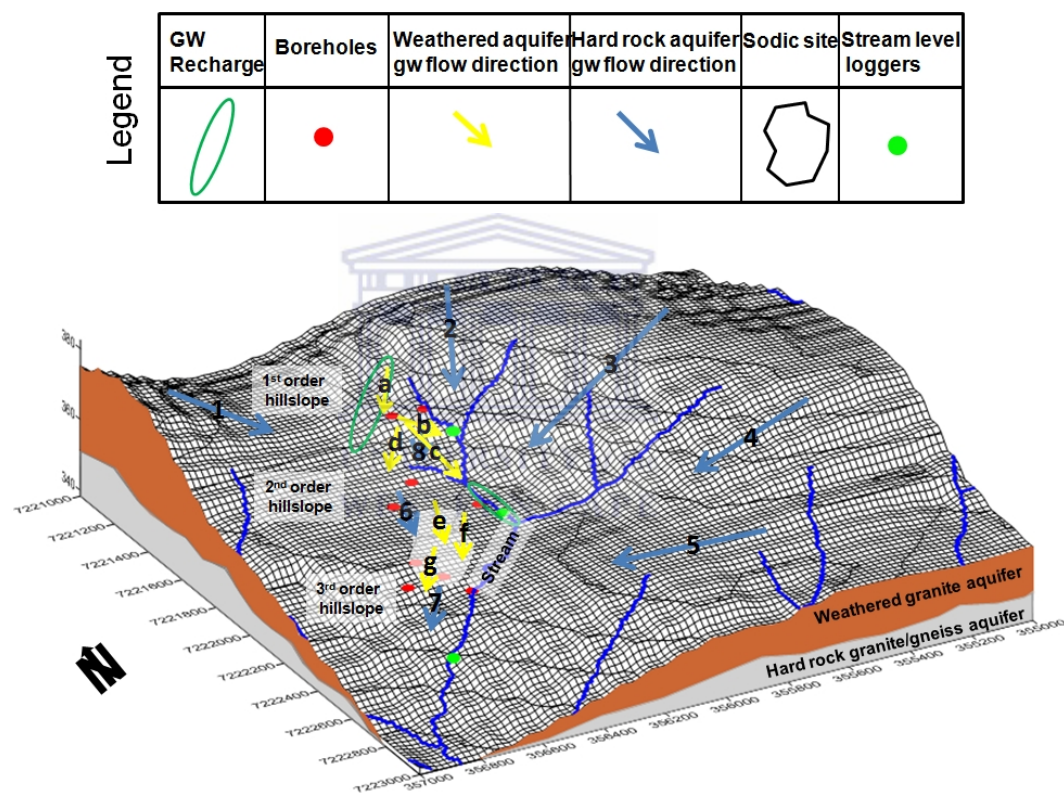


Figure 7.1 A hydrogeological conceptual site model of the southern granite supersite.

Chapter 8

Conclusions and Recommendations

8.1 Conclusion

In conclusion the lithological characterisations for the southern granite supersite based on the borehole lithology logs are described as a weathered and partially fractured /weathered hard rock granite/gneiss aquifer. The hard rock appears to be fractured in certain locations i.e. the 1st order crest position 103m borehole and 3rd order mid-slope position 49m borehole lithology log. The weathered aquifer ranges from highly weathered to completely weathered granite/gneiss.

Based on the groundwater hydraulic head spatial interpolation of all boreholes, the general weathered and hard rock aquifer groundwater flow direction extends from the 1st order hillslope towards the 3rd order hillslope. The groundwater flow path regime within these ephemeral 3rd order catchments are split into two domains, namely the weathered and hard rock groundwater flow paths. The weathered aquifer has a local groundwater flow system in that these boreholes responded rapidly to the moderate (5-35mm/day) and high (45-95mm/day) intensity sequence of rainfall events occurring in October 2012 and January 2013 respectively.

The fresh groundwater seen in the SC fluid logs adds to the possibility of a localized piston recharge process particularly confined to the 1st order crest position 17m borehole. The weathered aquifer also potentially plays a role in stream flow contribution via interflow processes at the 1st order hillslope given the hydraulic head generated from the perched water table toward the 1st, 2nd and 3rd order streams. The 2nd order hillslope riparian position 28m borehole within the weathered aquifer has likely responded to a gaining reach of the 2nd order stream during the high intensity (45-95mm/day) sequence of rainfall events during January 2013. This occurred as the borehole water level had risen and receded rapidly, and given its position relative to the stream it is possible via indirect recharge processes the stream could contribute to groundwater. The February 2013 specific conductance (SC) fluid logs of the 2nd order riparian position 28m

borehole also suggests a recent in- flux of fresh (low SC) water, likely 2nd order stream water.

The weathered aquifer boreholes along the 3rd order hillslope had negative hydraulic heads toward the 3rd order stream and a lengthy response time lag to the sequence of rainfall events over the hydrological season. This suggests no potential for localized recharge processes or interaction with the 3rd order stream. However the SC fluid logs revealed the possibility of fresh (low SC) water arriving at these boreholes due to the slight decrease in the SC values. This suggests a possible inflow of fresh groundwater from the lower order weathered aquifer.

The hard rock aquifer boreholes across the catchment had lengthy lags in response time (roughly 2-3 months) to the moderate (5-35mm/day) and high (45-95mm/day) intensity sequence of rainfall events. This suggests the hard rock aquifer is part of a regional groundwater flow system. The SC fluid logs for all the boreholes have not changed over the hydrological season, suggesting no flux of recent fresh groundwater. Therefore the boreholes within the hard rock aquifer could be seen as quite generic in their response.

The generally low transmissivity values and the continued rise in water levels for both weathered and hard rock aquifer boreholes after the wet season could be characteristic of hydraulic boundaries or buffer areas within these ephemeral landscapes. Similar observations in water level trend have been seen in certain boreholes i.e. Matlari borehole monitored by DWA within similar landscapes (see Appendix V figure V a). These potential hydraulic boundaries are likely to play a role in the regional hydraulic head sustainability throughout the dry season and generating the hydraulic gradient needed for groundwater to contribute baseflow to the perennial streams.

8.2 Recommendations for future research

In order to fully understand the response of the shallow and deep borehole water levels to the sequence of rainfall events, automatic level loggers with hydrochemical sensors (temperature, EC, pH, dissolved oxygen etc) are required. This would enable a detailed observation of groundwater regime across these catchments; in that majority of the response to rainfall events or stream and vadose zone interactions could be recorded. The true rise in groundwater levels will be known which could be correlated with the stream level loggers on a higher frequency. Additional groundwater, surface water and rainfall should be sampled for stable isotopes (i.e. oxygen 18 and deuterium) and major and minor constituents (i.e. silicon, magnesium, sodium, chloride) based on specific events or thresholds as during these events the interaction between the various sources of water is likely to occur. This could be achieved by installation of an incremental rainfall and stream sampler which could be calibrated to capture specific thresholds i.e. groundwater response to rainfall events. The incorporation of isotope and major and minor constituents would serve as an additional layer of insight into the correlation between these water resources and the dominant hydrological processes. The combination of the above mentioned parameters would provide greater insight on a groundwater interaction with the vadose zone and streams and vice versa.

To obtain the specific yield (S) for the boreholes of the southern granite supersite would provide an import parameter to quantify the recharge of the catchment. It is recommended that multiple borehole tests be performed to obtain the S parameter.

Once the current conceptual model has been updated with the above recommendations a numerical model i.e. modflow, Feflow etc, could be developed in order to predict future scenarios of various input and output factors such as groundwater recharge, discharge, interaction with surface water, vegetation transmission losses such as evapotranspiration for these water scarce environments. These predictions would assist in the integrated water management of these pristine catchments as the dominant hydrological processes would be revealed and applied to similar environmental settings.

8.3 Recommendations for management

An upscale of the supersite to higher stream orders would be beneficial in terms of understanding at which stream order the deep groundwater starts interacting with the stream, as the deeper groundwater system plays an important driving factor for these ecosystems when up scaling to a landscape or regional scale. It is likely that these areas are important hydrogeological boundaries or a buffer area that contributes to the regional hydraulic gradient driving baseflow into the perennial streams. Therefore the protection of these head water catchments could be part of a future protected area as in certain cases these ephemeral streams are mined for sand to grade tourist roads within KNP.

This study concluded that certain reaches of the stream is likely to contribute to groundwater recharge. Given the scarcity of water resources within semi-arid environments attention should be geared towards the sustainable development of water resources as a whole. When considering a water supply scheme scenario, these 3rd order scale head water streams within the granite landscapes are characteristic of low transmissive aquifer properties. Given the 19 boreholes drilled, the success rate of potentially high yielding boreholes was low and after Wright (1992) more than 0.25L/s are required for hand pumps in rural semi arid settings. Therefore these environmental settings are likely not to be part of a sustainable yield management plan for groundwater abstraction.

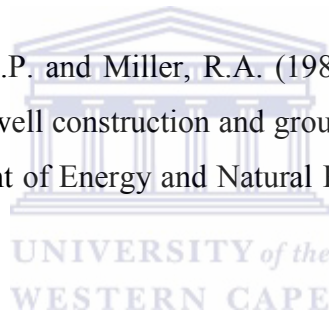
Reference

Abem. (2010). Instruction manual, Lund Imaging System, Abem Instrument AB, Sundbyberg, Sweden.

Anderson, M.P. (2005). Heat as a groundwater tracer. *Groundwater journal*, 43 (6): 951-968.

Australian Drilling Industry Training Committee Limited. (1997). *Drilling: The manual of methods, applications, and management*, 4th ed. CRC Press, LLC.

Barcelona, M.J., Gibb, J.P. and Miller, R.A. (1983). A guide to the selection of material for monitoring well construction and groundwater sampling. Illinois state water survey, Department of Energy and Natural Resources. SWS contract report 327.



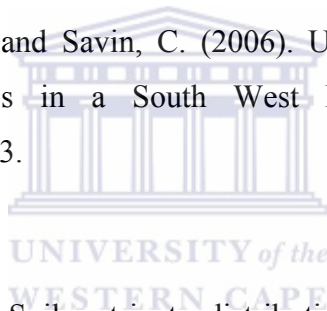
Brunke, M. and Gonser, T. (1997). The ecological significance of exchange processes between rivers and groundwater. *Fresh water biology*, 37: 1-33. Limnological research centre, Department of Limnology, EAWAG, 6047 Kartanienbaum, Switzerland. Blackwell science Ltd, special review.

Bouwer, H. and Rice, R.C. (1976). A slug test for determining hydraulic conductivity of unconfined aquifers with completely or partially penetrating wells. *Water Resources Research*, 12 (3): 423- 428.

Beauheim, R.L. and Pedler, W.H. (2009). Technical report: Fluid Electrical Conductivity Logging in Borehole DGR-1.DGR Site Characterization Document Intera Engineering Project 06-219. Available from http://www.nwmo.ca/uploads/DGR%20PDF/sitecharactechrep/TR-07-14_FEC-Logging-R2.pdf (Accessed April 2012).

Beauvais, A., Ritz, M., Parisot, J. C., Dukhan, M. and Bantsimba, C. (1999). Analysis of poorly stratified lateritic terrains overlying a granitic bedrock in West Africa, using 2-D electrical resistivity tomography, *Earth Planet. Sc. Lett* 173: 413–424.

Beauvais, A., Parisot, J. and Savin, C. (2006). Ultramafic rock weathering and slope erosion processes in a South West Pacific tropical environment. *Geomorphology*, 83: 1–13.



Ben-Shahar, R. (1990). Soil nutrients distribution and moisture dynamics on upper catena in a semi-arid nature reserve. *Vegetatio*, 89(1): 69-77. doi:10.1007/BF00134435.

Brink, A.B.A. and Bruin, R.M.H. (ed). (1990). Guidelines for soil and rock logging in South Africa. Proceedings of the Geoterminology Workshop. Association of Engineering Geologists, South African Institution of Civil Engineering, and South African Institute for Engineering and environmental Geologists. 2nd impression, 2002.

Birkhead, A.L., James, C.S. and Olbrich, B.W. (1995). Monitoring the bank storage dynamics component of the riparian water balance in the Sabie River, Kruger National Park. *Water SA*, 21 (3): 211-220.

Coulouma, C., Samyn, K., Grandjean, G., Follain, S and Lagacherie, P. (2011). Combining seismic and electric methods for predicting bedrock depth along a Mediterranean soil Toposequence. *Geoderma*, 170 39-47.

Cook, P.G. (2003). *A Guide to Regional Groundwater Flow in Fractured Rock Aquifers*. CSIRO Land and Water, Glen Osmond, SA, Australia.

Cooper, H.H. and Jacob, C.E. (1946). A generalized graphical method for evaluating formation constants and summarizing well field history. *American Geophysical Union Transactions* 27: 526–534. Available from: <http://core.ecu.edu/geology/spruill/spruill/Groundwater%20Notes%20No.%207.pdf> (Accessed January 2013).

Cullum, C. and Rogers, K. (2011). *A Framework for the Classification of Drainage Networks in Savanna Landscapes*. Report to the Water Research Commission. WRC Report No K5/1790.

Department of Water Affairs. (n.d.). *The Groundwater Dictionary* 2nd ed. Available from:

http://www.dwaf.gov.za/Groundwater/Groundwater_Dictionary/index.html?introduction_interflow.htm (Accessed June 2013).

Doughty, C. and Tsang, C.F. (2005). Signatures in flowing fluid electric conductivity logs. *Journal of Hydrology*, 310 157–180.

Dippenaar, M.A. (2013). Geological Characterisation at the Stevenson-Hamilton Southern Granite Research Supersite in the Kruger National Park (South Africa): Tors and Inselbergs. Unpublished document.

Driscoll, F.G. (1986). Well drilling methods. Chapter 10 in *Groundwater and wells*. 3rd ed, Johnson Filtration systems Inc. St Paul, MN.

Duffield, G.M. (1996-2007). AQTESOLV version 4.5. (Computer software) HydroSOLVE, Inc.



Du Toit, W.H., Verster H. and Smit I. (2009). Unpublished SANParks Project Progress Report (Aug 09).

Du Toit, J., Biggs, H. and Rodgers, K. (2003). *The Kruger experience: ecology and management of savanna heterogeneity*. Island press, Washington D.C USA.

Ebraheen, A.M., Garamoon, H.K., Riad, S., Wycisk, P., Seif, E.L and Nasr, A.M. (2003). Numerical modelling of groundwater resource management options in the East Oweinat area, southwest Egypt. Conference proceedings held at the Montpellier international symposium, April 2003.

Fischer, S., Witthüser, K.T., Birke, M., Leyland, R.C. and Schneider, M. (2009). Regional description of the groundwater chemistry of the Kruger National Park (KNP) using multivariate statistics. Groundwater Conference 2009, Somerset West, South Africa.

Freeze, R. and Cherry, J. (1979). Groundwater. Prentice Hall Inc.

Gabrielli, C.P., McDonnell, J.J and Jarvis, W.T. (2012). The role of bedrock groundwater in rainfall–runoff response at hillslope and catchment scales. Journal of hydrology, 450-451 and 117-133. Available from: <http://www.journals.elsevier.com/journal-of-hydrology> (Accessed August 2014).

Gertenbach, W.P.D. 1980. Rainfall patterns in the Kruger National Park.

Koedoe, 23: 35-43.



Gernand, J.D and Hietman, J.P .(1997). Detailed pumping test to characterize a fractured bedrock aquifer. Groundwater Journal, 4 (35).

Gomo, M., Steyl, G and Van Tonder, G. (2012). Investigation of Groundwater Recharge and Stable Isotopic Characteristics of an Alluvial Channel. Hydrol Current Res S12:002. doi:10.4172/2157-7587.S12-002.

Hantush, M.S. (1962). Flow of ground water in sands of nonuniform thickness; 3. Flow to wells in Kruseman, G.P. and De Ridder, N.A. (1994). Analysis and Evaluation of Pumping Test Data. 2nd ed. Available from:

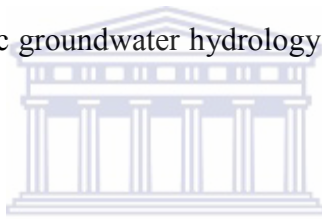
<http://content.alterra.wur.nl/Internet/webdocs/ilripublicaties/publicaties/Pub47/Pub47.pdf> (Accessed: March 2012).

Halford, K.J., Weight, W.D. and Schreiber, R.P. (2006). Interpretation of Transmissivity Estimates from Single-Well Pumping Aquifer Tests. *Groundwater journal*, 44 (3): 467.

Halford, K.J. and Kuniandy, E.L. (2005). United States Geological Survey (USGS) Aquifer test spreadsheets.

Healy, R.W. and Cook, P.G. (2002). Using groundwater levels to estimate recharge. *Hydrogeology journal*, 10 91-109.

Heath, R.C. (1983). *Basic groundwater hydrology*: U.S. Geological Survey Water Supply paper 2220.



International committee of the Red Cross (ICRC). (2010). Borehole drilling and rehabilitation under field conditions (Technical review). Available from: <http://www.icrc.org/eng/assets/files/other/icrc-002-0998.pdf> (Accessed March 2013).

Jacob, C.E. (1944). Well hydraulics and aquifer tests. Chapter 10 in the handbook of groundwater engineering 2nd ed. Taylor and Francis group, LLC.

Johnson, M.R., Anthaeusser, C.R. and Thomas R.J (Eds). (2006). *The Geology of South Africa*. Geological Society of South Africa, Johannesburg/Council for geosciences, Pretoria, 691pp.

Kearey, P. and Brooks, M. (1984). An Introduction to Geophysical Exploration. Blackwell scientific publications.

Kearey, P., Brooks, M. and Hill, I. (2002). An introduction to geophysical exploration. 3rd ed. Blackwell science Ltd.

Kresic, N. (2007). Hydrogeology and groundwater modelling. 2nd edition. CRC press. Taylor and Francis group, LLC.

Kresic, N. and Mikszewski, A. (2013). Hydrogeological conceptual site models. Taylor and Francis group, LLC.

Kohler, M.A. and Linsley, R.K. (1949). Predicting the runoff from storm rainfall. 30th Annual Meeting of the American Geophysical Union, Washington, D.C.

Kottek, M., Grieser, J., Beck, C., Rudolf, B. and Rubel, F. (2006). World Map of the Köppen-Geiger climate classification updated. Meteorologische Zeitschrift, 15 (3): 259-263. Available from:

http://www.schweizerbart.de/resources/downloads/paper_free/55034.pdf

(Accessed June 2013).

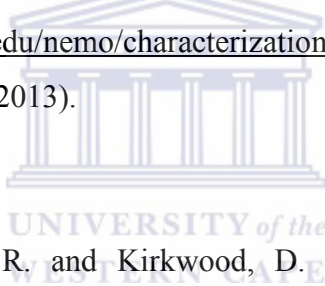
Kirchner, J. Changing rainfall- changing recharge. Pages 179-187 in Xu. Y., and H.E. Beekman, editors. 2003. Groundwater recharge estimation in Southern Africa. UNESCO IHP No. 64, UNESCO Paris. ISBN 92-9220-000-3.

Kruseman, G.P. and De Ridder, N.A. (1994). Analysis and Evaluation of Pumping Test Data. 2nd ed. Available from:

<http://content.alterra.wur.nl/Internet/webdocs/ilripublicaties/publicaties/Pub47/Pub47.pdf> (Accessed: March 2012).

Lerner, D.N., Issar, A.S. and Simmers, I. (1990). Groundwater recharge, guide to understanding and estimating natural recharge. International Association of Hydrogeologists, Kenilworth, Rep 8, 345 pp.

Leon, E. (2003). A Conceptual Model of Groundwater Flow in the Upper Agua Fria. Arizona Department of water resources. Available from: <http://www.snr.arizona.edu/nemo/characterizations/UpperAguaFria/AFconceptmodel.pdf> (Accessed May 2013).



Lemieux, J., Therrien, R. and Kirkwood, D. (2006). Small scale study of groundwater flow in a fractured carbonate-rock aquifer at the St-Eustache quarry, Quebec, Canada. Hydrogeology Journal, 14 603–612.

Loke, M. H. (1999). Electrical imaging surveys for environmental and engineering studies: A practical guide to 2-D and 3-D surveys, Available from: www.terrajp.co.jp/lokenote.pdf. (Accessed March 2012).

Loke, M. H. (2004). Tutorial: 2-D and 3-D electrical imaging surveys, Available from: www.goelectrical.com. (Accessed June 2012).

Loik, M., Breshears, D. D., Lauenroth, W. and Belnap, J. (2004). A multiscale perspective of water pulses in dryland ecosystems: climatology and ecohydrology of the western USA, *Oecologia*, 141, 269–281. Available from: http://research.eeescience.utoledo.edu/lees/papers_PDF/Loik_2004_Oecologia.pdf (Accessed April 2013).

Lorentz, S., Riddell, E., Koning, B. and Grant, R. (2006). The Influence of Catena Soil Water Dynamics on the Vegetation Patch Structure in the Northern Plains, KNP. HydroEco 2006, Karlovy Vary, Czech Republic, 11-14 September.

Nikas, K., Antonakos A., Lambrakis N. and Kallergis G. (2007). The use of Antecedent Precipitation Index and Delay Factor to estimate runoff from rainfall, a case study from eight drainage basins – Achaia, peloponessos, Greece. Proceedings held at the 11th International Congress, Athens, bulletin of the Geological Society of Greece 2007.



Maurice, L., Barker, J.A., Atkinson, T.C., Williams, A.T. and Smart, P.L. (2011). A Tracer methodology for Identifying Ambient Flows in Boreholes. *Groundwater Journal*, 49 (2):227-238.

Michalski, A. (1989). Application of temperature and electrical conductivity logging in groundwater monitoring. *Groundwater monitoring and remediation journal*, 9 (3): 112-118. Available from:

<http://onlinelibrary.wiley.com/doi/10.1111/j.17456592.1989.tb01158.x/abstract>. (Accessed: April 2013).

O'Keefe, J. and Rogers, K. H. (2003). Heterogeneity and Management of the Lowveld Rivers. In Du Toit, J. T., Rogers, K. and Biggs, H. C. (Eds.) *The Kruger Experience. Ecology and Management of Savanna Heterogeneity*. Washington DC, Island Press.

Osborne, P.S. (1993). *Suggested Operating Procedures for Aquifer Pumping Tests*. Environmental Protection Agency (EPA).

Pánek, T., Margielewshi, W., Taborik, P., Urban, J., Hradecky, J. and Szura, C. (2010). Gravitationally induced caves and other discontinuities detected by 2D electrical resistivity tomography: Case studies from the Polish Flysch Carpathians. *Geomorphology*, 123 165–180.

Peterson, R. (2011). Pers Comm relating to unpublished data for MSc in Geohydrology at the University of Western Cape.



Ratej, J. and Brencic, M. (2005). Comparative analysis of single well aquifer test methods on the mill tailing site of Borst Zirovski vrh Slovenija. *Geological survey of Slovenia. Materials and geo-environment*, 52(4):670 Available from: http://www.rmz-mg.com/letniki/rmz52/rmz52_0669-0684.pdf. (Accessed August 2012).

Robinson, D.A., Binley, A., Crook, N., Day-Lewis, F.D., Ferre, T.P.A., Grauch, V.J.S., Knight, R., Knoll, M., Lakshmi, V., Miller, R., Nyquist, J., Pellerin, L., Singha, L., Slater, L. (2008). Advancing process-based watershed hydrological research using near-surface geophysics: a vision for, and review of, electrical and magnetic geophysical methods. *Hydrol. Process*, 22 3604–3635.

Rogers, K. H. and O'Keefe, J. (2003). River Heterogeneity: Ecosystem Structure, Function & Management. In Du Toit, J. T., Rogers, K. and Biggs, H. C. (Eds.) The Kruger Experience. Ecology and Management of Savanna Heterogeneity. Washington DC, Island Press.

Sandberg, S.K., Slater, L.D. and Versteeg, R. (2002). An integrated geophysical investigation of the hydrogeology of an anisotropic unconfined aquifer. *Journal of hydrology*, 267: 227-243.

Smithers, J. C., Schulze, R. E., Pike, A., and Jewitt, G. P. W. (2001). A hydrological perspective of the February 2000 floods: A case study in the Sabie River Catchment. *Water SA*, 27(3): 325-332.

Smit, I.P.J., Riddell, E.S., Cullum, C. and Petersen, R., 2013, 'Kruger National Park research supersites: Establishing long-term research sites for cross-disciplinary, multiscaled learning', *Koedoe* 55(1), Art. #1107, 7 pages. <http://dx.doi.org/10.4102/koedoe.v55i1.1107>

South African National Standard (SANS) 663. (2009). Profiling and percussion and core borehole logging in South Africa for engineering purposes. Available from: http://www.saieg.co.za/uploads/Noticeboard/AZ%209610%20_DSS_%20633.pdf (Accessed May 2013).

Singh, K.P. (2005). Nonlinear estimation of aquifer parameters from surficial resistivity measurements. *Hydrol. Earth Sys. Sci. Discuss*, (2) 917–938.

Strahler, A. N. (1957). Quantitative analysis of watershed geomorphology. American Geophysical Union Transactions, 38: 913-920.

Talma, A.S. and Weaver, J.M.C. (2003). Published Water Research Commission Report on Evaluation of groundwater resources in fractured rock aquifers at a catchment scale using evidence of mixing of groundwater from CFC and isotope data. WRC Report no. 1009/1/03.

Tetzlaff, D., Carey, S.K., Laudon, H and McGuire, K.(2010). Catchment processes and heterogeneity at multiple scales benchmarking observations, conceptualization and prediction. Hydrol. Process. 24, 2203–2208.

The United Nations World Water Assessment Program. (2009). Introduction to IWRM guidelines at river basin level. Published by the United Nations Educational, Scientific and Cultural organisation. Available from: <http://unesdoc.unesco.org/images/0018/001850/185074e.pdf> (Accessed March 2012).

Toth, J. (1963). A theoretical analysis of groundwater flow in small drainage basins. Journal of Geophysical research, pp 63.

Tsang C.F., Hufschmeid, P. and Hale, F.V. (1990). Determination of fracture inflow parameters with a borehole fluid conductivity logging method. Water resources research, 26 (4): 561-57.

Van Tonder, G.J., Kunstmann, H. and Xu, Y. (2001). Flow characteristics. Version 3.0. (Computer software). Institute for groundwater studies, University of the Free State, Bloemfontein, South Africa.

Van Tonder, G.J. and Vermeulen, P.D. (2005). Applicability of slug tests in fractured rock formations. *Water SA*, 31 (2): 157-159.

Van Tol, J.J., Le Roux, P.A.L., Lorentz, S.A and Hensley, M. (2013). Hydropedological Classification of South African Hillslopes. *Vadose zone Journal*, 10.2136/vzj2013.01.0007.

Van Zijl, G., Le Roux, P.A.L. et al. (2011). KNP Supersites – Hydrological response models, internal report on KNP Supersite soil hydropedological characteristics.



Van Zijl, G.M. (2013). Developing a digital soil mapping protocol for Southern Africa using case studies. PhD thesis, University of the Free State, Bloemfontein, South Africa.

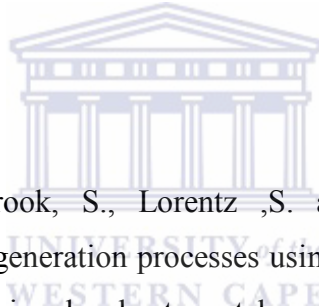
Vangins, M. and Simons, R. (1964). Rock Drill Bit. Patent No.273, 930. Available from:

<http://www.google.co.za/patents?hl=en&lr=&vid=USPAT3163246&id=zMFdAAAAEBAJ&oi=fnd&dq=%27percussion+drilling+method%27&printsec=abstract#v=onepage&q='percussion%20drilling%20method'&f=false> (Accessed March 2013).

Venter, F.J., Roberts, J.S. and Holger, C.E. (2003). The abiotic template and its associated vegetation pattern. Pages 86 - 87 in Du Toit, J.T., K. H. Rogers, and H. Biggs, editors. 2003. The Kruger experience: ecology and management of savanna heterogeneity. Island Press, Washington, and D. c.,USA.

Venter, F. (1990). A Classification of Land for Management Planning in the Kruger National Park. Doctoral Dissertation. South Africa. University of South Africa.

Winter, T.C., Harvey, J.W., Franke, O.L and Alley, W.M. (1998). Groundwater and Surface water a single resource. US Geological survey circulation 1139 ISBN 0-607-89339-7.



Wenninger, J., Uhlenbrook, S., Lorentz, S. and Leibundgut, C.h. (2008). Identification of runoff generation processes using combined hydrometric, tracer and geophysical methods in a headwater catchment in South Africa. Hydrological Sciences Journal, 53 (1): 65-80.

Wright, E.P. (1992). The hydrogeology of crystalline basement aquifers in Africa. Geological Society, London, special publications, 66 1-27. doi:10.1144/GSL.SP.1992.066.01.01

Appendix CD:

The following data are provided on the appendix CD to enable future analysis:

Appendix I: Southern granite supersite pump test and slug test data

Appendix II: Southern granite supersite fluid logging data

Appendix III: Southern granite supersite groundwater vs. surface water hydraulic head data

Appendix IV: Southern granite supersite borehole field logging form data

Appendix V: DWA monitoring borehole water level data in KNP

